NANYANG TECHNOLOGICAL UNIVERSITY

PURIFICATION AND CHARACTERIZATION OF A POTENT DENDRITIC CELL ACTIVATOR RELEASED BY T CELLS

LIN MIN

SCHOOL OF BIOLOGICAL SCIENCES

2011

PURIFICATION AND CHARACTERIZATION OF A POTENT DENDRITIC CELL ACTIVATOR RELEASED BY T CELLS

LIN MIN

School of Biological Sciences

A thesis submitted to the Nanyang Technological University in partial fulfillment for the degree of
Doctor of Philosophy

2011

ACKNOWLEDGEMENT

- The most sincere thanks to my supervisor, A/P Christiane Ruedl, for her patient supervision and broad knowledge, giving me a bright view in the field of immunological researches
- Special thanks to Prof Klaus Karjalainen for his experienced suggestions in my experiments, directing me in the correct tracks
- Thanks to our collaborators, A/P Julien Lescar, Asst/P Newman Sze, Asst/P Peter Cheung, Dr Kotako Masayo, Tiannan Guo, and Dai Liang for their advices and technical support in my experiments
- Thanks to my colleagues, Shuai, Winnie and Siti for their helps in my experiments
- Thanks to my colleague, Dr Piotr Tetlak for his teaching of the molecular techniques in my work
- And thanks to my supervisor and all labmates for giving me this valuable memory of my PhD life in this lab

TABLE OF CONTENTS

SUMMARY

$CD8^+$ T lymphocytes, during priming, can induce robust maturation of dendritic cells (DCs) in a CD40 independent manner by secreting licensing factor(s). I have isolated this so far elusive licensing factor and identified it as GM-CSF. Signaling through the GM-CSF receptor in *ex-vivo* purified DCs upregulates the expression of costimulatory molecules and provides a positive feedback loop in stimulation of $CD8^+$ T cell proliferation. Combined with a variety of microbial stimuli, GM-CSF supports the formation of potent 'effector' DCs capable in screening a variety of proinflammatory cytokines guiding the differentiation of T cells during the immune responses.

I have extended this principle to a strong synergism in particular between the Dectin-1 agonist, β-glucan curdlan, and GM-CSF. Both together act in synergy in inducing a strong inflammatory signature which converts immature DCs to potent effector DCs. The synergistic effects of both stimuli resulted in strong IκBα phosphorylation, in its rapid degradation and in enhanced nuclear translocation of all NF-κB subunits. We further identified MAPK ERK as one possible integration site of both signals, since its phosphorylation was clearly augmented when curdlan was co-applied with GM-CSF. Our data demonstrate that the immunomodulatory activity of curdlan requires an additional inflammatory signal provided by GM-CSF to successfully initiate a robust β-glucan specific cytokine and chemokine response. The integration of both signals clearly prime and tailor a more effective innate and adaptive response against invading microbes and fungi.

ABBREVIATIONS

APC: Antigen-presenting cell

ASC: Apoptosis-associated speck-like protein containing a CARD

BAFF: B-cell-activation factor of the TNF family

β_C: Common β subunit

BCL: B cell lymphoma

BLC: B-lymphocyte chemoattractant

BM: Bone marrow

CARD: Caspase recruitment domain

CCL24: Chemokine (C-C motif) ligand 24

cDC: Conventional DC

CLCF1: Cartrophin-like cytokine factor-1

CLP: Common lymphoid progenitor

CLR: C-type lectin receptor

CMP: Common myeloid progenitor

COX: Cyclooxygenase

CpG: Unmethylated CpG DNA of bacteria and viruses

CTL: Cytotoxic T lymphocyte

CXCL13: Chemokine (C-X-C motif) ligand 13

DETC: Dendritic epidermal T cells

DC: Dendritic cell

DN: Double negative

dsRNA: Double-stranded RNA

ELC: Epstein-Barr virus-induced molecule 1 ligand

ENS: Predicted gene, ENSMUSG00000073266

ERK: Extracellular signal-related kinase

FACS: Fluorescent-activated cell sorting

FLT3L: Fms-like tyrosine kinase 3-ligand

Foxp: Forkhead transcription factor

FPLC: Fast protein liquid chromatography

Gdf: Growth differentiation factor

GM-CSF: Granulocyte-Macrophage colony-stimulating factor

Grn: Granulin

H2-Eb2: Histocompatibility 2, class II antigen E beta2

Hdgf: Hepatoma-derived growth factor

HPLC: High performance or high pressure liquid chromatography

HSP: Heat shock protein

ICAM: Intercellular adhesion molecule

IEF: Isoelectric focusing

IFN: Interferon

IKK: IκB kinase

IL: Interleukin

IMDM: Iscove's modified Dulbecco's medium

iNOS: Inducible nitric oxide synthase

ITAM: Immunoreceptor tyrosine-based activation motif

ITIM: Immunoreceptor tyrosine-based inhibitory motif

JAK: Janus (tyrosine) kinase

JNK: Jun amino-terminal kinase

LC: Langerhans cell

LCMV: Lymphocytic choriomeningitis virus

LN: Lymph node

LPS: Lipopolysaccharide

LRR: Leucine-rich repeat

Ltb: Lymphotoxin-beta

MACS: Magnetic-activated cell sorting

MALT: Mucosa-associated lymphoid tissue lymphoma translocation gene

MAPK: Mitogen-activated protein kinase

MCP: Monocyte chemotactic protein

MDP: Muramyl dipeptide

MDP: Macrophage and DC progenitor

MHC: Major histocompatibility complex

MIF: Microphage migration inhibitory factor

MIP: Macrophage inflammatory protein

MKK: MAPK kinase

MS: Mass spectrometry

NFAT: Nuclear factor of activated T cells

NF-κB: Nuclear factor-kappa B

Ngp: Neutrophilic granule protein

NIK: NF-κB-inducing kinase

NK: Natural killer

NLR: Nucleotide-binding oligomerization domain (Nod)-like receptor

PAMPs: Pathogen-associated molecular patterns

pDC: Plasmocytoid DC

PE: Phycoerythrin

pI: Isoelectric point

PLA: Phospholipase A

PRR: Pattern recognition receptor

Ptma: Prothymosin-alpha

RA: Retinoic acid

RLR: Retinoic acid inducible gene (RIG)-I-like receptor

ROR: Retinoid-related orphan receptor

ROS: Reactive oxygen species

RT-PCR: Reverse transcriptase PCR

S100a9: S100 calcium binding protein A9

SAPK: Stress-activated protein kinase

SCF: Stem-cell factor

SDF: Stromal cell-derived factor

SLC: Secondary lymphoid tissue chemokine

STAT: Signal transducer and activator of transcription

TCF: T cell factor

TCR: T cell receptor

T_{FH}: Follicular helper T cell

TGF: Transforming growth factor

T: Helper T cell

TIR: Toll/IL-1R

TLR: Toll-like receptor

TNF: Tumor necrosis factor

Tnfrsf13b: TNF (Tumor necrosis factor) receptor superfamily, member 13B

T_{REG}: Regulatory T

TSLP: Thymic stromal lymphopoietin

VCAM: Vascular cell adhesion molecule

LIST OF TABLES

LIST OF FIGURES

LIST OF PUBLICATIONS

1. Lin Min, Siti Aminah Bte Mohammad Isa, Fam Wee Nih, Sze Siu Kwan Newman, Ottavio Berretta, Alessandra Mortellaro and Christiane Ruedl S**ynergism between Curdlan and GM-CSF confers a strong inflammatory signature to dendritic cells**, ***submitted to J. Immunol.***
2. Hanif Javanmard Khameneh*, Siti Aminah Bte Mohammad*, Lin Min, Fam Wee Nih and Christiane Ruedl (2011) **GM-CSF Signalling Boosts Dramatically IL-1 Production,** ***Plos ONE,*** 6(7): e23025.
3. Lin Min, Siti Aminah Bte Mohammad Isa, Wang Shuai, Cher Boon Piang, Fam Wee Nih, Masayo Kotaka and Christiane Ruedl (2010) **Granulocyte-Macrophage Colony-Stimulating Factor is the major CD8 $^{+}$ T cell-derived licensing factor for dendritic cell activation,** ***J. Immunol***. 184: 4625-4629.

CONFERENCES AND AWARD

- **11th International Symposium on Dendritic Cells in Fundamental and Clinical Immunology**, Lugano, Switzerland - Poster Presentation
- **1st to 4th International Singapore Symposium of Immunology**, Singapore - Poster Presentation
- **1st to 2nd Singaporean Immunology PHD Student Retreat** - Poster presentation
- **Young Investigator Travel Award**, 11th International Symposium on Dendritic Cells in Fundamental and Clinical Immunology, Lugano, Switzerland

INTRODUCTION

Chapter I: Dendritic cells and the control of immunity

1 Immune regulations by dendritic cells

Dendritic cells (DCs) were first described by Ralph Steinman in the 1970s as the potent accessory cells involved in the priming of immune responses (1). Thereafter, more studies revealed DCs to be the key regulators of immune reactions and the link between innate and adaptive immune responses (2). DCs are the sentinels of the mammalian immune system because they are the first to detect, encapture and process the invading infectious agents for the scrutiny of T cells. Hence, the optimal 'collaboration' of DCs and T cells is absolutely crucial for the successful immunity. As a matter of fact, DCs have been long known to be the most efficient antigen-presenting cells (APCs) capable of priming naïve T cells but only recently it became clear that DCs are also involved in establishing tolerance to self-antigens and non-pathogenic foreign antigens (3). In fact, interaction of naïve T cells with immature resting DCs results in antigen-specific T cell tolerance, whereas mature DCs induce T cell priming (4).

As the first DC subtype discovered, Langerhans cell (LC) was considered as the archetypal DC with the typical DC life cycle: to encounter and capture the pathogens in the peripheral tissues, and with the process of maturation marked by upregulation of the costimulatory molecules and major-histocompatibility complex (MHC) molecules, to migrate to the draining lymph nodes (LNs) and activate the naïve T cells. This process is named as the "Langerhans cell paradigm" (**Fig. 1**) (5, 6).

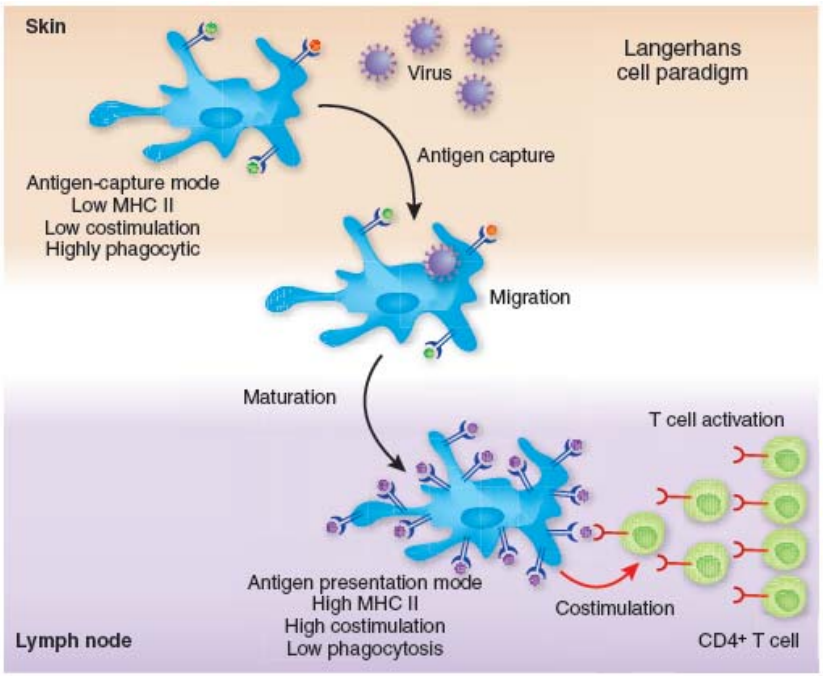

Figure 1: The life cycle of LCs as the archetypal DCs. The cells capture antigens in the skin, and with antigen processing and DC maturation by upregulation of the costimulatory molecules and MHC class II on the surface, LCs migrate to the draining lymph nodes and activate naïve T cells. (Heath and Carbone, 2009).

However, this LC paradigm, might not apply to the DCs found in other tissues. In the revised model integrating the functions of more subtypes of DCs, the DCs acting as sentinels in both peripheral and lymphoid tissues, continuously sampling the antigenic environment are in their 'immature' stage. Once encountering the antigenic stimulators, they initiate the maturation processes as mentioned and migrate to the T cell areas of the secondary lymphoid organs and present antigen to naïve T cells, to initiate either T cell activation when the microbial products or inflammatory stimuli are present or tolerance if these signals are absent (7-9).

1.1 The dendritic cells family

With numerous approaches, the established results have supported the multiple roles of DCs as being a family of extremely heterogeneous subsets. More literature supports the idea that each DC subset is unique and associated with distinct, although potentially overlapping, functions (5). Their distinct locations, surface makers, and probably developmental stages define the complexity of the heterogeneity of the DC subsets (10).

Recently, Heath and Carbone proposed the following DC subsets based on their expressed cell surface markers and anatomical locations (**Fig. 2**).

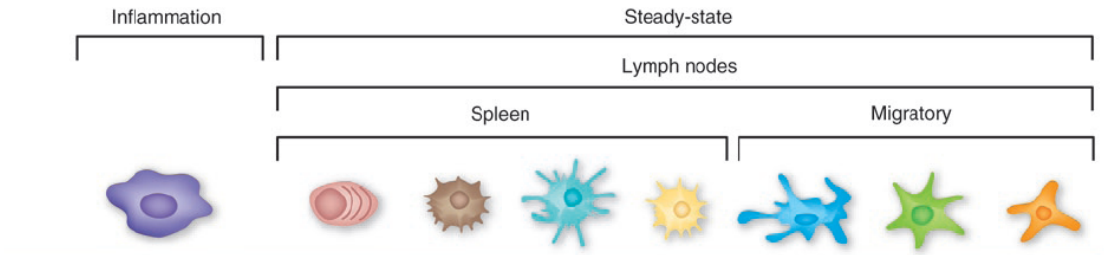

	Mono-DC	Plasmacytoid	CD8$^+$	CD4$^+$	DN	CD11b$^+$ (e.g. classic dermal)	CD103$^+$ (e.g. langerin$^+$ dermal)	Langerhans
CD205	?	–	+	–	–	+	++	++
CD11b	+	–	–	+	+	+	–	+
Ep-CAM (CD326)	–	–	–	–	–	–	+/–	+
Langerin (CD207)	–	–	+	–	–	–	++	++
B220	–	+	–	–	–	–	–	–

Figure 2: Phenotype and location of DC subsets. The subsets are defined by the surface expression of the key phenotypic markers, categorizing the DCs according to the following criteria: whether they are present in the steady state or only after infection; whether they are resident or migratory DCs; and the DC locations in the lymphoid organs. DN, $CD4^-CD8^-$ (double-negative) DCs. (Heath and Carbone, 2009).

The monocytes-derived DCs are inflammation-associated DCs. Monocytes are phagocytic cells of the myeloid lineages located in blood and BM in the steady state. During infection-associated inflammatory responses, they are converting DCs and are recruited into the lymphoid organs for innate immune functions (11). As reported by Yrlid, et. al., both the short-lived 'inflammatory' monocytes ($Ly6C^+GR1^+$) and the long-lived 'non-inflammatory' monocytes ($Ly6C^-GR1^-$) can convert DCs (12, 13). *In vitro,* the monocytes converte $CD11c^+MHCII^+$ DCs upon stimulation of GM-CSF, with or without interleukin (IL)-4 (14-17).

The subdivision of DCs into myeloid DCs and plasmacytoid DCs (pDCs), which was initially described for human DCs, was parallel discovered in mouse DCs (18, 19). Different from the other DC subsets, which are collectively named as conventional DCs (cDCs), the pDCs have the plasma-cell morphology and are primarily involved to initiate immune responses to viral infections (20, 21). The naïve pDCs in the steady state are considered as pre-DCs, which can acquire the typical DC morphology upon activation, and are found in many tissues of the mouse, including blood, thymus, BM, liver and lymphoid organs. Upon exposure to viruses, bacteria and certain TLR agonists they produce the inflammatory cytokines, especially the type I interferon (IFN), which is essential for the generation of antiviral adaptive immune responses. The secreted type I IFNs are essential in the antiviral responses and stimulate both T cells and Ag-presenting DCs (22, 23).

Mouse cDCs residing in lymphoid organs in the steady state, named lymphoid organ-resident DCs, can be categorized into three subsets on the basis of their surface expression of CD4 and CD8α, including $CD8\alpha^+$, $CD4^+$ and double-negative (DN) populations (24). However, more studies simply defined the subsets into $CD8\alpha^+$ cDCs ($CD11b^-$) and $CD8\alpha^-$ cDCs ($CD11b^+$) because the DN and $CD4^+$ were

collectively referred to as CD8α$^-$ DCs (5). The resident DCs constitute half of the lymph-node DCs and all of the splenic and thymic DCs (25). And they are developed from the bone-marrow precursors within the lymphoid organs without previously trafficking through peripheral tissues (26-28). The lymphoid organ-resident DCs are normally found in a MHC II^{low} 'immature' states, clearly distinct from the mature MHC II^{hi} migratory DCs (6, 29). Being the most numerous resident cDCs in the spleen, CD8$^-$ cDCs are only a minor population in the lymph nodes. Anatomically, CD8$^+$ cDCs are found in the T cell areas of the spleen and lymph nodes, while the CD8$^-$ cDCs are found in the marginal zones (30).

There are at least three different subpopulations of migratory DCs in the skin, named LCs, dermal DCs and CD103$^+$ DCs. To elaborate more by the key surface phenotype markers, the full description of the dermal DCs is classic CD11b$^+$ dermal DCs while the CD103$^+$ DCs are the langerin-positive CD11b$^-$CD103$^+$ DCs. CD103$^+$ DCs are not purely dermal DCs because they also reside in other sites. For example, the lung contains its equivalent type as also being langerin positive and CD103$^+$ (31). Besides, the lymph nodes draining the gut, liver, kidney, lung and skin also contain their counterparts reflecting the wide distribution of this newly identified CD103$^+$ DC population (32-34).

1.2 The innate immune recognition and dendritic cell maturation

The hallmark of DC maturation is the upregulation of cell-surface expression of MHC molecules, CD40, CD80, CD83 and CD86, which is described by the cell surface phenotype. Because expression of these molecules often correlates with the

increased T cell-priming ability, it is generally accepted that DCs that are mature phenotypically also bear the functional potency to be immunogenic, thus are considered as the functionally mature DCs (35). However, as mentioned, this traditional view was challenged by recent observations that phenotypically mature DCs do not always promote T cell immunity, and sometimes rather induce T cell tolerance (3, 8).

Studies showed that with the maturation of DCs associated with the surface marker upregulations and the migration of DCs to the secondary lymphoid organs for antigen presentation to T cells, they gradually lost the capacity to phagocytose (36). In fact, immature DCs in the periphery capture and process antigens, after which they migrate to the secondary lymphoid tissues as mature DCs that decrease antigen-sampling functions but increase T cell priming abilities (37).

Immature DCs express a series of receptors on surface to capture the pathogen-associated molecular patterns (PAMPs) from microbes and secondary inflammatory compounds from the host (**Fig. 3**). Such receptors include Toll-like receptors (TLRs), nucleotide-binding oligomerization domain (NOD) proteins (NLRs), RIG-I-like receptors (RLRs), C-type lectin receptors (CLRs), cytokine receptors, and chemokine receptors (25, 38). Once encountering their respective binding partners, these receptors deliver the maturation stimuli intracellularly to initiate the increased expressions of the maturation markers, migratory molecules and the inflammatory cytokines. These phenotypic changes allow DCs to initiate immune responses, or rather tolerance (25, 35).

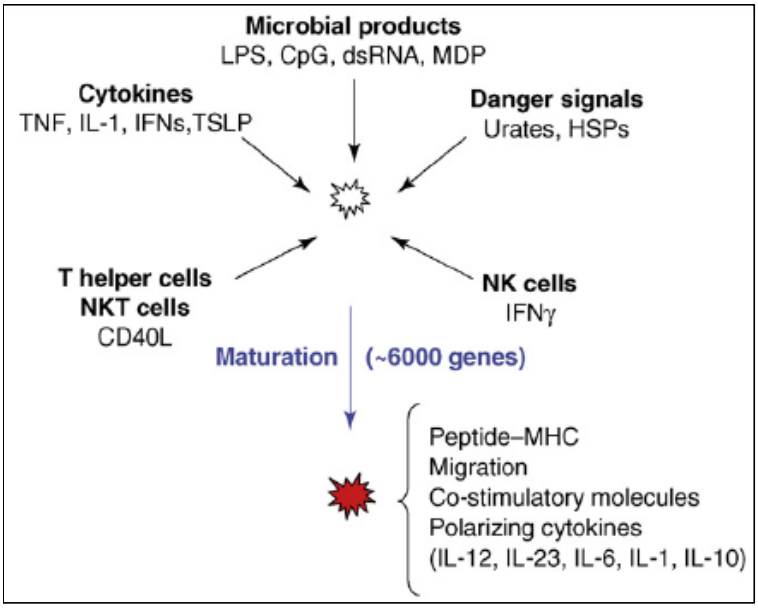

Figure 3: Stimuli for dendritic cell activation. Steady state DCs can be activated by microbial products [lipopolysaccharide (LPS), unmethylated CpG of bacterial DNA, double-stranded viral RNA (dsRNA) and muramyldipeptide (MDP)], endogenous signals [urates and heat shock proteins (HSPs)] and feedback signals from cells of the innate and adaptive immune systems (cytokines, T helper cells, NKT cells and NK cells). Activated DCs integrating one or more stimuli undergo a maturation process that includes upregulation of the surface peptide-MHC molecule complexes, increase of the migratory ability, and the ability to stimulate T cell proliferation and polarization. (Macagno et. al., 2007).

1.2.1 The Toll-like receptors as archetypal pattern recognition receptors

The microbial stimuli, including lipopolysaccharide (LPS), unmethylated CpG DNA of bacteria and viruses (CpG), double-stranded RNA (dsRNA), muramyl dipeptide (MDP), etc, are detected by different receptors on DCs (38), which are collectively called pattern recognition receptors (PRRs), while these above mentioned PRR-ligands are PAMPs. PAMPs are normally essential for the survival and functions of the pathogens and thus are resistant to the frequent mutations in the lifecycle of the microbes. This ensures the fast and specific recognition during innate immune defense (39). The expressions of PRRs are nonclonal and constitutive on the cell

surface. Different PRRs recognize different PAMPs with specificity, initiating different signaling pathways which ultimately lead to distinct antimicrobial responses (40).

The most important family of PRRs identified so far are TLRs, which include 12 members in mice (41). Belonging to type I integral membrane glycoproteins, TLRs are composed of the leucine-rich repeats (LRRs) bearing extracellular domains, which are involved in ligand binding, and the cytoplasmic domains called Toll/IL-1R homoloy (TIR) domains, which interact with TIR-domain containing adaptor molecules for signaling transduction (40, 42).

Species	PAMPs	TLR Usage
Bacteria, mycobacteria	LPS	TLR4
	lipoproteins, LTA, PGN, lipoarabinomannan	TLR2/1, TLR2/6
	flagellin	TLR5
	DNA	TLR9
	RNA	TLR7
Viruses	DNA	TLR9
	RNA	TLR3, TLR7, TLR8
	structural protein	TLR2, TLR4
Fungus	zymosan, β-glucan	TLR2, TLR6
	Mannan	TLR2, TLR4
	DNA	TLR9
	RNA	TLR7
Parasites	tGPI-mutin (*Trypanosoma*)	TLR2
	glycoinositolphospholipids (*Trypanosoma*)	TLR4
	DNA	TLR9
	hemozoin (*Plasmodium*)	TLR9
	profilin-like molecule (*Toxoplasma gondii*)	TLR11

Table 1: PAMP detection pattern of different TLR members. Different TLRs recognize different types of pathogenic ligands with certain overlapping. (Kawai and Akira, 2011).

Within the TLR family, TLR1, TLR2, TLR4, TLR5, and TLR6 are localized on the cell surface to capture the surface components of the invading pathogens, whereas TLR3, TLR7, TLR8 and TLR9 are expressed in the intracellular compartments to recognize nucleic acids which are released upon digestion of

microbes (**Table 1**) (41, 43). Examples of PAMPs recognized by particular TLRs are LPS recognized by TLR4, CpG via TLR9, bacterial lipoproteins and lipoteichoic acids via TLR2, flagellin through TLR5, poly(I:C) through TLR3 and single-stranded viral RNA detected by TLR7 (43).

Upon engagement, TLRs transduce intracellular signals via either MyD88-dependent or -independent pathways. MyD88 belongs to TIR-domain-containing adaptor proteins, which also include TIRAP, TRIF and TRAM involved in TLR signaling. In response to different pathogenic signaling received by different TLR members, the specific combination of these adaptor proteins are recruited to the receptor cytoplasmic domain for signals transmission (44). MyD88 is employed by all TLRs (with the only exception TLR3) in the absence or with combination of other adaptors, to activate the NF-κB and MAPK signaling pathways for the induction of inflammatory cytokines. TLR3 and TLR4 use TRIF to signal an alternative pathway resulting in NF-κB and IRF3 activation and the induction of type I IFN release. TLR2 and TLR4 recruit MyD88 indirectly via TIRAP. TLR4 utilizes TRAM as the adaptor for TRIF binding in the TRIF-dependent pathway besides the MyD88-dependent one. The differential binding of adaptors is crucial for TLRs, providing them with specificity for downstream intracellular responses (41, 45).

As the archetypal PRRs, the functions of TLRs have been well elaborated. With recognition of a vast range of pathogens, they play a central role in anti-microbial defense with involvement of both innate (42) and adaptive immunity (43). The host defense delivered by TLRs often requires a crosstalk between the different TLR members (41-43). As the invading microorganisms usually contain multiple PAMPs recognized by different TLRs, the signaling integration between them make

advantages in tailoring the pathogen clearance mechanisms involving release of inflammatory cytokines and induction of adaptive immune responses for prolonged immunological memory (41). In addition, the signaling integration also happens in between TLRs and other PRRs. For example, the NLRP3 (NACHT-LRR-PYR-containing protein 3) inflammasome machinery needs the TLR signaling for cytokine expressions, which will be further discussed later (46).

1.2.2 Other pattern recognition receptors as microbial sensors

Besides the TLRs, as conventional PRRs, NLRs, RLRs, and the newly identified CLRs also belong to the PRRs family (38, 41).

The NLRs are cytosolic receptors capable of detecting bacterial products and endogenous danger signals (9, 47). The family members include Nod1, Nod2, which induce NF-κB signaling, and NLRPs that activate caspase-1 for the processing of pro-IL-1 and pro-IL-18 to their active form (9). Signals via NLRs are shown to be essential for the onset of adaptive immunity. From recent studies, upon recognition of ligand peptidoglycan, Nod1 alone was sufficient to drive T_H2 and B cell responses (48). In combination with TLR signals, Nod1 mediates T_H1, T_H2, and T_H17 responses while favoring anti-bacterial T_H17 responses (9).

The cytosolic RLRs are sensors for viral nucleic acids. Upon ligand activation, they mediate the activation of interferon (IFN)-regulatory factor for the induction of antiviral type I IFNs (49). RLR signaling contributes to the adaptive immunity via the induction of $CD8^+$ T cell responses in response to certain viral infection, while the protection against re-infection needs the help from TLRs (9, 50).

The CLRs detect bacterial and fungal carbohydrate moieties. Dectin-1 is its representative with the best-revealed functions (9). Dectin-1 induced signals were shown to induce adaptive immunity favoring both T_H1 and T_H17 polarization (51). Besides the tailored antifungal effects, Dectin-1 also mediates the clearance of fungal infection, using a signaling pathway with involvement of the kinase adaptor Syk (52-54).

1.2.3 Endogenous signals

Besides the PAMP-dependent signals, DC maturation can also be stimulated by endogenous 'danger signals', e.g., molecules released from the necrotic host cells (**Fig. 3**) (2, 55). Some of those signals may mimic the PAMPs and stimulate PRRs responses. Examples include hyaluran degradation products, fibronectin A, heat shock proteins, etc (56). In contrast, others are PRR-independent and include ATP (recognized by purinergic receptors) and bradykinins (via bradykinin receptors) (57). The significance of this danger signal-induced DC maturation is still unknown.

1.2.4 Cytokines as signals from immune cells

Equipped with receptors for inflammatory cytokines, DCs can be stimulated by tumour necrosis factor (TNF), IL-1β, and type I and II IFNs, which are released by immune cells at early stage of infection (38). These cytokines function in an autocrine or paracrine feedback loop to stimulate DC maturation.

1.3 Development of dendritic cells

1.3.1 *In vivo* development

With a high developmental flexibility at early stages of haematopoiesis, pDCs and all subtypes of splenic cDCs can be generated from either common myeloid (CMP) or common lymphoid precursors (CLP) (58, 59). All the early precursors of different DC subsets are within the BM $FLT3^+$ precursor population, regardless of their lymphoid or myeloid origins (**Figure 4**) (60, 61).

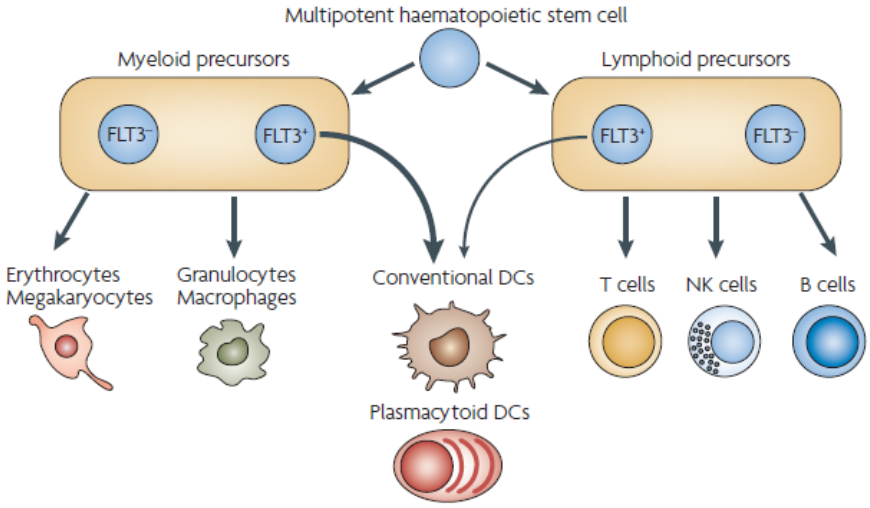

Figure 4: Dendritic cell development from haematopoitic precursors. The common myeloid progenitors and common lymphoid progenitors are the two lineage-defining precursor stages, while the DCs are derived from both lineages that express the FLT3 (FMS-related tyrosine kinase 3) receptor. Both the lymphoid organ resident conventional DCs (cDCs) and the plasmacytoid DCs (pDCs) can be generated from either $FLT3^+$ precursor type. NK, natural killer. (Shortman and Naik, 2007).

The above mentioned different types of pre-DCs are the last precursor stage of DC development, while intermediate precursors of DCs can be sought among bone

marrow cells lacking lineage-specific markers (lin^-), but not yet expressing DC markers such as CD11c or surface MHC II molecules and still expressing some early haematopoitic-precursor markers such as CD117 (10, 27). Based on the limited information available so far, lymphoid tissue cDCs, pDCs and monocytes can be derived from a common progenitor called the macrophage and DC precursor (MDP) that is identified by the surface phenotype as $Lin^-cKit^{hi}CD115^+CX_3CR1^+Flt3^+$ (62), whereas a distinct progenitor called the common DC precursor, which is $Lin^-cKit^{lo}CD115^+Flt3^+$, is restricted to produce DCs but not macrophages (10, 63).

1.3.2 *In vitro* development

In the GM-CSF culture, the progenitor cells generate a relatively homologous population of $CD11c^+CD11b^+CD8^-MHC\ II^+$ DCs, resembling the $CD8^-$ myeloid DCs residing in the lymphoid organs, thus they were for a longtime considered as the key precursors for steady state DCs generation. However, more recent studies proved the importance of GM-CSF derived DCs only during inflammation (26, 64, 65). In the steady state mice, GM-CSF levels are too low to derive DC development (66-68). In addition, knocking-out the GM-CSF functions had effects neither on the normal ratios and numbers of the splenic DC subtypes, nor on their expected functions (69, 70).

In contrast, the cytokine FLT3L (FMS-related tyrosine kinase 3 ligand) is crucial for steady state pDC and cDC development. Evidence was from the FLT3L knock-out mice that have low levels of myeloid-related ($CD11c^+CD8\alpha^-$) and lymphoid-related ($CD11c^+CD8\alpha^+$) DCs (71).

It was always a tedious process to obtain DCs *ex vivo* because of their high heterogeneity and low abundance in the lymphoid tissues. With background information about both *in vivo* and *in vitro* development of DCs, the cytokine derived *in vitro* cultures were well established and made big advantages to allow the easier access and study of DCs (27). The widely applied culture models used to derive *in vitro*-DCs are listed in **Table 2**.

Precursors	Cytokines, conditions	DC type generated	References
Human monocytes	GM-CSF (+IL-4)	Inflammatory DCs (monocyte-derived DCs)	32
	Transendothelial migration	Interstitial DCs, migratory DCs	107,108
	Epidermal equivalents	LCs	106
Human $CD34^+$ precursors	GM-CSF (±TNF, ±IL-3, ±TGFβ, ±SCF)	Interstitial DCs, LCs, inflammatory DCs (through monocytes)	31, 126–128
Mouse bone marrow, enriched precursors, lin^-KIT^+ precursors	GM-CSF (±TNF, ±SCF)	Interstitial DCs, LCs, inflammatory DCs (through monocytes)	57,74,129
Mouse bone marrow	FLT3L	pDC, $CD8^+$ cDC and $CD8^-$ cDC equivalents	40,41, 112,130
Mouse thymus, early T-cell precursors	Seven-cytokine mix, no GM-CSF	Thymic cDC equivalents	94
Mouse spleen cells	GM-CSF (+3T3 supernatant)	DCs (inflammatory DCs?)	84,85
	Medium alone	$CD11c^-$ MHC class II^- cells (DC equivalence uncertain)	83

Table 2: Culture models of dendritic-cell development. cDC, conventional dendritic cell; DC, dendritic cell; FLT3L, FMS-related tyrosine kinase 3 ligand; GM-CSF, granulocyte/ macrophage colony-stimulating factor; IL, interleukin; lin^-, negative markers of mature haematopoietic cell lineages; LC, Langerhans cell; pDC, plasmacytoid dendritic cell; SCF, stem-cell factor; TGFβ, transforming growth factor-β; TNF, tumour-necrosis factor; 3T3 supernatant, supernatant from cultures of the 3T3 fibroblast cell line. (Shortman and Naik, 2007).

As the well established and widely applied method to derive BMDCs *in vitro*, GM-CSF cultures have been providing the fundamental basis for DC research for a long time, supporting the studies on the development, functionalities and potential applications of DCs in the directions of their immuno-stimulatory effects (10, 27). However, it was gradually realized that GM-CSF derived DCs represent more the

inflammatory DCs that do not appear during steady state, whereas FLT3L derived BMDCs better represent the steady state resident DCs, including pDCs and CD8α$^+$ cDCs and CD8α$^-$ cDCs (**Table 2**) (27, 72).

2 Translation of the innate signals to adaptive responses

Different from the innate immunity, which include fast immune responses to clear the invading pathogens, the adaptive immunity is involved to eliminate the pathogens at the late stage of infection and to generate the immunological memories for future protection of the host (73).

2.1 T cells priming by dendritic cells

Apart from the other APCs, DCs are unique in their ability not only to efficiently trigger the primary T cell responses, but also to function in the secondary T cell responses (5). The interactions between T cells and DCs involve the functions of the different DC subsets, which are demonstrated in **Fig. 5**.

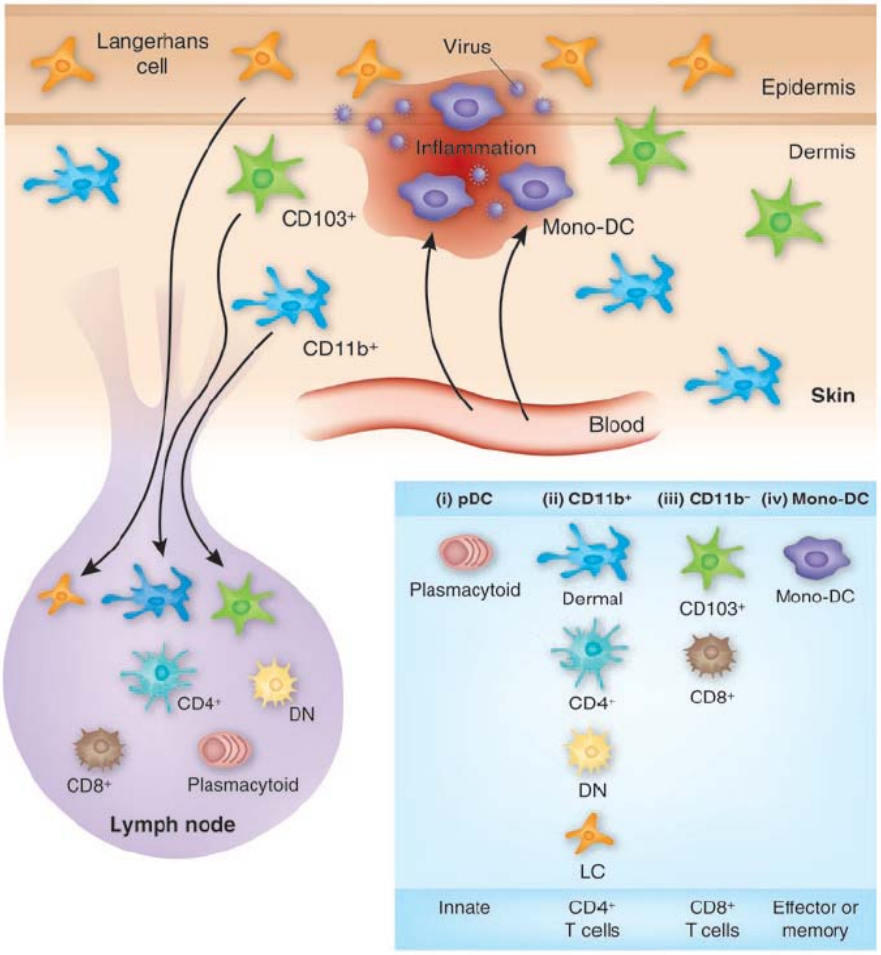

Figure 5: A general model for DC subsets to initiate and maintain T cell responses during infection. Taking skin infection as example, antigenic stimuli drive the skin DCs migration to the draining lymph nodes, and the inflammatory responses recruite monocytes to the site of infection to form inflammatory DCs. In the draining lymph nodes, mature migratory DCs activate T cells and provide the antigen to lymph node-resident $CD8\alpha^+$ cDCs. DC subsets contribute to T cell responses in the following ways: i) innate signals released by pDCs in the lymph nodes to boost the adaptive immunity; ii) $CD11b^+$ DCs contributing to $CD4^+$ T cell responses by antigen presentation; iii) $CD11b^-$ DCs contributing to $CD8^+$ T cell responses; iv) monocyte-derived DCs acting as local stimulators for the functions of effector or memory DCs at the site of infection. (Heath and Carbone, 2009).

The priming of T cell responses is initiated by binding of TCR (TCRα:β heterodimer and CD3 complex) to its cognate antigen presented by MHC molecules on the surface of the DCs. The MHCs are peptide-binding proteins subdivided into two types, MHC class I and MHC class II, which bind to $CD8^+$ and $CD4^+$ T cells

with antigen specificity to initiate cytotoxic T lymphocyte (CTL) and T helper cell (T_H) responses, respectively. Referring to **Fig. 5**, the $CD11b^+$ DCs, including dermal DCs, lymphoid organ resident $CD4^+$ cDCs and DN cDCs, derive the $CD4^+$ T cell differentiation, whereas the $CD11b^-$ DCs, including $CD103^+$ DCs and $CD8\alpha^+$ DCs, drive the $CD8^+$ T cell response (5). The pDCs and monocyte-derived DCs contribute to T cell responses indirectly by secretion of proinflammatory cytokines to boost and reinforce the adaptive response, which has been discussed in the subset introduction part (23, 74).

In the steady state without inflammatory stimulants, DCs can tolerize peripheral $CD4^+$ and $CD8^+$ T cells by inducing death, anergy or regulatory T cell (T_{Reg}) development (8). The tolerogenic DCs, residing in the secondary lymphoid organs, are essential for the inactivation of those autoreactive T cells that escaped from the thymic deletion. It is shown that negative selection in the thymus is not sufficient to eliminate all potentially pathogenic autoreactive T cells. Without deletion, those cells might be activated by the immunogenic mature DCs bearing both the self and foreign antigens during infection, resulting in auto-toxicity (75, 76).

2.2 $CD4^+$ T cell lineage differentiation

The tailoring of T cell responses consists of multiple events mediated by a vast number of different cell types. One of the key events involved is the T_H cell polarization to shape the secondary T cell responses (77). Upon interaction with antigen-presenting DCs, $CD4^+$ T cells differentiate into different effector subsets, including conventional T_H1 and T_H2 cells, the recently identified T_H17 cells,

follicular helper T (T_{FH}), and induced regulatory T (iT_{Reg}) cells. The differentiation into different subsets is driven by cytokines in the local environment (77, 78), and probably also the strength of antigen binding to T cell receptors (79). DCs contribute to the direction of T_H differentiation via secretion of tailored cytokines in response to particular pathogens detected by PRRs (9, 80).

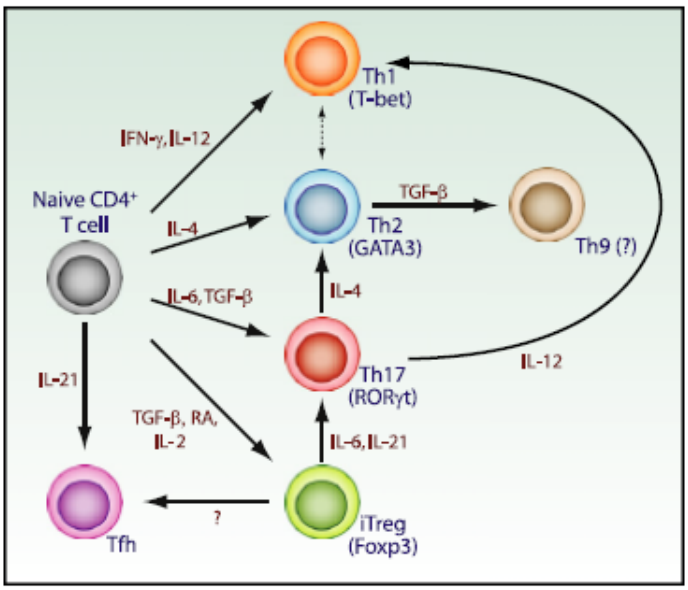

Figure 6: The lineage-determining cytokine milieu that drives $CD4^+$ T cell differentiation. The differentiation of T_H subsets is controlled by the local cytokine milieu. From the traditional view of T_H1 and T_H2 paradigm, IL-12 and IFN-γ support T_H1 fate, while IL-4 derives T_H2 cells. Recent studies revealed T_H17 population, which is driven by TGF-β and IL-6, whereas iT_{Reg} is by TGF-β, retinoic acid (RA), and IL-2. T_{FH} cell differentiation needs IL-21. Meanwhile, the differentiation of specific T_H subsets is orchestrated by their respective transcription factors: T-bet for T_H1 cells, GATA3 for T_H2 cells, RORγt for T_H17 cells, and Foxp3 for iT_{Reg} cells. More evidences illustrated the plasticity for convention of certain T_H subsets under cytokine stimulation. For example, switching of iT_{Reg} to T_H17 or T_{FH} cells has been identified. Besides, T_H17 cells can also convert to T_H1 or T_H2 cells. But the significance of the conversion of T_H2 to T_H9 is still to be discussed. (Zhou et al, 2009).

As shown in **Fig. 6**, the differentiation of T_H subsets is controlled by cytokines released by innate immune cells in the local microenvironment. In response, the

developed T_H effector cells release different cytokines to further modulate the adaptive immune responses (78). In the conventional T_H1/T_H2 paradigm model, the T_H1 cells are IFN-γ producers and involved in host defense against intracellular pathogens, whereas T_H2 cells produce IL-4, IL-5 and IL-13, and are involved in helminthes and other extracellular pathogens-induced immunity. The T_H1 lineage is driven by the IL-12 released by innate immune cells and IFN-γ from natural killer (NK) and T cells and is characterized by the transcription factor T-bet. In contrast, the T_H2 lineage is driven by IL-4 and involves the transcription factor GATA-3 (77).

However, more recent research expanded the T_H cells population with the newly identified T_H17, T_{Reg} and T_{FH} cells carrying different defense or regulatory functions. T_H17 cells produce IL-17A, IL-17F, IL-22 and their differentiation requires IL-6, TGF-β and the transcription factor retinoid-related orphan receptor (ROR)-γt (81). T_H17 cells are essential for the clearance of extracellular bacteria and fungi, especially at mucosal surface. T_{FH} cells are helpers of the maturation of B cell responses (82).

Besides the above mentioned effector types, T_H family also includes a regulatory population called regulatory T cells (T_{Regs}), which are important regulators in the immunity against self antigens and commensal microbes (83, 84). T_{Reg} cells are characterized by the expression of CD25 (the IL-2 receptor α chain, which is part of the high-affinity IL-2 receptor) and forkhead transcription factor (Foxp3), while the latter characterizes the T_{Reg} lineages (84). The T_{Reg} population includes two subtypes: the naturally occurring $CD4^+CD25^+$ T_{Reg} (nT_{Reg}) developed in the thymus and the TGF-β-induced iT_{Reg} cells in the periphery. The development of iT_{Reg} also needs signals from retinoic acid (RA) and IL-2. The T_{Reg} populations

participate in the regulations of peripheral tolerance for the prevention of auto-immune responses. The detailed mechanisms are still to be revealed (83).

It has longtime been considered that the differentiation of the T_H subsets is irreversible, while more recent data demonstrated a lineage plasticity that allows the conversion of certain T_H subsets to others (77, 85). Examples include the switch of iT_{Reg} to T_H17 cells in the presence of IL-6 and IL-21 (86, 87), and the conversion of T_H17 cells to either T_H1 or T_H2 with stimulation from IL-12 or IL-4, respectively (88) (**Fig. 6**). This plasticity might provide the host with a higher flexibility to fine-tune the defense with lifted specificity against certain invading pathogens (77).

2.3 The 'licensing' model for DC activation via T cells

The 'licensing' model was detected in the late 1990s. This model explains DC maturation signals delivered by T_H cells, for the elevated potency of DCs to mediate the CTL killing effects (89). As discussed, the steady state immature DCs express low levels of MHC and co-stimulatory molecules, which in combination mark their low immuno-stimulatory potency. Therefore, in the absence of strong inflammatory stimuli, an additional maturating signal is needed to further elevate the maturation status of DCs and eventually drive them into potent 'effector' DCs. In the proposed 'licensing' model, the maturating signal is delivered by T_H cells via CD40L-CD40 axis, in which the CD40 ligand (CD40L) on T_H cells bind to receptor CD40 on DCs for maturation stimulation (90-92).

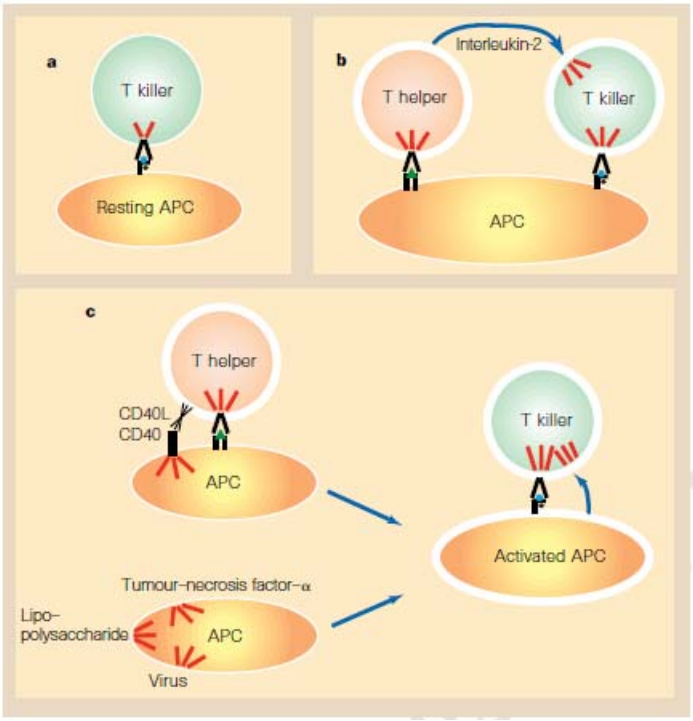

Figure 7: Antigen-presenting cells (APCs) need a licence to help T-killer cells. a, naïve $CD8^+$ T cells (T-killer precursors) recognize antigen on resting APCs, which do not provide enough signals for their activation. b, The traditional model assumed that the T helpers and T killers recognize antigen on the same APC. The activated T helper produces interleukin-2 which helps to activate the T-killer. c. In the new model, The APCs are licensed to activate T-killer cells by T helpers or by other stimuli. (Lanzavecchia, 1998).

The proposed model for the licensed help is given in **Fig. 7**. It was previously demonstrated that the activation of CTL responses needs the help from a T_H cell which binds to the same APC as the CTL (93). In the traditional model, the help is mediated by cytokines, e.g., IL-2 secreted by activated APC (**Fig. 7, b**). However, the data from Ridge, et al., Bennett, *et al.*, and Schoenberger *et al.* simultaneously suggested a more dynamic 'licensing' model for CTL activation with the help from T_H cells. In this model, the signal delivered from T_H cells, later proven to be CD40L which binds to CD40 on DCs, promotes the maturation of DCs. Upon activation, DCs upregulate the co-stimulatory molecules and secrete IL-12 and become potent activators for CTL responses. The maturation stimuli for DCs could also be TNF-α,

LPS, virus, etc. provided by invading pathogens or inflammatory responses (**Fig. 7, b**).

The signal provided by CD40 elevats the maturation status of DCs, sustains their IL-12 production, and enhances the antigen presentation via MHC I on DC surface. CD40L-CD40 ligation is revealed to be necessary for the induction of the combined $CD4^+$ T_H1 and $CD8^+$ CTL immunity (94). The $CD40^{-/-}$ DCs lose their ability to present the antigen well to $CD4^+$ and $CD8^+$ T cells although they still express high levels of surface maturation markers CD80 and CD86.

Besides this T_H-dependent DC maturation, viruses are often able to induce T_H-independent and CD40-independent CTL priming (95). $CD8^+$ T cells were later shown to mediate this CD40-independent maturation of DCs (96). According to Ruedl, *et al*. (1998), in the process of infection by lymphocytic choriomeningitis virus (LCMV), the virus-specific CTLs were able to elicit their own help *in vivo* to trigger the maturation of DCs. Surpringly, this maturation was triggered by $CD8^+$ T cells and not by the viral infection per se. This DC maturation could also be established by injection of specific peptides into a TCR-transgenic mouse. Moreover, this activation could be mediated *in trans*, leading to the widespread activation of DCs in the lymphoid organs, indicating the potentially soluble property of the cellular mediator involved in this interaction.

Using T cells or DCs derived from various genetically deficient mice combined with neutralizing antibodies or other blocking molecules, one could exclude, so far, known maturation stimuli, such as CD28, CD40L, TRANCE, TNF-α, IL-1, IL-6, IFN-α/β and IFN-γ. In addition, the function of the active factor(s) involved was shown to be MyD88-independent, thus TLR-independent since MyD88 is the necessary adaptor molecule involved in TLR-induced signaling pathway. In this

case, it would be interesting to isolate this soluble factor and furthermore to study its potential interactions with other stimuli for DC maturation.

Chapter II: Signaling integrations between different dendritic cell maturation stimuli

The maturation of DCs is a sophisticated process involving the regulated expression of thousands of genes controlling phagocytosis, the upregulation of costimulatory molecules and MHC molecules on the cell surface, chemokine receptor expression, the secretion of inflammatory cytokines and chemokines, and the capability to present antigens (97). Therefore, mature DCs are the most potent APCs capable to efficiently prime T cells. The resulting T cell polarization link the innate recognitions to adaptive responses (2, 38).

3 Signaling pathways involved in dendritic cell activation

The complicated DC maturation process described above could be stimulated by a vast repertoire of DC activators and may involve the integrated regulations of different signaling events. As previously described, the signaling through various PRRs induces a vast majority of cellular events delivered by multiple signaling pathways, including NF-κB pathway, MAPK pathway, NFAT pathway (41, 98). In addition, the inflammasome acts as a two-level-regulated molecular platform to release the potent proinflammatory cytokines during infection (46).

3.1 NF-κB signaling pathways

Nuclear factor (NF)-κB transcription factors are the key regulators involved in the inflammatory responses (99, 100). The genes regulated by NF-κB include the ones

coding for cytokines (e.g., IL-1, IL-2, IL-6, IL-12, TNF-α, LTα, LTβ, and GM-CSF), chemokines (e.g., IL-8, MIP-1α, MCP-1, RANTES, and eotaxin), adhesion molecules (e.g., ICAM, VCAM, and E-selectin), acute phase proteins (e.g., SAA), and also inducible effector enzymes (e.g., iNOS and COX-2) (101).

Functionally, NF-κB regulates gene expression in the nuclei of the cells by binding to discrete DNA sequences, called κB elements (102). Their family members include RelA (p65), RelB, c-Rel, p50/p105 (NF-κB1) and p52/p100 (NF-κB2). NF-κB1 and NF-κB2 are synthesized as large precursors, p105 and p100, that can be post-translationally processed to p50 and p52, respectively. The p50 and p52 proteins lack a transcription activation domain, while the other three contain the domain. The NF-κB proteins form numerous homo- and hetero-dimers that are associated with specific gene transcription profiles to regulate different biological responses. Generally, due to the lack of the transcription activation domain, p50 and p52 homodimers are repressors of gene expression, while dimers containing RelA or c-Rel are activators for transcription. In contrast, RelB retains a bigger regulatory flexibility, being able to either activate or repress the transcription (99, 100, 103).

In the steady state, NF-κB homo- or heterodimers form complexes with inhibitors of NF-κB (IκBs) thus are retained in the cytoplasm. IκBs include IκBα, IκBβ, and IκBγ. Stimulatory signals activate the IκB kinase (IKK) that in turn phosphorylates IκB and promotes its degradation. IKK is a complex composed of three subunits: IKKα, IKKβ, and IKKγ. IKKα and IKKβ are the catalytic subunits of the complex, while IKKγ is the regulatory subunit (101). With IκB degradation, the NF-κB dimers are thus released and translocate into the nuclei to regulate gene expression.

There are two major signaling pathways that lead to the NF-κB nuclear translocation, the canonical pathway and the non-canonical one (**Fig. 8**) (102, 103).

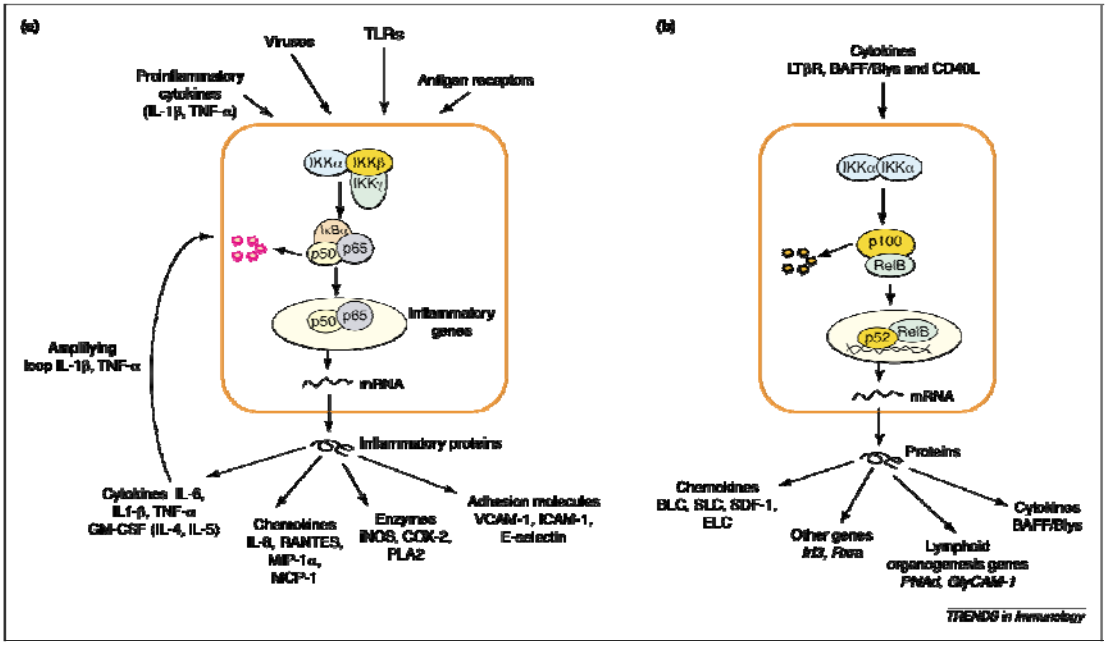

Figure 8: Canonical and non-canonical NFκB pathways. (a) The classical NF-κB pathway is activated by different inflammatory signals, resulting in the expression of inflammatory cytokines and other innate immune genes. The cytokines IL-1β and TNF-α, induced by NF-κB activation, form an amplifying feedback loop. (b) The non-canonical pathway for NF-κB results in nuclear translocation of p52–RelB dimers, is strictly dependent on IKKα homodimers and is activated by LTβR, BAFF and CD40L by NIK. BAFF, B-cell-activating factor belonging to the TNF family; BLC, B-lymphocyte chemoattractant; CD40L, CD40 ligand; COX-2, cyclooxygenase 2; ELC, Epstein–Barr virus-induced molecule 1 ligand CC chemokine; GM-CSF, granulocyte/macrophage colony-stimulating factor; ICAM-1, intercellular adhesion molecule 1; IKK, IκB kinase; IL-1β, interleukin-1β; iNOS, inducible nitric oxide synthase; LT, lymphotoxin; MCP-1, monocyte chemotactic protein-1; MIP-1α, macrophage inflammatory protein-1a; NIK, NF-kB-inducing kinase; PLA2, phospholipase 2; SDF-1, stromal cell-derived factor-1α; SLC, secondary lymphoid tissue chemokine; TLRs, Toll-like receptors; TNF-α, tumor necrosis factor α; VCAM-1, vascular cell adhesion molecule-1. (Bonizzi, 2004).

The canonical pathway is induced by the various inflammatory stimuli, including proinflammatory cytokines TNF-α and IL-1, engagement of the T-cell receptor

(TCR) or exposure to the microbial components such as LPS (**Fig. 8, a**) (104). In this pathway, the IKK complex that contains three core subunits, IKKα, IKKβ and IKKγ, transduces the activation signals, while IKKβ plays the most important role. In response, IκBα is rapidly phosphorylated and degraded. IκBβ and IκBε respond slower. In the canonical pathway, the most common NF-κB dimers are p50-RelA heterodimers. With translocation into the nuclei, they induce the transcription of genes encoding chemokines, cytokines, adhesion molecules, enzymes that produce secondary inflammatory mediators and inhibitors of apoptosis, which in combination are important for phagocytosis and inflammatory responses in innate immunity.

In contrast, the non-canonical pathway is activated by stimuli including CD40 and lymphotoxin-β receptors, B-cell-activating factor of the TNF family (BAFF), LPS and latent membrane protein-1 (LMP1) of Epstein-Barr virus, etc (**Fig. 8, b**) (100, 103). In this mechanism, the activation of IKKα by the NF-κB-inducing kinase (NIK) results in the formation of p52 from the inactive form p100. The active p52 then binds to RelB to form a heterodimer, which has high affinity to bind to κB elements and to regulate gene transcription. The non-canonical pathway is regulated by the IKKα homodimers and is independent of the IKK heterotrimer complex. The non-canonical pathway plays an important role in the transcription of genes encoding chemokines, cytokines, and other regulators that are involved in the development of secondary lymploid organs, thus functions in the regulation of the adaptive immunity (105).

3.2 MAPK signaling pathways

Mitogen-activated protein kinase (MAPK) cascades are universal signal transduction modules that are highly conserved among species. The core unit of this cascade includes three members, a MAPK kinase kinase (MKKK), a MAPK kinase (MKK), and a MAPK (106, 107). In response to chemical or physical stresses, the different members of MKKKs are activated. MKKKs are serine/threonine kinases, which phosphorylate and activate MKKs to transduce the signaling downstream. The activated MKKs are dual specificity kinases which then phosphorylate both tyrosine and threonine residues on MAPKs for activation. In vertebrates, the most extensively studied MAPK cascades include extracellular signal-related kinase (ERK1/2), Jun amino-terminal kinase (JNK1/2/3) and p38 proteins (p38α/β/γ/δ), whose activation and impact on cellular processes are under tight control of the signaling cascades with details been reveled (**Fig. 9**). Other so far identified MAPK members include ERK7/8, ERK3/4 and ERK5, but their functional regulations are yet unclear (107-109).

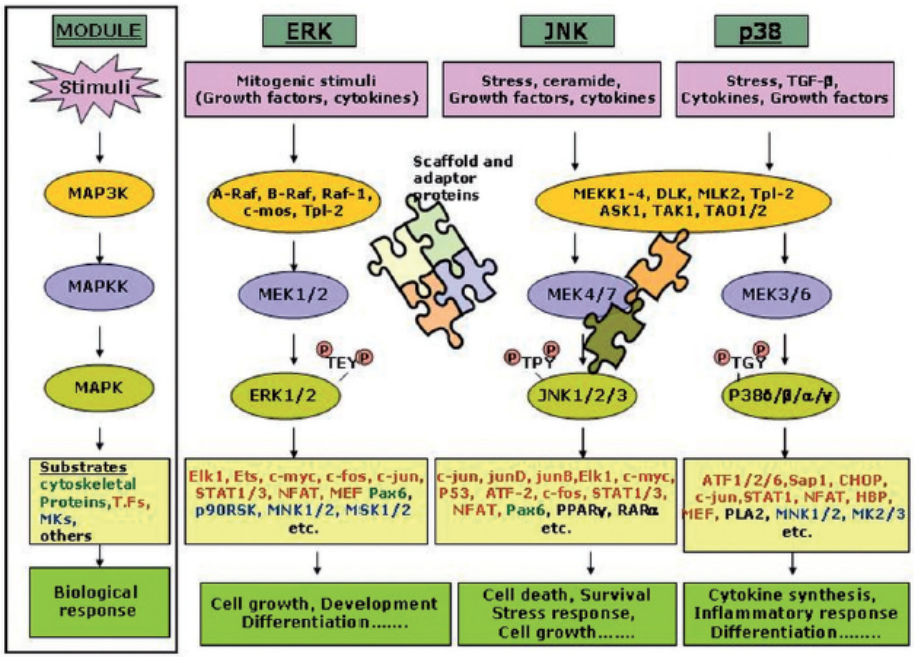

Figure 9: Mitogen-activated protein kinase cascades. The MAPK module consists of a MKKK, a MKK, and a MAPK. In response to a variety of extracellular signals, MKKK initiates the signaling cascade involving a series of phosphorylation events that activates MAPK, which in turns activates the transcription factors controlling cellular responses including growth, differentiation, and apoptosis. (Krishna and Narang, 2008).

Specificity of MAPK responses is achieved by activation of different cascades. The activation stimuli include growth factors, hormones, cytokines and cellular stresses, e.g., irradiation, heat shock, osmotic imbalance, DNA damage and bacterial products. In response to these diverse stimuli, the MKKKs contain diverse members. This MKKKs diversity is maintained by employing different defined regulatory motifs, which help them to be differentially regulated by the upstream inputs, while these motifs are not found in MKKs or MAPKs. In contrast, the variety of MKKs and MAPKs is less, so that the coupling of MKK-MAPK is quite consistent, e.g., ERK1/2 is regulated by MEK1/2, JNK1/2/3 is regulated by MKK4/7, p38 members are coupled to MKK3/6, and ERK5 is under MKK5 regulation (**Fig. 9**) (106, 107).

The transcription factors involved in these responses normally belong to activator protein 1 (AP-1) family that consists three subfamilies: Jun, Fos, and ATF-2. Regulation of AP-1 members involves different MAPKs. In the regulation, different MAPK members may have overlapping functions. For example, c-Jun is regulated by both JNK and ERK, c-Fos is a substrate for ERK, while ATF-2 is phosphorylated by JNK and p38 (110). ERKs are stimulated by growth factors, neurotrophins, and phorbol esters. Its three level signaling cascades involve Raf (MKKK), MEK (MKK), and ERKs. The c-Jun amino-terminal kinases (JNKs), also known as stress-activated protein kinases (SAPKs), were first known as kinase responsible for phosphorylation of transcription factor c-Jun. Other transcription factors activated by JNKs are ATF-2 and Elk-1 (111). ATF-2 and Elk-1 are also substrates for p38, while the other targets of p38 include MAPLAP kinase and Max. Signaling of p38 might be involved in the negative regulation of cell proliferation (109, 112).

In general, ERK signaling is involved in the control of cell proliferation and differentiation, while JNK and P38 mediate responses to cellular stresses, such as cell damage repair, cell growth arrest and cell death (109, 110). With the complicated regulations of signaling cascades involved in MAPK pathways, crosstalk between different members exists to fine-tune their functions. For example, the pro-survival ERK pathway may play a role of balancing the pro-apoptotic JNK pathway (113).

In addition, other signaling pathways can modulate the functions of MAPK signaling cascades. Examples include Rac1/CDC42-PAK1 cascade, PI3K-PDK-Akt pathway and NIK-IKK-NF-κB pathway (109). To illustrate, the PI3K-PDK-Akt pathway activates protein kinase C (PKC), which in turn activates Raf. As the key player of ERK signaling, Raf potentiates the ERK signaling upon activation.

Besides, the Rho subfamily members Rac1 and cdc42 regulate JNK and p38 rather than ERK possibly through adaptor PAK1 (114).

3.3 NFAT signaling pathways

The nuclear factor of activated T cells (NFAT) was first identified as an inducible nuclear factor that could bind to the IL-2 promoter in activated T cells (115). More recent finding demonstrated the roles of NFAT proteins in other cells rather than T cell only (116). Although their expression is among diverse organs, the function and regulation of NFAT proteins are best studied in immune cells (117, 118).

The NFAT family has five members: NFAT1 (or called NFATp or NFATc2), NFAT2 (NFATc or NFATc1), NFAT3 (NFATc4), NFAT4 (NFATx or NFATc3) and NFAT5. All members have a highly conserved DNA-binding domain, called REL-homology region (RHR), which is structurally related to the one contained in the REL-family transcription factors. The only non-calcium-regulated NFAT protein is NFAT5, which controls the osmotic stress responses, while the mechanism we going to discuss here is based on the calcium-dependent members (116-118).

The activation of NFAT is induced by the engagement of receptors that are coupled to the calcium-signaling pathway that eventually activates calmodulin after a series of signaling transduction events. The activated calmodulin then activates the calmodulin-dependent phosphatase calcineurin. This phosphatase dephosphorylates NFAT from their steady state phosphorylated form and induces their activation. The activated NFATs then migrate to the nuclei and induce the NFAT-mediated gene transcription. In the nuclei, the NFAT proteins can interact with different

transcription factors with functional integrations. The AP-1 family transcription factors, c-Fos and c-Jun, are their main partners (119). Upon interaction, they play various roles involved in immune regulations including T cell anergy, DC maturation, B cell responses, etc (116).

3.4 Inflammasome

The inflammasome is a special platform associated with the activation of NLR signaling. The NLRs are normally cytosolic proteins that function as intracellular PRRs, which may eventually induce the NF-κB activation and adaptive immune responses (48, 120). The recognition of molecules from invading pathogens or damaged host cells by NLRs may lead to the activation of caspase-1 through the assembly of a cytosolic protein complex. This complex is called inflammasome which induces the proteolytic processing of pro-caspase-1 to its active form (46, 121).

The different inflammasomes slightly vary in their components and functions (122), while the major one involved in innate immunity is NLRP3 inflammasome consisting of the intracellular adaptor protein ASC (apoptosis-associated speck-like protein containing a CARD) and the receptor NLRP3 (NACHT-, LRR- and pyrin-domain containing protein 3), together with pro-caspase-1 and caspase-11 (46, 123).

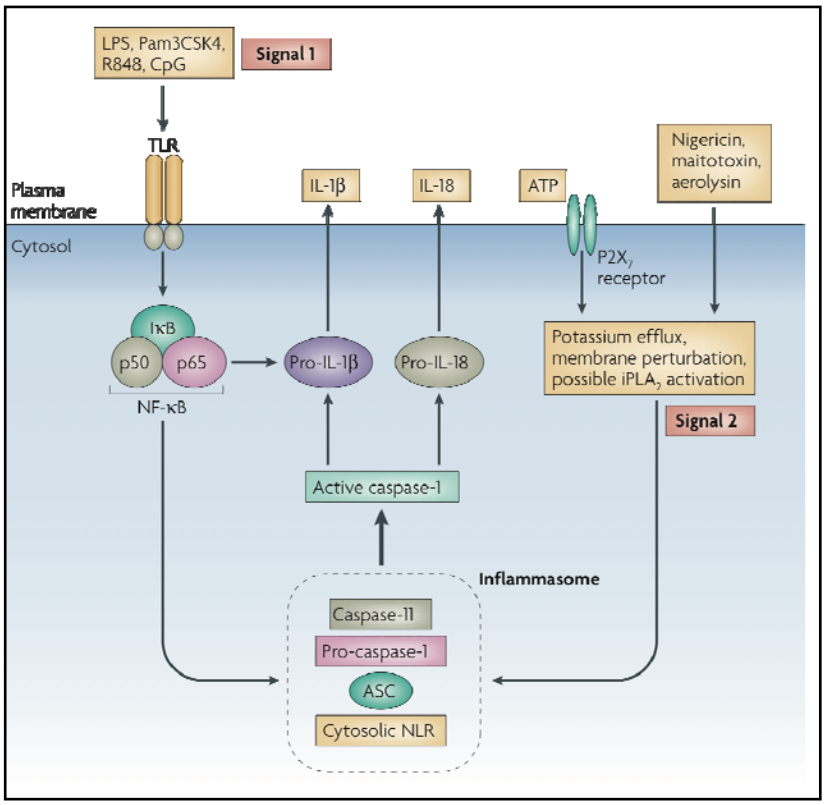

Figure 10: Activation signals for IL-1β release. The activation of IL-1β needs two signals. The first signal is the stimulation from TLRs for the synthesis of pro-IL-1β. In mice, macrophages and dendritic cells express ASC and pro-caspase-1 constitutively, but not caspase-11, which is also upregulated by TLR stimulation. The second signal is delivered by "danger signals" which cause membrane blebbing and pore formation. The danger molecules, including ATP, nigericin, maitotoxin and aerolysin, cause ionic perturbations, specifically potassium efflux. Possibly with activation of calcium-independent phospholipase A2 (iPLA2), this ionic change mediates IL-1β processing. (Mariathasan, 2007).

It is generally accepted that the activation of IL-1β needs two signals (**Fig. 10**). The first signal is delivered by TLRs for the synthesis of pro-IL-1β. In mice, macrophages and dendritic cells express ASC and pro-caspase-1 constitutively, but not caspase-11, which is also upregulated by TLR stimulation. The second signal is given by "danger signals" which cause membrane blebbing and pore formation. The danger molecules, including ATP, nigericin, maitotoxin and aerolysin, cause ionic perturbations, specifically potassium efflux. Possibly with the involvement of

calcium-independent phospholipase A2 (iPLA2) activation, this ionic change mediates IL-1β processing (46, 121). More recent data revealed the existence of multiple models for NLRP3 inflammasome activation rather than potassium efflux pathway only (124, 125).

4 Signaling via GM-CSF receptor

Granulocyte-macrophage colony-stimulating factor is a cytokine that is known to stimulate proliferation, differentiation and survival of various hematopoietic cells (126). More recent studies focus on its roles in the regulation of the development and remodeling of the myeloid cells of the granulocyte and macrophape lineages, particularly during host defense and inflammatory reactions. It is produced by almost all tissues and organs and by various cell types such as activated T cells, macrophages, endothelial cells and fibroblasts in response to cytokines, antigens and other inflammatory stimuli (127).

GM-CSF receptors (GM-CSFRs) contain two subunits, α and β, both of which belong to the cytokine receptor superfamily. The β subunit, also called common β subunit (βc), is shared by IL-3, IL-5 and GM-CSF receptors. In contrast, the α subunit is specific for each cytokine receptor (128). The α subunit, by itself, binds to the specific cytokine with low affinity, while in combination with the non-ligand binding βc, they form a high affinity receptor. Further studies show that this βc is the major player in the signaling transduction of these receptors (129).

GM-CSFR activation is associated with receptor dimerization and tyrosine phosphorylation of cytoplasmic domains (130). The receptor itself does not have

intrinsic tyrosine kinase function, and the tyrosine kinase Janus kinase 2 (JAK2) acts as the adaptor to phosphorylate the βc (131). The rapid tyrosine phosphorylation then activates the adaptors Ras, Raf-1 and the downstream MAPKs. The transcription factors induced by MAPKs here are c-myc, c-fos, and c-jun. Cytoplasmic deletion mutants of βc domain showed that the signal transduction of GM-CSFR involves two distinct cytoplasmic regions on βc (129, 132). One membrane proximal region is responsible for induction of transcription factors c-myc and pim-1. This induction signaling is mediated by JAK2 that binds to βc directly. The signal transducer and activator of transcription 5 (STAT5) then transduces the induction signals further downstream. STAT5 forms a DNA-binding complex and functions in the nucleus. In contrast, the membrane distal region is stimulating the MAPK cascades involving the activation Ras-Raf-1, followed by activation of transcription factors c-fos and c-jun. Additionally, the latter is probably involved in the PI3K activity (129). However, the detailed events involved in these signaling transductions are still unrevealed.

Although the GM-CSFR α subunit is not involved in the binding of JAK2 for signaling transduction directly, its involvement in GM-CSF signaling transduction for cell growth and differentiation has been identified (133). Crystallographic studies suggested that, although lacking an efficient cytoplasmic domain, the GM-CSFR α subunits, with the bound GM-CSF ligands, might form the dodecamer complex with βc subunits that can eventually transduce signals through JAK2 (131).

More studies linked the JAK2-mediated signaling transduction to the activation of both ERK, which is the key member of the MAPK pathway, and the Akt, which is the signaling molecule in the PI3K pathways, for gene transduction (134, 135).

Besides, evidences revealed the roles of a Src-like adaptor protein (SLAP) in the regulation of GM-CSF signaling (136).

5 Signaling via myeloid C-type lectin receptors

C-type lectins are a large family of proteins that are highly conserved in vertebrates. They are defined as any protein containing one or more C-type lectin domain(s). The term C-type lectin was first introduced as Ca^{2+}-dependent carbohydrate binding lectins. The CLR family was then expanded to the receptors with C-type lectin domain homologs (137). CLRs include both soluble and transmembrane members. Although not all CLRs function as PRRs to participate in innate pathogen recognition, some of them do promote phagocytosis and induce cytokine production in macrophages, DCs and other leukocytes (138).

As introduced previously CLRs are non-TLR type of PRRs (9, 139). They may function to modulate the TLR signaling during the immune responses (140-142). Besides, the CLR signals also directly induce cytokine gene expression via NF-κB pathways, allowing the further modulation of the $CD4^+$ T cells differentiation into both T_H1 and T_H17 lineages for antifungal defense (51, 80, 87, 143). More and more evidences suggested the important roles of CLR-triggered signaling events in the modulations of both innate and adaptive immune responses (80, 144).

CLRs expressed by DCs recognize most classes of human pathogens. The PAMPs involved in their recognition include mannose, fucose and glucan carbohydrate. The CLRs may trigger the diverse immune responses via complex signaling processes which also include crosstalk with other PRRs (80). Generally, they are categorized into four groups (**Fig. 11**) (98, 144). The CLRs bearing a

hemITAM (immunoreceptor tyrosine-based activation motif) on their cytoplasmic tails, which allow them to bind to Syk kinase directly for signaling transduction, are among the best-examined CLR group with clear regulatory functions revealed in both innate and adaptive immunity. Different from ITAM that has tandem dual YxxL motifs, the hemITAM contains only a single YxxL motif for Syk recognition (139). Dectin-1 is a typical representative in this group which is widely employed for the functional studies (54). The second group associates with and induces signaling pathways through ITAM-containing adaptor molecules, such as Fc receptor γ-chian (FcRγ) or DAP12. The adaptors allow their binding to Syk kinase thus the downstream signaling transduction. Members in this group include macrophage-inducible C-type lectin (mincle), dectin-2, blood DC antigen 2 protein (BDCA2), etc. Besides these myeloid activating members, the third group mediates inhibition of myeloid functions and is common in NK cells. They bear an immunoreceptor tyrosine-based inhibitory motif (ITIM) on the cytoplasmic tails to recruit SHP-1, SHP-2, and SHIP phosphatases rather than kinases (98, 145). Last but not least, the tyrosine-based signaling-independent CLRs modulate the cell activation in a so far unidentified mechanism (80).

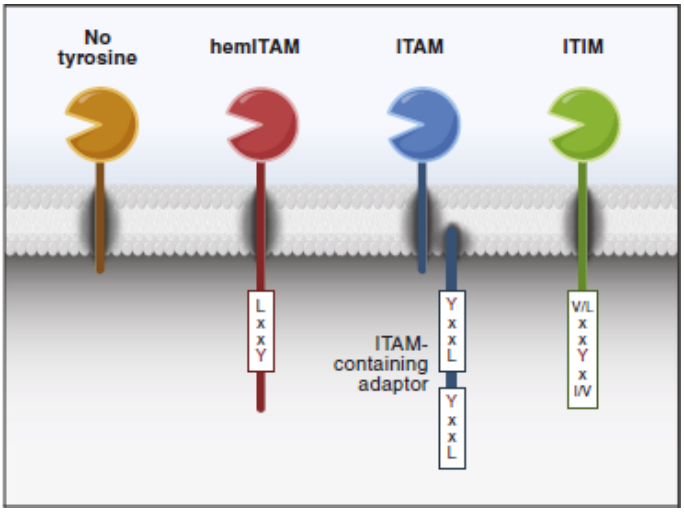

Figure 11: Distinct myeloid CLR groups bearing different tyrosine-based signaling motifs. Myeloid CLRs can be classified by their employment of different tyrosine-based motifs for signaling transduction. The CLRs recruit signaling kinases via hemITAM directly or through binding to ITAM-bearing adaptors. ITIM-containing CLRs may inhibit myeloid cell activation by coupling phosphatases. The so far identified last group of CLRs function through the nontyrosine-based signaling pathways. (Osorio and Reis e Sousa, 2011).

The key signal mediator, Syk kinase, was previously known as a signaling molecule downstream of B-cell receptor for executing of adaptive immune responses. Syk is then found to be the key adaptor for signaling of many CLRs, possibly with the help from some other adaptor molecules, bearing Syk-binding motif. The signaling transduction downstream of Syk consists of complicated events mediated by different signaling cascades. Take Dectin-1 signaling as an example, adaptors CARD9 (caspase recruitment domain family, member 9), BCL-10 (B cell lymphoma 10) and MALT1 (mucosa-associated lymphoid tissue lymphoma translocation gene 1) form a scaffold complex to activate the NF-κB pathway for the induction of inflammatory cytokines, which will be explained in more details in the next part (80).

Dectin-1 recognizes the exogenous β-glucan, a component of the fungal and bacterial cell walls. The formally employed Dectin-1 agonist is zymosan, which is

the raw extract from the yeast cell walls. However, as a crude preparation, zymosan is a complex product containing multiple ligands, e.g., glucans, mannan, proteins, chitin and glycolipids (146). Therefore, besides the Dectin-1 signaling induction, it also triggers the activation of TLR-2 signaling cascade (147). In order to have target-specific Dectin-1 activation, curdlan, a linear β-1, 3-glucan (148), is used as a purified preparation of Dectin-1 agonist. Curdlan induced dendritic cell activation, marked by elevated expressions of both costimulatory molecules and inflammatory cytokines, is MyD88-independent but Dectin-1-dependent (51), which excludes the potential involvement of TLR signaling effects in its functions.

The Syk-coupled Dectin-1 signaling plays a key role in the innate responses through the production of reactive oxygen species (ROS) (149) and activation of multiple signaling pathways, including NF-κB pathway (52, 54), MAPK pathway and NFAT pathway, for induction of inflammatory cytokines (150) (**Fig. 12**). Dectin-1 is unique in CLRs as the first one to be identified to activate both the canonical and non-canonical NF-κB pathways (80). In the Syk-dependent signaling transduction, the scaffold complex, CARD9-BCL10-MALT1, induces the NF-κB activation, probably through the recruitment of TNF receptor-associated factor 2 (TRAF2)-TRAF6 complex. The elevated signaling transduction stimulates the activation of canonical NF-κB subunits p65 and REL and their efficient translocation into the nuclei (143). In contrast, in the non-canonical pathway, the NF-κB heterodimer RelB-p52 is activated through the activation of NF-κB-inducing kinase (NIK) and IκB kinase-α (IKKα). How the signaling transduction happens in the non-canonical pathway remains unclear (143).

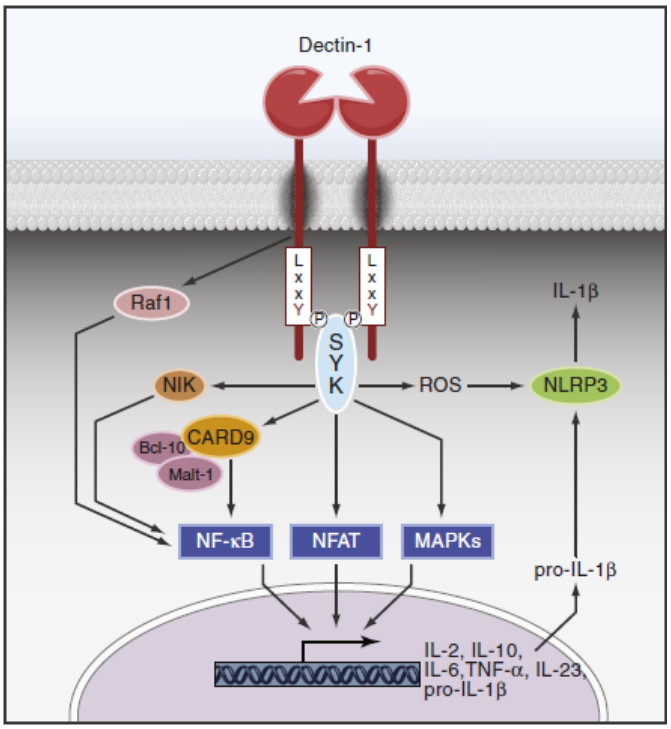

Figure 12: Dectin-1 signaling transduction. Upon ligand binding, the Dectin-1 receptor mediates signaling transduction via events possibly involving the receptor dimerization, which trigger the phosphorylation of the hemITAM motifs by Src family kinases and the follow up recruitment and activation of Syk. The Syk-dependent signaling induces activation of NF-κB, MAP kinase, and NFAT pathways, for the regulation of innate gene expressions. Besides, the Raf-1 transduces signals in a Syk-independent manner, but the signaling integrates with the Syk-induced signaling at the NF-κB levels. (Osorio and Reis e Sousa, 2011).

In addition to the Syk-dependent signaling pathway, Dectin-1 induces a second signaling pathway that involves the Raf-1 activation (143). Although Raf-1 does not interact with Syk for its activation, its signaling eventually combines to Syk signaling at the NF-κB levels. The Raf-1 activation triggers the phosphorylation of Syk-induced p65 at Ser276, and this phosphorylation event induces the acetylation and elevated transcriptional activity of p65, resulting in the induction of IL-6, IL-10, and IL-12 transcription (140). With controlling both the Syk- and Raf-1-dependent

signaling, Dectin-1 is able to fine-tune other NF-κB induced cytokines, including IL-1β and IL-23, for the potentiated T_H cell differentiation efficacy.

Dectin-1 recognizes a number of fungal species and plays an important role in antifungal immunity. This defense is associated with the T_H1 responses and fungicidal mechanisms of phagocytic cells, such as respiratory burst. In addition, the killing is coupled with the production of protective inflammatory cytokines and chemokines, including TNF and CXCL2 (151). It was suggested that the Dectin-1 induced IL-10 and IL-2 are involved in the development of regulatory T cell responses. With this regulatory function, Dectin-1 signaling might modulate the immune responses via limiting the inflammatory pathogens and promoting the fungal persistence for a long-term immunity.

AIM

The major goals of this thesis were:

(1) To characterize a still unidentified dendritic cell-targeted immunostimulant released by activated T cells (herein referred to simply as TCF).

(2) To decipher the nature of potential intracellular signals triggered by the identified TCF (GM-CSF) and the β-glucan curdlan.

MATERIALS AND METHODS

1 Materials

1.1 Mice

C57BL/6 WT mice were purchased from the animal facility, National University of Singapore (Singapore). OVA-specific OT1 and OT2 BL/6 and GM-CSFR$^{-/-}$ BL/6 mice were purchased from the Jackson Laboratory (Bar Harbor, ME) and breed in the animal facility, School of Biological Sciences, Nanyang Technological University.

1.2 Cells

The T cells lines A5, BEKO and EL4 were given by Prof Klaus Karjalainen and maintained in the medium SF-IMDM with 2% FCS at 37ºC.

NUP98-HOX B4 transduced bone marrow cells were established by transducing bone marrow cells with retroviral vectors carrying NUP98-HOX B4 fusion gene.

1.3 List of reagents

Name	Company	Note
Acetic acid	Merck	
Acrylamide	Bio-Rad	
Ammonium bicarbonate	Sigma-Aldrich	
Ammonium chloride	Sigma-Aldrich	0.89% solution and antoclave
ATP	InvivoGen	In endotoxin-free H_2O
BSA	Sigma-Aldrich	
Chloroform	Fisher	
CpG	Alexis	In endotoxin-free H_2O
Curdlan	Wako	Prepared in 0.15 N NaOH
EDTA	Fluka	500 mM stock solution
EGTA	Sigma-Aldrich	500 mM stock solution
Endotoxin-free H_2O	Sigma-Aldrich	
Endotoxin-free OVA	Hyglos	
Ethanol	Merck	
Fat-free milk powder	Bio-Rad	
Fetal Bovine Serum	GibcoBRL	2% in SF-IMDM medium
Glycine	Bio-Rad	
GM-CSF	BioLegend	
HEPES	Sigma-Aldrich	
Iscove's modified Dulbecco's medium	Sigma-Aldrich	
β-mecaptoethanol	Sigma-Aldrich	
Methanol		
Nonidet P-40	Merck	10% stock solution
LPS	Sigma-Aldrich	In endotoxin-free H_2O
OptiPrep	Sigma-Aldrich	
Paraformaldehyde	Merck	
Poly(I:C)	Sigma-Aldrich	In endotoxin-free H_2O
Potassium chloride	Merck	
Proteinase K	Promega	
Sodium chloride	Sigma-Aldrich	
Sodium	Sigma-Aldrich	10% stock solution
Sodium fluoride	Sigma-Aldrich	
Sodium orthovanadate	Sigma-Aldrich	100 mM stock solution
Sodium pyrophosphate	Sigma-Aldrich	
Sucrose	MP Biomedicals	
Tris	Bio-Rad	
Triton X-100	Merck	
Trizol	Invitrogen	
Trypsin	Promega	
Tween-20	Sigma-Aldrich	
Zymosan	Sigma-Aldrich	In endotoxin-free H_2O

1.4 List of primary antibodies for signaling molecules

Name	Company	Catalog Number	Species	Dilutions
α-c-Rel	Santa Cruz	sc-71	Rabbit	1:500
α-caspase-1	Santa Cruz	sc-514	Rabbit	1:200
α-caspase-11	Biolegend	647201	Rat	1:500
α-ERK	Santa Cruz	sc-153	Rabbit	1:1000
α-p ERK	Santa Cruz	sc-7976	Goat	1:1000
α-IκBα	Cell Signaling	9242	Rabbit	1:1000
α-p IκBα	Cell Signaling	2859S	Rabbit	1:1000
α-IL-1β	R&D	MAB4011	Rat	1:500
α-p JAK2	Cell Signaling	3771	Rabbit	1:1000
α-JNK	Cell Signaling	9252	Rabbit	1:1000
α-p JNK	Invitrogen	44682G	Rabbit	1:1000
α-NLRP3	Alexis	804-881-C100	Mouse	1:1000
α-p38	Cell Signaling	9212	Rabbit	1:1000
α-p p38	Cell Signaling	9215	Rabbit	1:1000
α-PAK1	Cell Signaling	2602	Rabbit	1:1000
α-p PAK1	Cell Signaling	2601	Rabbit	1:1000
α-PLCγ2	Cell Signaling	3872	Rabbit	1:1000
α-p PLCγ2	Cell Signaling	3874	Rabbit	1:1000
α-p STAT5	Cell Signaling	9359	Rabbit	1:1000
α-Syk	Cell Signaling	2712	Rabbit	1:1000
α-p Syk	Cell Signaling	2710	Rabbit	1:1000
α-tubulin	Santa Cruz	sc-32293	Mouse	1:1000
α-USF-2	Santa Cruz	sc-862	Rabbit	1:500

All secondary antibodies (α-Rabbit, α-Mouse α-Rat and α-Gout) used in Western blotting were purchased from BioLegend (San Diego, CA) and used in the dilution 1:1000.

2 Immunological methods

2.1 Isolation of T cells

T cells were isolated from spleens and lymph nodes of BL/6 mice. The cells were first prepared by smashing the organs through a sieve and resuspended into PBS solution with 2% FCS. The T cells were then purified from the total cell suspension by using either MACS (magnetic-activated cell sorting) or panning experiments.

2.1.1 MACS separation

MACS columns, microbeads and separators were purchased from Miltenyi Biotec (Bergisch Gladbach, Germany). The microbeads with tagged antibodies used to isolate T cells were α-CD4, α-CD8α, and α-Thy1.2.

Following the manufacturer's instruction, the cell suspension was first incubated with the microbeads. 100 µl beads solution was added into 10^6 cells. The mixed samples were incubated for 30 min at 4ºC. The cells were then washed once with PBS 2% FSC and applied through the MACS column in MACS buffer (PBS with 2% FCS and 2 mM EDTA, pH 7.2). After washing three times with MACS buffer, the cells were eluted into 5 ml MACS buffer and washed once using the medium for the next step experiment.

2.1.2 Panning experiment

In panning experiments, we pre-coated the Petri dishes (Greiner) with α-MHC class II antibodies. The antigen-presenting cells (APCs) bind to the α-MHC II antibodies after incubation at 4°C for 2 h. Supernatant was collected with gentle shaking.

2.2 Bone marrow-derived dendritic cells

Bone marrow cells were isolated from the BL/6 mice. The erythrocytes lysis was done using 0.89% Ammonium Chloride for 10 min at room temperature. The progenitor cells were recovered by centrifugation and resuspended into medium (SF-IMDM, 2% FCS) supplemented with FLT3L (100 ng/ml). The cell suspension was then distributed into dishes (100 mm × 20 mm, Corning), 20×10^6 cells in 15 ml medium per dish. The cell culture was incubated at 37°C with 7% CO_2. After 3-4 days, 5 ml fresh medium supplemented with FLT3L was added. The cells were harvested at day 7.

2.3 DC activation assay

The FLT3L-derived bone marrow dendritic cells were collected and distributed into 96-well round-bottom plate, 0.3×10^6 cells/well in 100 µl medium (SF-IMDM, 2% FCS). Another 100 µl of sample-containing medium was added into each well to stimulate the DCs. The cells were then incubated at 37°C with 7% CO_2 for 24 h.

After incubation, the cells were recovered by centrifugation and stained with PE-conjugated α-CD80 or α-CD86 antibodies (BioLegend) for 20 min at 4ºC. The stained cells were washed and resuspended into PBS with 2% FCS and analyzed by FACSCaliber^{TM} flow cytometer (Beckton Dickinson). The mean value of fluorescence intensity was calculated in order to visualize the surface expression of both CD80 and CD86, reflecting the DC maturation levels.

2.4 T cell activation and preparation of serum-free supernatant containing T cell factor (TCF) in large-scale

The MACS isolated T cells were washed twice by serum-free Iscove's modified Dulbecco's medium (IMDM) and resuspended in solution, which was then distributed into the 12-well plate pre-coated by α-CD3 and α-CD28 antibodies, 10×10^6 cells in 2 ml IMDM per well. After 24 h incubation at 37ºC with 7% CO_2, the medium was collected gently while avoiding the cell debris at the plate bottom. The supernatant was further purified by centrifugation then filtration with 0.2 μm filters to remove cell debris.

For A5 cell activation, the cultured A5 cells were washed and resuspended in serum-free IMDM medium and put into the α-CD3/CD28 pre-coated Petri dishes, 20×10^6 cells in 20 ml per dish. The culture was incubated at 37°C with 7% CO_2 for 24 h. The supernatant was then collected and cells were removed by centrifugation and then 0.2 μm filtration. The BEKO and EL4 cells were used in the same way as the A5 cells.

2.5 Isolation of splenic DCs

The spleens were taken from BL/6 mice and smashed across the sieve. The cells were digested with Collagenase D (1 mg/ml) (Sigma-Aldrich) for 1 h at 37ºC. The digested cells were then enriched using OptiPrep (Sigma-Aldrich) gradient centrifugation at room temperature at 650 g for 10 min. The clear cell layer at the interface between the OptiPrep and medium were carefully collected and recovered by centrifugation and resuspension into normal medium. The recovered cells were stained with α-CD11c and α-CD8 and then sorted using FACSCalibur™ flow cytometer (Beckton Dickinson, USA).

2.6 Isolation of NKT, DETC and γ/δ T cells

The NKT cells were isolated from the livers of the BL/6 mice. Livers were cut and smashed across the sieve. The cells were resuspended into medium with 2% FCS and digested with Collagenase D (1 mg/ml) (Sigma-Aldrich) for 1 h at 37ºC. The digested cells were then enriched using OptiPrep (Sigma-Aldrich) gradient centrifugation at room temperature at 650 g for 10 min. The clear cell layer at the interface between the OptiPrep and medium were carefully collected and recovered by centrifugation and resuspension into normal medium. The recovered cells were stained using α-NK1.1 and α-Thy1.2. The NKT cells were collected by flow cytometer.

The DETC and γ/δ T cells were isolated from the ear skin epidermal layers and spleens, respectively. Widetype BL/6 mice were used in the experiments. For DETC

isolation, the cells were stained by both α-Thy-1 and α-γ/δ TCR. For γ/δ T cell isolation, the cells were stained by α-γ/δ TCR. The cells were sorted by FACSCalibur^{TM} flow cytometer (Beckton Dickinson, USA).

2.7 Blocking experiments

T cells were isolated from WT or and stimulated on α-CD3/CD28 pre-coated plates or with 10^{-6} M SIINFEKL or 10^{-6} M OVA-pulsed DCs in co-culture. BMDCs were derived by FLT3L from WT or GM-CSFR$^{-/-}$ BL/6 mice and stimulated with T cell factor (TCF)-containing supernatant, recombinant GM-CSF (BioLegend, San Diego, CA), LPS, polyinosinic:polycytidylic acid [poly(I:C)], zymosan (all from Sigma-Aldrich), and CpG [ODN 1668, TLRgrade, Alexis (Enzo Life Sciences, Farmingdale, NY)] at their respective concentration indicated in the corresponding figure legend. The reagents were suspended in endotoxin-free water (Sigma-Aldrich). The endotoxin-free OVA peptides were purchased from Hyglos (Regensburg, Germany).

2.8 Co-culture experiments

For the co-culture experiment using both wildtype (WT) and GM-CSFR$^{-/-}$ (KO) DCs, a 50:50 mixture of FLT3L-derived BMDCs (Ly5.1^{+} WT and Ly5.1^{-} KO) was pulsed with SIINFEKL and put into co-culture with OVA-specific CD8^{+} T cells from OT-1 mice. Cells were triple-stained with Ly5.1, CD11b, and CD80/CD86.

Neutralizing α-GM-CSF and α-CD40L antibodies were purchased from BioLegend (USA). GM-CSF and IL-2 released from activated T cells were detected by ELISA kits (BioLegend, USA).

2.9 Proliferation assay

The *ex vivo*-isolated splenic DCs were sorted into $CD11c^+CD8^+$ and $CD11c^+CD8^-$ population. The sorted cells were stimulated in the absence or presence of 10 ng/ml recombinant GM-CSF for 24 h. The cells were then washed and pulsed with OVA for 30 min at 37ºC. Naïve $CD4^+$ T cells isolated from OT2 BL/6 mice were put into co-culture with pulsed DCs and incubated at 37ºC with 7% CO_2. 72 h later, T cell proliferation was visualized by thymidine incorporation in a 16 h pulse.

3 Proteomics approaches

3.1 Sample concentration

The starting material (500-1000 ml), serum-free supernatant collected from the activated T cells, was concentrated by Centricon (10 kDa Cut-off, Millipore) into 1 ml solution, followed by ultracentrifugation at 80,000 rpm for 1 h. Supernatant was carefully taken out and desalted by PD-10 column (GE Healthcare). The H_2O dissolved sample was then frozen at -80°C for 1 h and lyophilized by lyophilizer (FreezeMobile) overnight.

3.2 Silver staining

The SDS-PAGE was run at 80 V for 15 min followed by 100 V for 1 h. The gel was then fixed with fixation buffer (50% Methanol, 12% acetic acid) for 2 h at room temperature. The fixed gel was then washed three times with 35% ethanol, each for 20 min. The gel was sensitized with 0.02% sodium thiosulfate for 2 min and washed with H_2O for 3 times, 5 min each. The gel was then stained with silver nitrate solution for 20 min (0.2% silver nitrate, 0.076% formalin). After extensive washing with H_2O for 40 s, the gel was developed in the developing solution (6% sodium carbonate, 0.05% formalin, 0.0004% sodium thiosulfate) until color visible, at which time the stopping solution (50% methanol,12% acetic acid) was added.

3.3 HiTrap Q HP

The sample was prepared in PBS, pH 7.2. The HiTrap Q HP 5 ml column (GE Healthcare) was run at a flowrate 5 ml/min. The starting buffer was PBS with 1 M NaCl, pH 7.2 and the elution buffer is PBS, pH 7.2. The samples were collected into fractions and desalted using PD-10 columns and sterilized by boiling at 95ºC before applying into *in vitro* DC activation assay.

3.4 Preparative isoelectric focusing

After overnight lyophilization, the samples, which appeared in the white powders, were disolved in Milli-Q water with 2% Bio-Lyte ampholytes (pH 3-10, Bio-Rad) in

a volume of 60 ml. The Rotofor apparatus, which is the Bio-Rad branded liquid-phase IEF system, was cooled to 4°C and washed by pre-running with Milli-Q H_2O for 5 min at 5 W constant power, which could efficiently remove the residual electrolytes. Then the sample mixtures were carefully and slowly loaded into the chamber. The chamber was sealed tightly after sample loading. The standard Rotofor chamber was then run at 15 W constant power for 4 to 6 h. The run was completed when the constant stopped decreasing for at least 1 h.

The sample was collected in 20 fractions, each 2.5 ml in a 5 ml tube. 10 times concentrated PBS solution was added into each fraction to get 1 time PBS in the solution which could exchange the ampholytes from the proteins. After vortexing, the fractions were buffer-exchanged into PBS (pH 7.2) by PD-10 columns (GE Healthcare). Aliquots of all 20 fractions were then tested by DC activation assay after sterilization using 95°C boiling for 30 min and applied into.

The fractions with peak DC-stimulatory activities were then combined and the proteins were recovered by desalting and lyophilization.

3.5 FPLC-gel filtration

The Superdex 200 (10/300, GE Healthcare) was run under native condition with buffer PBS (pH 7.2). The lyophilized protein powders were dissolved in 500 µl PBS and loaded into the column. The flowrate of the run was 0.5 ml/min and the fractions were collected in 0.5 ml each. The aliquots of all fractions were sterilized by filtration and applied into DC activation assay.

The fractions with peak bio-activities in DC activation assay were then dialyzed and lyophilized to recover the proteins.

3.6 Mass spectrometry coupled protein identification

The samples after two-dimentional purification, including Rotofor and gel filtration, was then dissolved in Milli-Q water and sent for liquid chromatography coupled mass-spectrometry (LC-MS) with protein identification from mouse genome database. This MS experiment with sample digestion was performed by the MS core facility, School of Biological Sciences, Nanyang Technological University.

4 Molecular and cellular approaches

4.1 RNA preparation

Total cytoplasmic RNA was extracted from un-activated and activated T cells using RNA extraction kit (Invitrogen). After stimulation, the different T cells, including *ex vivo*–isolated naïve T cells and the T cell lines A5, Beko and EL4, were lyzed by Trizol reagent (Invitrogen). After 5 min incubation on ice, 0.2 ml chloroform (Fisher) was added into each ml of Trizol solution followed by vigorous shacking for 15 s. After 2 min incubation on ice and 10 min centrifugation at 4,000 g at 4ºC, the upper clear layer was carefully collected and loaded into the column from the RNA extraction kit (Invitrogen) and washed with the commercial buffers and

RNase-free 70% ethanol (Merck). For each sample, the RNA was eluted into 30 µl RNase-free H_2O from the kit.

4.2 RT-PCR

The selected candidate genes were then validated by RT-PCR to monitor their expression levels in both un-activated and activated (CD3/CD28 crosslinking) T cells, A5 cells, BEKO cells and EL4 cells. 10 µg of extracted RNA was then mixed with 2 µl random primer (Roche), diluted by H_2O to 17.8 µl. The mixture was incubated at 65°C for 15 min. Then reverse transcriptase (Roche) was used to synthesize the first stand cDNA at 37°C for 60 min in a volume of 33 µl. After synthesis, the system was diluted into 100 µl. The cDNAs of A5 cell, BEKO cell and EL4 cell were prepared in the same way.

The primer pairs, spanning from 100 bp to 500 bp for different candidate genes, were designed and ordered from 1st Base (Singapore). PCR was performed by Taq polymerase as following: denaturation for 30 s at 94°C, annealing for 30 s at 55°C, extension for 1 min at 72°C for 30 cycles.

4.3 Intracellular staining

The $CD11b^+CD11c^+$ BMDCs were purified from 7-day FLT3L culture using CD11b microbeads (Miltenyi Biotec). For α-p-Syk, α-Syk, α-p-PLCγ2, and α-PLCγ2 staining, the purified $CD11b^+CD11c^+$ BMDCs were stimulated for 5min, followed by fixation with 2% paraformaldehyde (Sigma Aldrich) in PBS for 30 min. The cells

were then washed by 0.1% Saponin (Sigma Aldrich) in PBS with 2% serum as permeabilization buffer, followed by staining with α-p Syk and α-Syk for 2 h in permeabilization buffer. The cells were washed again and stained with the FITC-conjugated α-Rabbit secondary antibody (Southern Biotechnology, USA) for 30 min. During staining, 1 mM sodium orthovanadate (Sigma Aldrich) was always added in the solution. FACScalibur^{TM} flow cytometer (Beckton Dickinson, USA) was used to detect the fluorescence intensity.

4.4 Immunoprecipitation

The sample was pre-cleared using 5 µl of protein G agarose (Thermo Scientific). The cleared sample was then mixed with antibodies and incubated at 4ºC overnight. The mixture was then added into 20 µl protein G agarose and shaken at 4ºC for 2 h. The samples were then washed with lysis buffer (50 mM Tris pH 7.5, 0.27 M sucrose, 0.1 mM EGTA, 1 mM sodium orthovanadate, 50 mM sodium fluoride, 5 mM sodium pyrophosphate, 1% Triton X-100 and 0.1% β-mecaptoethanol with 500 mM NaCl) twice followed by wash buffer (50 mM Tris pH 7.5, 0.27 M sucrose and 0.1% β-mecaptoethanol) twice. The beads were then loaded into acrylamide gel for Western blotting.

4.5 Western blotting

The FLT3L-derived BMDCs were purified by CD11b microbeads and stimulated with GM-CSF or curdlan or the combination of both, followed by cell lysis using

lysis buffer [50 mM Tris pH7.5, 0.27 M sucrose, 0.1 mM EGTA, 1 mM sodium orthovanadate, 50 mM sodium fluoride, 5 mM sodium pyrophosphate, and 1% Triton X-100, and the protease inhibitor cocktail (Roche) and 0.1% β-mecaptoethanol were added just before use]. The concentration of the protein sample was measured by Bradford assay (Bio-Rad). Equal amounts of proteins for all samples were loaded into the acrylamide gels followed by Western blotting using nitrocellulose membrane (BioRad). The wash buffer used in the Western experiment is PBS with 0.05% Tween-20, and the blocking buffer is 5% fat-free milk powder (Bio-Rad) dissolved in the wash buffer. After incubation with HRP-conjugated secondary antibodies, the membrane was developed by chemiluminescence (PerkinElmer, USA) following manufactures' instructions. The digital image of the chemiluminescence was captured by the CCD camera in Las 4000IR (FUJIFILM).

4.6 Nuclear protein extraction

The FLT3L-derived BMDCs were purified by CD11b microbeads and stimulated by GM-CSF and curdlan. After 20 h, the cells were washed by PBS and put into hypotonic buffer A [10 mM HEPES with pH 7.9, 10 mM KCl, 1 mM EDTA and 1 mM EGTA, with addition of 1 mM DTT and protease inhibitor cocktail (Roche) just before use]. After 5 min incubation on ice, 0.5% Nonidet P-40 was added into the buffer followed by vortexing. The samples were spun down at 16,000 g for 3 min and washed by buffer A twice. The pellets were then resuspended into the hypertonic buffer B (20 mM HEPES with pH 7.9, 420 mM NaCl, 10 mM EDTA and 10 mM EGTA, with addition of 1 mM DTT and protease inhibitor just before use)

and incubated at 4°C with gentle shaking for 2 h. The samples were then spun down at 16,000 g for 10 min at 4°C and kept at -20°C. All chemicals used in this protocol were purchased from Sigma-Aldrich.

4.7 ELISA

4.7.1 Cytokines

IL-1β, IL-12p70, IL-2, TNF-α and IL-6 ELISAs, and recombinant GM-CSF were purchased from BioLegend (San diego, CA). ELISA experiments were performed following manufacturers instruction. Capture antibodies dissolved in PBS were pre-coated at 4ºC overnight. The samples and detection antibodies were prepared in assay diluent that is PBS with 1% BSA. 0.05% Tween-20 was dissolved into PBS for sample washing after each step. The chemiluminescent signals were developed by the enzymatic substrates from the kit and detected by the Multiskan Spectrum spectrophotometer (Thermo Scientific).

4.7.2 NF-κB subunits

Using the extracted nuclear samples, which was standardized using α-USF-2 in the Western blot, nuclear translocation of c-Rel was visualized by Western blot, while for the other four NF-κB subunits, including p65, p50, RelB and p52, their levels in the nuclear samples were detected by the NF-κB binding consensus-coated ELISA kit (TransAM NF-κB transcription factor kit, Active Mitif, Carlsbad, CA, USA)

following the manufacturers' instructions. After standardization, 2 μg of each sample was loaded into separate wells of a 96-well plate and incubated directly with the κB consensus DNA pre-coated well. Following sample incubation, NF-κB subunits-specific primary antibodies, HRP-conjugated secondary antibodies were applied following each washing session. Lastly, the signals were developed by the enzymatic substrates from the kit and read by the Multiskan Spectrum spectrophotometer (Thermo Scientific).

5 Phospho-proteomics

$CD11b^{+}CD11c^{+}$ BMDCs were isolated from 7-day FLT3L culture derived from NUP-HOX B4-transduced BM cells and stimulated by curdlan or/and GM-CSF for 20 min at 37ºC. After stimulation, the cells were washed once with PBS and lyzed by lysis buffer as described above. The lysate was collected by centrifugation at 4ºC, 16,000 g for 10 min. Sample concentration was measured by Bradford assay and 3 mg of each sample was taken for phosphor-proteomics.

Each sample lysate was loaded into one separate 10% commercial acrylamide gel (Bio-Rad) and run for 1 h at 100 V. After coomassie blue (Bio-Rad) staining, the gel was then washed by ethanol and cut into 1 mm^3 for in-gel digestion using Trypsin (Promega), 37°C overnight.

After digestion, the phospho-peptides containing samples were recovered by spin-vacumn (eppendorf), 45°C for 6 h. Electrostatic repulsion-hydrophilic interaction chromatography (ERLIC) was run to enrich the phospho-peptides,

followed by LC-MS and peptide identification, and performed by the MS core facility, School of Biological Sciences, Nanyang Technological University.

RESULTS

1 T cell factor released by activated T cells maturates DCs

To characterize the TCF functions, we have established an easy *in vitro* screening system, which allows us to monitor the immunostimulatory activities by flow cytometry. DCs derived from FLT3L BM cultures were incubated 24/48 h with culture supernatants obtained from α-CD3/CD28 stimulated T cells or with purified preparations ($CD8^+$ T cells or $CD4^+$ T cells) thereof. Upregulation of co-stimulatory receptors (e.g. CD80 and CD86) on DC surface was monitored by flow cytometry and used as parameters for DC maturation. An example is given in **Fig. 13**, in which the TCF sample was from total T cells. We used CpG (the bacterial DNA which is the agonist of TLR4) as a positive control. As shown in **Fig. 13,** the TCF-containing supernatant is even more potent in the stimulatory efficacy for DC maturation.

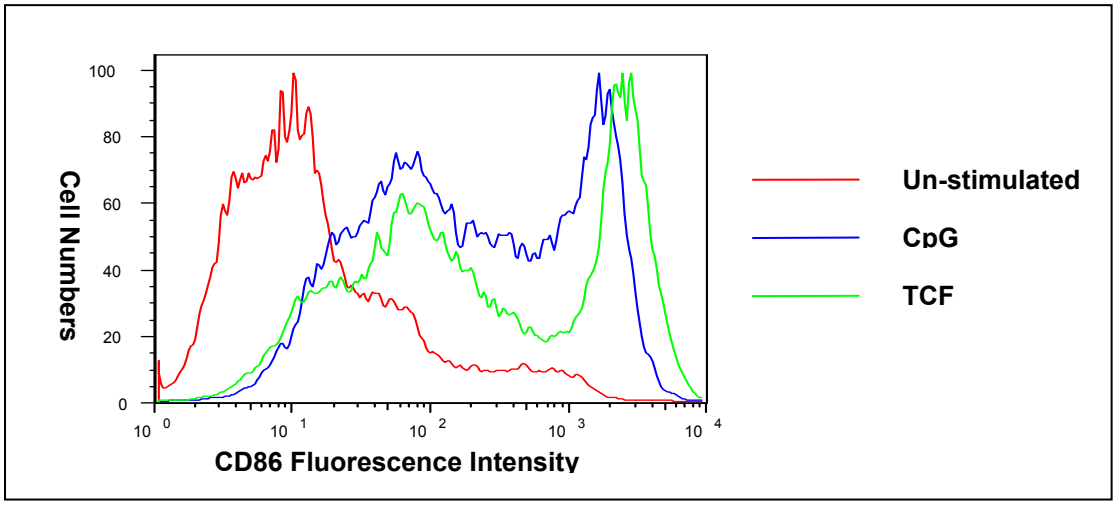

Figure 13: Upregulation of the costimulatory molecule CD86 on DCs after stimulation by the supernatant from activated T cells. The red line is the fluorescence intensity of un-stimulated dendritic cells. Blue line is the one of CpG stimulated DCs. And the green line is the one of the TCF-containing supernatant stimulated DCs.

To further validate the potency of T cell subtypes in their TCF production abilities, the $CD4^+$ and $CD8^+$ T cells were purified from the spleens and lymph nodes. The obtained cells were stimulated by α-CD3/CD28 and the sample activities were tested using the established DC maturation assay as described in **Fig.13**. The results are summarized in **Fig. 14**. $CD8^+$ T cells are more potent TCF producers compared with $CD4^+$ T cells.

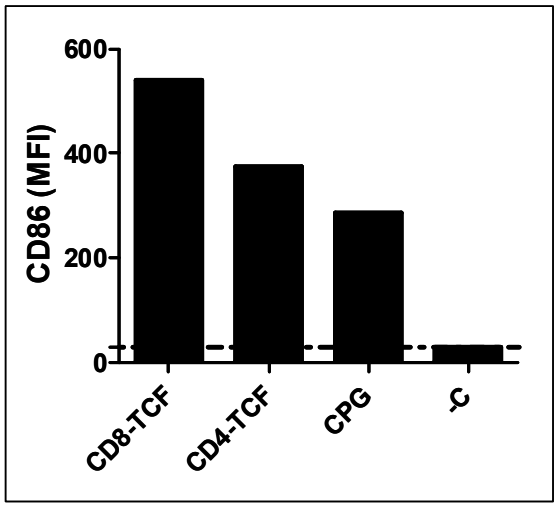

Figure 14: $CD8^+$ T cell derived TCF-containing supernatant is more potent than the $CD4^+$ derived one. The $CD8^+$ T cells or $CD4^+$ T cells were purified by microbeads and stimulated by CD3/CD28 crosslinking. The serum-free supernatants collected from 24 h-stimulated cells were then applied into DC maturation assays. After 24 h, the upregulation of CD86 was measured by flow cytometer. IMDM was used in the assay as the negative control. This is the representitive of at least five experiments.

This unidentified TCF was furthermore proved to be a protein. Protein digestion of the TCF-containing supernatant by Proteinase K at 37°C for 2 h efficiently abolished its DC stimulatory activities (**Fig. 15**). Additionally, TCF was heat-resistant. Boiling of the samples at 95°C for 30 min did not obviously diminish its activity (**Fig. 15**). This heat-resistant property matches with many cytokines according to the literature (152).

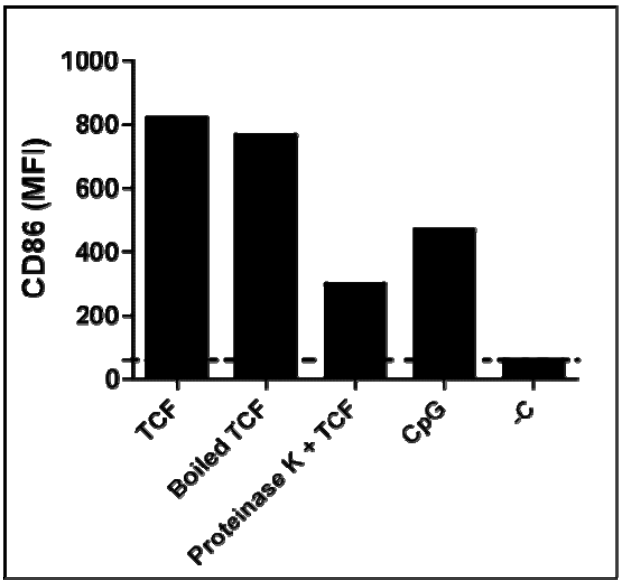

Figure 15: The TCF as a heat-resistant protein. The serum-free TCF-containing supernatant was either boiled at 95ºC for 30 min or digested with Proteinase K for 2 h at 37 ºC. The samples were then applied in the DC maturation assay. CpG was used as A positive control while pure IMDM medium was the negative control. After 24 h stimulation, the CD86 MFI was detected by flow cytometer. This is a representitive of three independent experiments.

2 TCF enrichment for efficient protein identification

To purify TCF, different approaches were tested for their potential applications. These approaches included ion-exchange columns, consisting the cation exchanger HiTrap SP HP, anion exchanger HiTrap Q HP columns, Heparin column and gel filtration columns. The BioRad® isoelectricfocusing apparatus Rotofor was also included in our studies. After series of preliminary experiments, the flowchart of the whole protein purification procedure was fixed as shown in **Fig. 16**. In this procedure, the serum-free TCF-containing supernatant was collected and concentrated. Then two purification approaches were applied to enrich the target protein based on its pI and size, respectively. The final step was a MS analysis.

Selected candidates from MS results were then validated by RT-PCR monitoring their gene expression levels in un- and activated T and A5 cells, while using BEKO and EL4 cells as negative controls (see 2.1). Along this procedure, the immunostimulatory activities of TCF were always traced by the *in vitro* DC activation assay.

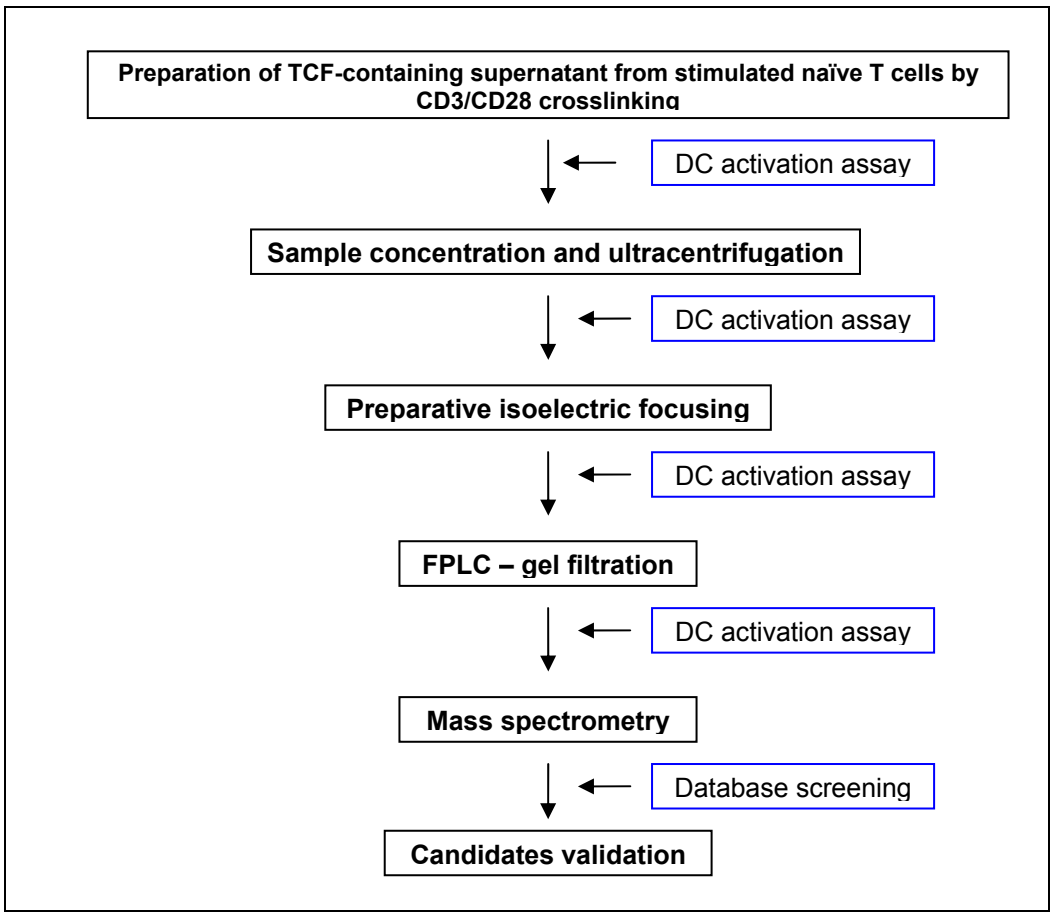

Figure 16: The purification schedule of TCF. The black boxes show the purification line, while the blue boxes show the monitoring methods after each purification step. DC activation assay was employed in the whole purification procedure to track the TCF activity.

2.1 Screening of cell lines for large-scale production

As the MS sample preparation needs a large amount of starting proteins, we tested several different T cell lines for their TCF-producing abilities. The tested cell lines included the A5 cell line, which is a HA specific $CD4^+$ T cell hybridoma line, and two thymoma cell lines, BEKO and EL4 cell lines. The TCF-activities from these cells were summarized in **Fig. 17**. From the data, A5 cells were potent TCF-producers, which might be employed to replace the T cells as the TCF sources for large-scale production. In contrast, BEKO and EL4 cells were not the good targets.

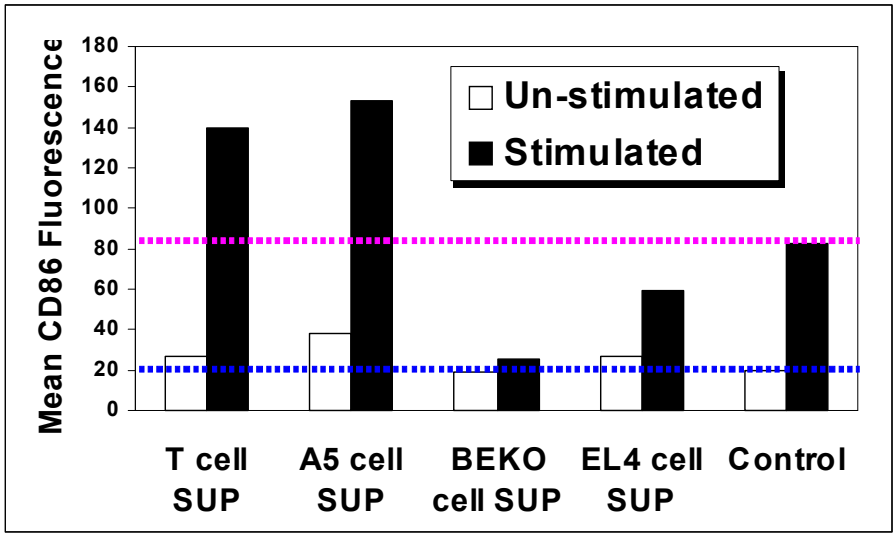

Figure 17: The amount of TCF from different cell sources. The different cell types used in the screening were tested in the *in vitro* DC maturation assay in terms of their TCF-secreting abilities after α-CD3/CD28 stimulation. CD86 mean fluorescence intensity was calculated to monitor the TCF activities. The lower dashed line indicates the activation level of the negative control (IMDM), while the upper dashed line indicates the stimulation level of CpG as the positive control. This represents at least three independent experiments.

2.2 Preparation for TCF purification

The sample was prepared from 500-1000 ml serum-free TCF-containing supernatant collected from the α-CD3/CD28 activated T cells or A5 cells. The protein concentrator Centricon with 10 KDa cut-off used for sample concentration was able to retain the TCF successfully, indicating that the size of TCF is larger than 10 KDa. After this step, the amount of total proteins (traced by Bradford assay) became 1/2 of the amount in the primary supernatant while the TCF activities reflected by DC activation assay retained. In other words, our target protein was enriched by 2 times. The next step was ultracentrifugation, after which the total proteins were reduced by another 2/3 while the TCF was still retained because of its high solubility. In this case, another 3 times enrichment was established. Above all, the whole sample preparation process established 6 times enrichment of our target protein (**Fig. 18**).

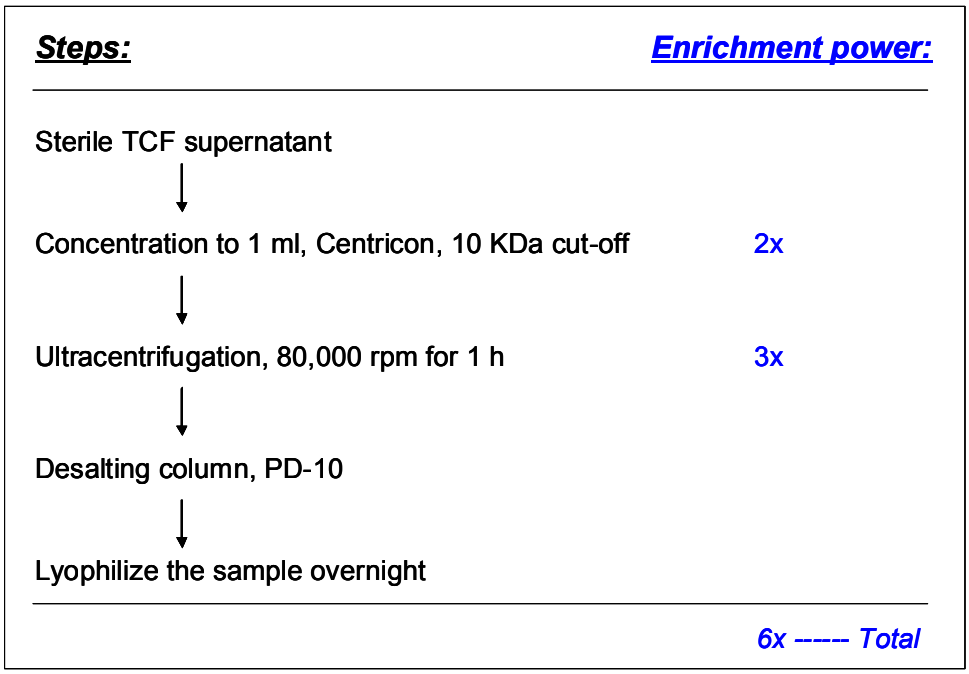

Figure 18: The protein enrichment power of the sample preparation approaches. In the process of MS sample preparation, the enrichments of our targeted TCF were established by Centricon and unltracentrifugation steps, which in total gave 6 times TCF enrichment, monitored by DC maturation assay, while the total protein amounts were monitoring by Bradford assay to measure the sample protein concentrations.

2.3 Preparative isoelectric focusing

After sample preparation, two-dimensional protein purification approaches were applied. The first dimension is the Rotofor apparatus, a preparative isoelectrical focusing approach. This Rotofor apparatus was run with ampholyte mixture to establish a pH gradient with the value 3 - 10. The pH gradient was increased from fraction 1 to fraction 20, but the rate of the increase was not even. The different sample mixtures applied to be separated also affected the local pH. After sample collection and buffer exchange to PBS by PD-10 column, the pH values of the fraction 1 to fraction 20 were successfully neutralized to pH 7 to 8.

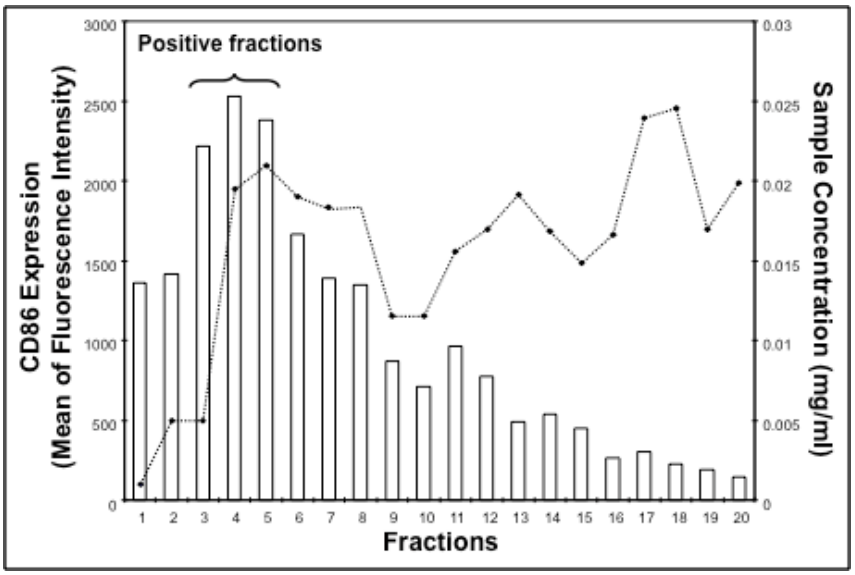

Figure 19: The sample activities coupled to protein concentrations of all 20 fractions in a Rotofor run. The X-axis is the fraction number along pH gradient pH 3 to pH 10. The blank columns are the respective fraction sample activities in DC activation assay. The left Y-axis shows the mean values of CD86 fluorescence intensity. The dashed line shows the corresponding fraction concentrations. The right Y-axis is the sample concentration in mg/ml.

DC activation assay showed that our target protein was successfully narrowed down into 2 to 3 fractions with pH values roughly from 3.5 to 4.5 in the original Rotofor fractions (**Fig. 19,** pH value not shown), indicating the pI value of TCF is around this range. In addition, other small activity peaks, e.g. the one in fraction 11, might indicate other DC stimulatory factor in the sample mixture since it was visualized by our DC maturation assay *in vitro*.

The concentration of each fraction was measured by Bradford assay. Many contaminating proteins were efficiently separated away from TCF (**Fig. 19,** dashed line). In this case, the enrichment power of TCF was great and it could be calculated using the following concentration ratio: (sum of concentrations of all fractions) / (sum of concentrations of the fractions with peak TCF activities validated by DC activation assay). After Rotofor run, the peak fractions (fractions 3 to 5) were then combined and processed for gel filtration - Superdex 200 10/300.

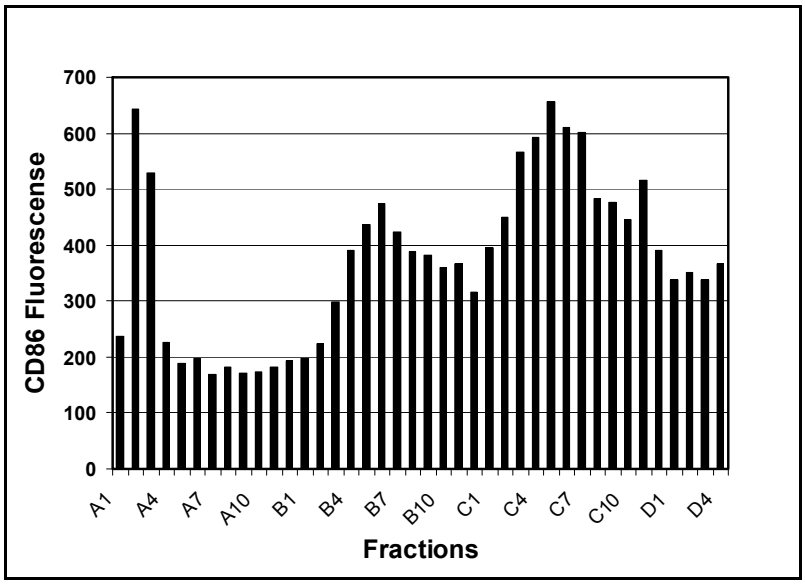

Figure 20: The sample activities screened by DC maturation assay after HiTrap Q HP fractionation. The factions collected from HiTrap-Q were sterilized and applied into the DC maturation assay. The activities reflected by CD86 upregulation were measured by flow cytometer.

The observation from the Rotofor results that the pI value of TCF was around 3.5 to 4.5 was consistent with the one from the HiTrap Q HP results (**Fig. 20**). The sample activities were captured from this anion exchanger, indicating that the targeted TCF carried a negative change under neutral pH. Thus the pI value of the TCF protein is predicted to be less than 7. Besides, the double peaks from the HiTrap Q HP run had indicated the existence of more than one active factors potentially being our targeted TCF.

2.4 FPLC - gel filtration

The combined TCF-containing Rotofor fractions (**Fig. 19,** fractions 3 to 5) were then applied to a Superdex 200 10/300 column. The sample collection began from 1/3 of the bed volume after injection, which was the point where the proteins began to reach the bottom of the column. Visualized via UV curve, the sample was well processed by this column, giving resolved peaks (**Fig. 21,** flow curve). After analyzing the fraction activities by our established DC activation assay, we found the factor was distributed in two positions: one in the beginning of sample collection corresponding to the protein aggregates, while the other in the middle of the run corresponding roughly to proteins ranging from 10 KDa to 50 KDa in size.

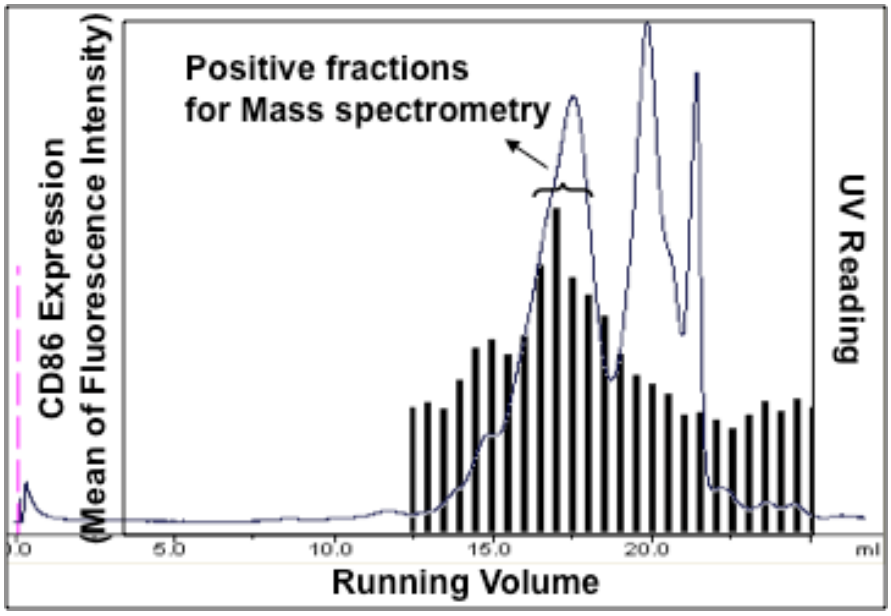

Figure 21: The Superdex 200 run coupled to fraction activities given by DC activation assay. The left side vertical dashed line indicates the injection point. The flow curve is the UV reading curve to capture the total protein distribution along the run, while the black columns are the corresponding activities for the collected fractions.

The central fractions in the second peak, which contained the native proteins, were combined and sent for LC-MS analysis and protein identification. Meanwhile, the SDS-PAGE coupled to silver staining was used to visualize the sample components and a complex mixture of proteins was detected (**Fig. 22**), indicating our purification procedure was not efficient enough to separate out TCF. Rather, it was just an enrichment process to make the final MS detection more specific. The purification of TCF was so difficult because the serum-free supernatant contains a wide spectrum of secreted proteins as well as proteins from dead cells resulted from activation-induced cell death, which is a common phenomenon coupled to T cell activation.

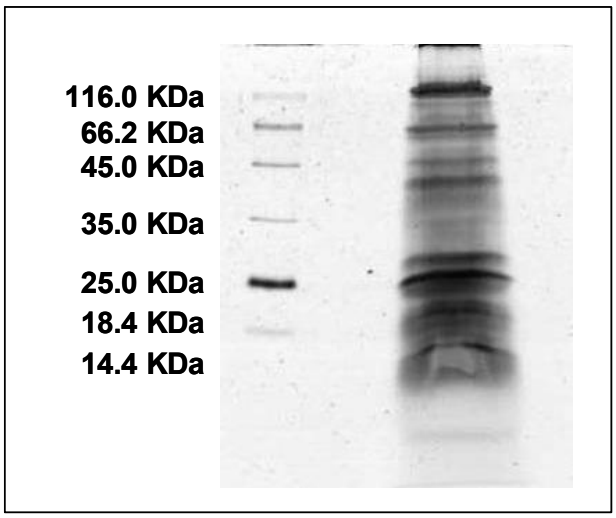

Figure 22: The silver staining of the MS sample. An aliquot of the sample prepared for MS analysis was run via SDS-PAGE followed by silver staining. The protein markers on the left indicated the sizes of the protein bands on the gel.

3 Candidates selection and validation

MS analysis, a long list of proteins, normally in the scale of hundreds, were detected and identified through database searching. The list was then analyzed with approaching literature reviewing and NCBI searching. Several papers were published to show the comparison of gene expressions of T cells before and after activation by CD3/CD28 crosslinking (153-155). The NCBI gene database provided a good resource for gene browsing. Based on our results and the related background information, the candidate selection was generally focused on the following groups: cytokines, chemokines, growth factors, or secreted receptors.

Using different batches of BMDCs, we repeated 4 times the MS analysis. Combining all five sets of MS results we have successfully established, we eventually narrowed down the candidates to 18 genes as given in **Table 3**. RT-PCR monitoring their mRNA levels in un- or activated T cells was applied to screen their

respective expression pattern. The cDNA templates were prepared from both un-activated and activated T cells, A5 cells, BEKO cells, and EL4 cells. As already shown in **Fig. 17**, the four cell types were tested in terms of their TCF-producing potency. We might assume that their DC stimulatory levels reflected by DC activation assay corresponded to their respective TCF gene expression levels (mRNA quantities), which were summarized in a semi-quantitative way (**Fig. 23**, red bottom table).

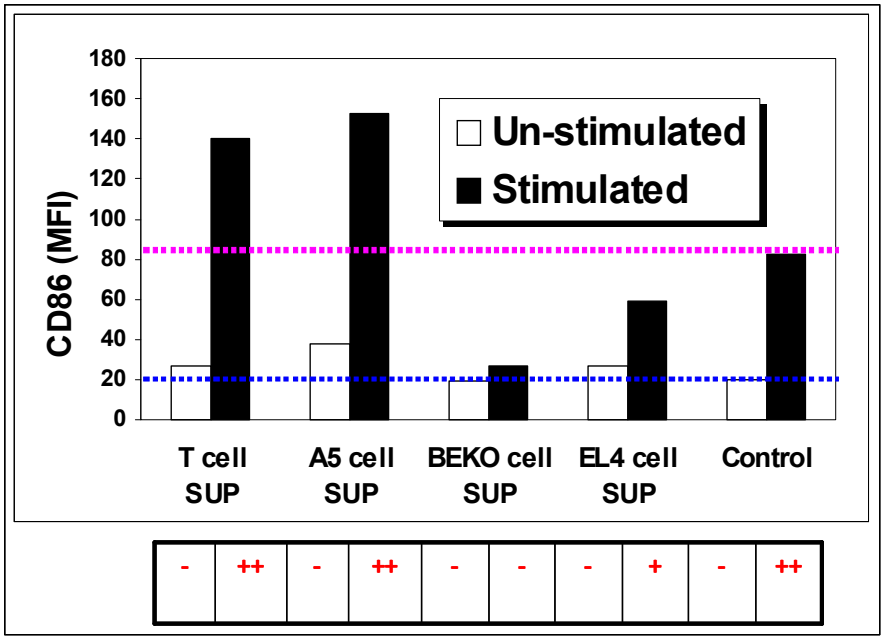

Figure 23: The amount of TCF from different cell sources. The different cell types used in the screening were tested in the *in vitro* DC maturation assay for their TCF-secreting abilities after α-CD3/CD28 stimulation. CD86 mean fluorescence intensity was calculated to indicate the TCF activities, which in turn reflect the TCF gene expression levels.

The semi-quantitative TCF expression pattern was included in **Table 3** [TCF (Predicted)] and used as an indicator for target selection after RT-PCR of each candidate. The screening results of the candidate genes were shown in **Table 3** and further summarized in **Table 4** in the semi-quantitative way.

Gene	Full Name	0 h T Cells	18 h T Cells	0 h A5 Cells	24 h A5 Cells	0 h Beko Cells	24 h Beko Cells	0 h EL4 Cells	24 h EL4 Cells	- C
CCL24	Chemokine (C-C motif) ligand 24									
CLCF1	Cardiotrophin-like cytokine factor 1									
CXCL13	Chemokine (C-X-C motif) ligand 13									
ENS	Predicted gene, ENSMUSG00000073266									
Gdf7	Growth differentiation factor 7									
Gdf11	Growth differentiation factor 7									
GM-CSF	Granulocyte-macrophage colony-stimulating factor									
Grn	Granulin									
H2-Eb2	Histocompatibility 2, class II antigen E β2									
Hdgf	Hepatoma-derived growth factor									
IL-19	Interleukin-19									
IL-22	Interleukin-22									
Ltb	Lymphotoxin-β									
MIF	Macrophage migration inhibitory factor									
Ngp	Neutrophilic granule protein									
Ptma	Prothymosin-α									
S100a9	S100 calcium binding protein A9									
Tnfrsf13b	TNF receptor superfamily, member 13B									
TCF (Predicted)		-	++	-	++	-	-	-	+	-
HPRT										

Table 3: Validation of candidate genes by RT-PCR in comparison with predicted expression levels of TCF gene. cDNA templates were prepared from both un-activated and 16 h α-CD3/CD28 activated T cells, A5 cells, BEKO cells and EL4 cells. RNase-free H_2O was the negative control. TCF expression levels predicted from **Fig. 23** were given as reference. House-keeping gene HPRT was used as control for RNA quantity.

Table 4 is the semi-quantitative representation of the data in **Table 3**.

Gene	Full Name	0 h T Cells	18 h T Cells	0 h A5 Cells	24 h A5 Cells	0 h Beko Cells	24 h Beko Cells	0 h EL4 Cells	24 h EL4 Cells	- C
CCL24	Chemokine (C-C motif) ligand 24	+	+	-	+	-	-	-	-	-
CLCF1	Cardiotrophin-like cytokine factor 1	++	++	-	+	-	+	-	-	-
CXCL13	Chemokine (C-X-C motif) ligand 13	-	-	-	-	-	-	-	-	-
ENS	Predicted gene, ENSMUSG 00000073266	+	+	-	-	+	-	-	-	-
Gdf7	Growth differentiation factor 7	+	+	+	+	+	+	+	+	-
Gdf11	Growth differentiation factor 7	+	++	+	+	+	+	-	+	-
GM-CSF	Granulocyte-macrophage colony-stimulating factor	-	++	+	++	-	+	-	++	-
Grn	Granulin	++	++	++	++	++	++	++	++	-
H2-Eb2	Histocompatibility 2, class II antigen E β2	+	+	+	+	+	+	+	+	-
Hdgf	Hepatoma-derived growth factor	++	++	++	++	++	++	++	++	-
IL-19	Interleukin-19	-	-	-	-	-	-	-	-	-
IL-22	Interleukin-22	-	++	-	++	-	-	-	+	-
Ltb	Lymphotoxin-β	++	++	+	++	-	++	+	-	-
MIF	Macrophage migration inhibitory factor	++	++	++	++	++	++	++	++	-
Ngp	Neutrophilic granule protein	++	+	-	-	-	-	-	-	-
Ptma	Prothymosin-α	++	++	++	++	++	++	++	++	-
S100a9	S100 calcium binding protein A9	++	+	-	-	-	-	-	-	-
Tnfrsf13b	TNF receptor superfamily, member 13B	+	+	-	-	+	-	-	+	-
TCF (Predicted)		-	++	-	++	-	-	-	+	-
HPRT		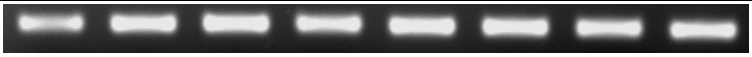								

Table 4: Validation of candidate genes by RT-PCR in comparison with predicted expression levels of TCF gene in a semi-quantitative way. This table shows the same results as in **Table 3**, but in a semi-quantitative way.

The expression levels of the house-keeping protein HPRT were used to standardize the amounts of each template cDNA used in the experiments and shown at the bottom of this table. RNase-free H_2O was the used as the negative control. None of the primer pairs used in the experiments showed any positive bands in the negative control H_2O sample when the template was not around (data not shown).

From **Table 3** and **Table 4**, four genes matched the predicted TCF gene expression pattern. Their expression patterns visualized via RT-PCR are representatively shown in **Table 5**. We would then discuss their expression patterns.

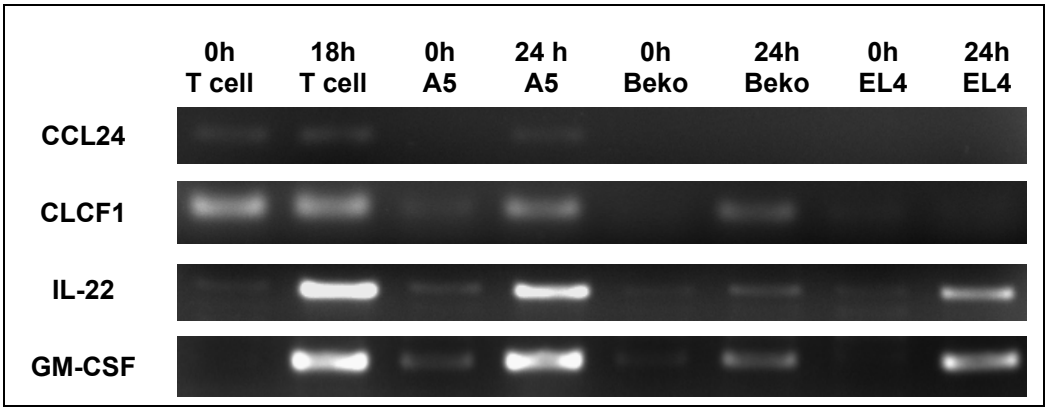

Table 5: The positive candidates from RT-PCR validation and their PCR pattern on agarose gel. These genes showed the similar pattern as the predicted TCF gene expression pattern.

Among these genes, CCL24 is a chemokine according to its name [Chemokine (C-C motif) ligand 24]. We chose this candidate because it was expressed in both activated T and A5 cell, but not in BEKO or EL4 cells. However, it was also visible in un-activated T cells. And one problem is its expression visualized on the gel was too weak to be considered as reliable. CLCF1 (Cardiotrophin-like cytokine factor 1) is another gene with similar expression pattern as CCL24. Additionally, it was

visible in activated BEKO cells, although the expression level was much lower than the one in positive cells (T and A5 cells). As introduced, the BEKO cell line was a negative source. Thus the possibility of these two factors being TCF is low.

IL-22 belongs to the IL-10 family (156). We tested its possibility to be TCF by applying the recombinant IL-22 to DC maturation assay. We did not observe any stimulatory effects. This was the major reason why we excluded the IL-22 from the list of candidates.

The last interesting target was GM-CSF. GM-CSF is a glycoprotein of 22 KDa, in the range of predicted TCF size. As we know, GM-CSF is a known stimulator for DC differentiation, hence we focused on its property to induce DC maturation.

4 GM-CSF as the licensing factor for DC maturation

To validate whether GM-CSF was the targeted DC-stimulatory TCF, we tested whether the blocking antibody α-GM-CSF was capable to neutralize the TCF activity. To achieve this, bone marrow-derived FLT3L-DCs were incubated overnight without or with 50 µl or 25 µl TCF-containing supernatant in the presence or absence of the blocking antibody. The results, monitoring expression levels of co-stimulatory molecule CD86, showed that α-GM-CSF antibody was able to block the TCF activities in a does-dependent manner (**Fig. 24**).

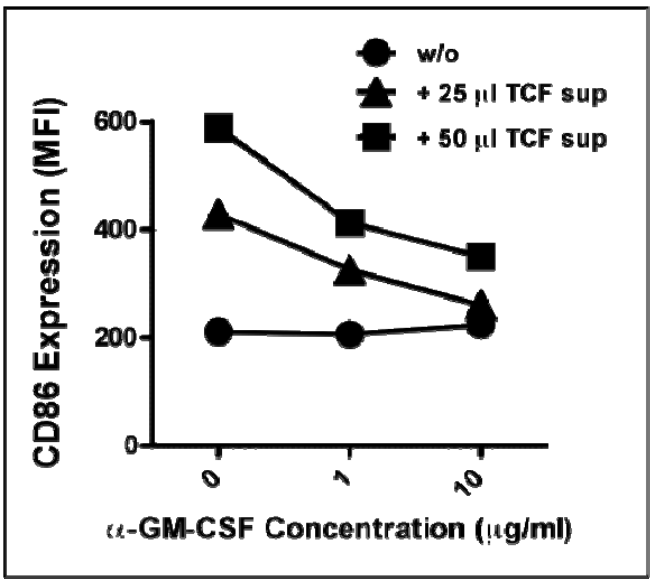

Figure 24: Neutralizing α-GM-CSF antibody blocked TCF activities in the DC maturation assay *in vitro*. The FLT3L-derived BMDCs were incubated with 50 or 25 μl of TCF-containing serum-free supernatant in the absence or presence of 1 or 10 μg/ml blocking α-GM-CSF. After 24 h incubation, CD86 expression was then analyzed by flow cytometer.

This assay successfully proved that it was the GM-CSF that played a major role in our TCF screening assay. We then analyzed the different T cells subsets, including both naïve and effector types of either $CD4^+$ or $CD8^+$ T cells, to screen their DC stimulatory functions. The effector types ($CD44^+$) of either $CD4^+$ or $CD8^+$ T cells isolated from spleens and lymph nodes of the BL/6 mice were stained with α-CD44 and sorted by flow cytometer. Besides the effector T cells, the $CD44^-$ group which represents the naïve T cell population was also collected. The plot of flow cytometer detection of stained spleen cells and gated cell subpopulation is given as an example (**Fig. 25**).

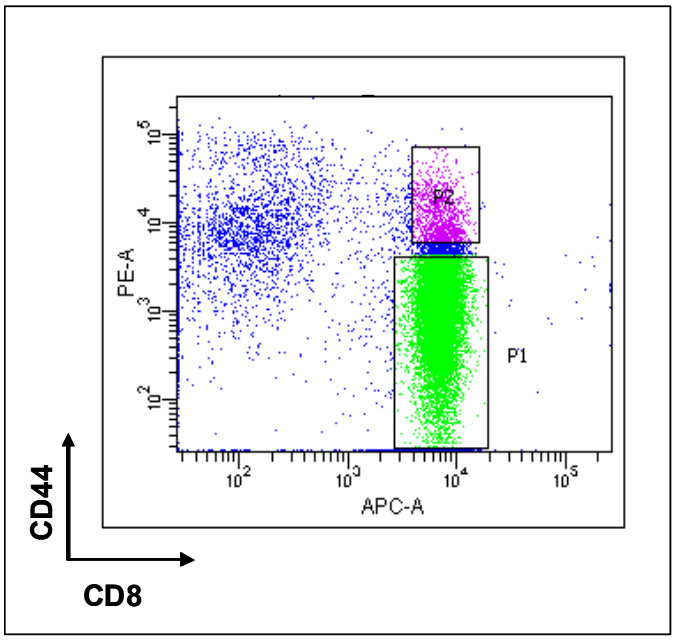

Figure 25: The sorting of CD8$^+$ T cells into effector (CD44$^+$) and naïve (CD44$^-$) subsets. The CD8$^+$ T cells isolated from the spleen and lymph nodes of the BL/6 mice were purified by α-CD8 microbeads and stained with both α-CD8 and α-CD44 antibodies. The cells were then sorted by flow cytometer. Both effector CD8$^+$ T cells (CD8$^+$CD44$^+$) and naïve CD8$^+$ T cells (CD8$^+$CD44$^-$) were collected.

The sorted cells were then cultured in a α-CD3/CD28-coated plate to allow GM-CSF secretion overnight. The collected GM-CSF-containing supernatant was then applied into DC maturation assay to test the CD86 upregulation. Both effector and naïve groups of CD8$^+$ T cells showed increased DC stimulatory abilities in the assay. Effector CD8$^+$ T cells were more potent than the naïve cells (**Fig. 26**).

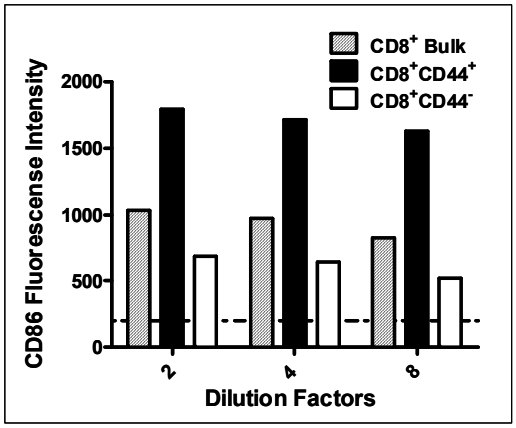

Figure 26: GM-CSF is secreted by both effector and naïve CD8$^+$ T cell upon activation *in vitro*. The sorted CD8$^+$ T cells were stimulated by α-CD3/CD28 crosslinking for 24 h. The supernatants were then applied into DC maturation assay with serial dilutions (2 to 8 times). CD86 up-regulation was measured by flow cytometer. The dashed line indicates the negative control. The experiment was repeated twice.

However, in the case of CD4$^+$ T cells, only the effector cells can stimulate the DCs upon activation *in vitro*, while the naïve type didn't participate at all (**Fig. 27**). Thereafter, our further experiments focused mainly on the CD8$^+$ T cells to target the involvement of these cells in DCs/T cells interactions.

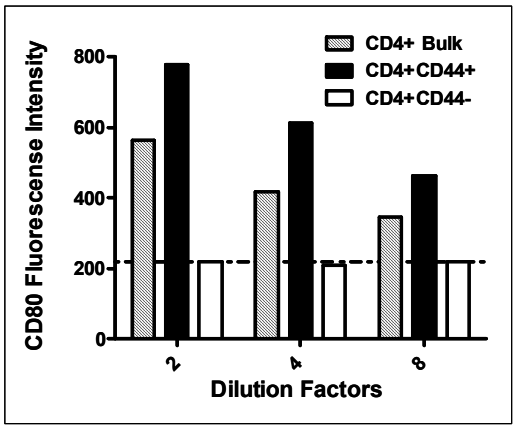

Figure 27: GM-CSF is not secreted by naïve CD4$^+$ T cell upon *in vitro* activation. The sorted CD4$^+$ T cells (CD4$^+$CD44$^+$ and CD4$^+$CD44$^-$) were stimulated by α-CD3/CD28 crosslinking for 24 h. The supernatants were then applied into DC maturation assay with serial dilutions (2 to 8 times). CD86 up-regulation was measured by flow cytometer. The dashed line is the value of the negative control (IMDM). This experiment was repeated twice.

To further validate the crucial role of GM-CSF in the $CD8^+$ T cell-mediated DC maturation, we then co-cultured isolated $CD8^+$ T cells together with FLT3L derived BMDCs. Blocking α-GM-CSF and α-CD40L were added separately or in combination to analyze the importance of GM-CSF and CD40L in their interactions. From **Fig. 28**, neutralizing the activities of GM-CSF in the culture efficiently blocked the OVA-specific interactions between $CD8^+$ T cell and DCs, while blocking of CD40L-CD40 interactions did not further enhance this inhibitory effect in the co-culture. This data shows that GM-CSF, but not CD40L, is the licensing factor for the $CD8^+$ T cell-mediated DC maturation (157).

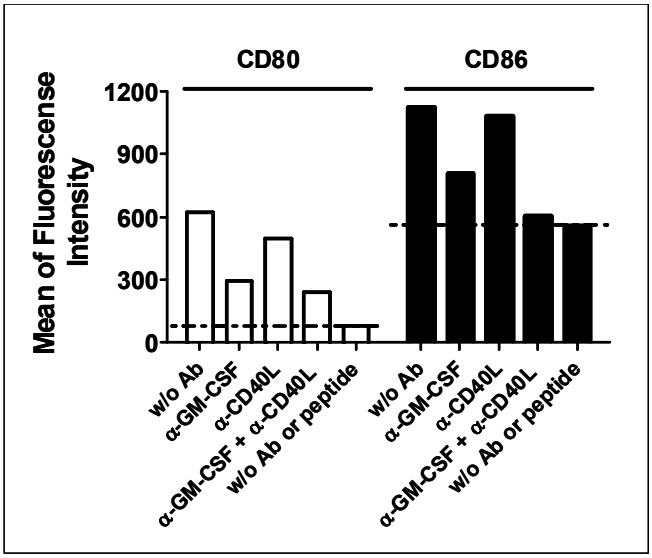

Figure 28: GM-CSF rather than CD40L is the major player in the $CD8^+$ T cell mediated FLT3L BM DC activation *in vitro*. The OVA-specific $CD8^+$ T cells were put in co-culture with OVA-pulsed FLT3L BMDCs, with addition to 10 μg/ml blocking antibodies α-GM-CSF and α-CD40L separately or in combination. Non-pulsed DCs were used in the negative control sample. After 24 h, the CD86 expression was analyzed by flow cytometry. This figure shows the representitive of three independent experiments.

The important role of GM-CSF was further proved by testing GM-CSFR$^{-/-}$ DCs, which do not respond to GM-CSF. The FLT3L BMDCs were prepared from both wildtype (Ly5.1^{+}) and GM-CSFR$^{-/-}$ (Ly5.1^{-}) mice and both types were put into co-culture in a 50:50 ratio. The DCs were pulsed by OVA peptide and incubated with OVA-specific CD8^{+} T cells for 24 h. The expression levels of CD80 and CD86, for both WT and GM-CSFR$^{-/-}$ DCs, distinguished by Ly5.1 staining, were measured and plotted in **Fig. 29**. From this figure, even in the same co-culture, GM-CSFR$^{-/-}$ DCs could not receive the maturation signals from CD8^{+} T cells, while the WT DCs were activated as usual. This indicated that GM-CSF is the key player in the observed DC maturation mediated by CD8^{+} T cells in the OVA-specific co-culture.

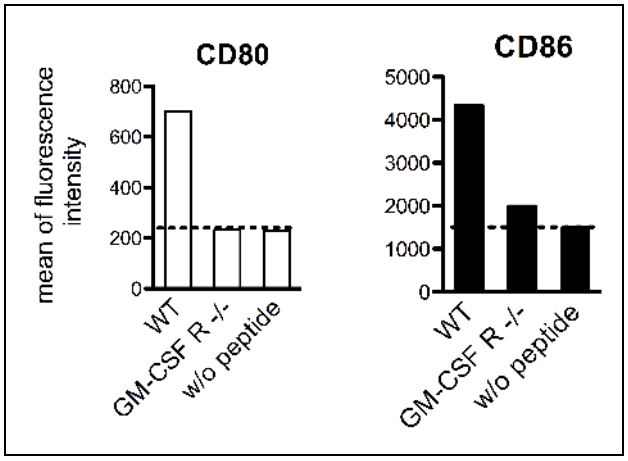

Figure 29: Comparison of the maturation of DCs from WT or GM-CSF-R$^{-/-}$ mice in DC/CD8^{+} T cells co-culture. A 50:50 ratio of FLT3L-derived Ly5.1^{+} WT and Ly5.1^{-} GM-CSFR$^{-/-}$ DCs were pulsed by SIINFEKL and incubated with OT-1 CD8^{+} T cells for 24 h. CD80 and CD86 expressions for both WT and GM-CSFR$^{-/-}$ DCs were then analyzed by flow cytometry. This data represents three sets of experiments.

To further validate the licensing role of GM-CSF in the maturation of DCs, the time series of GM-CSF secretion from activated CD8^{+} and CD4^{+} T cells was measured. Both CD8^{+} and CD4^{+} T cells isolated from spleens and lymph nodes of

the BL/6 mice were sorted into both effector and naïve types. The sorted cells were then activated by CD3/CD28 crosslinking. The supernatant was collected in a time series and monitored by ELISA to measure the secretion levels of GM-CSF. IL-2 was measured as the positive indicator for T cell activation.

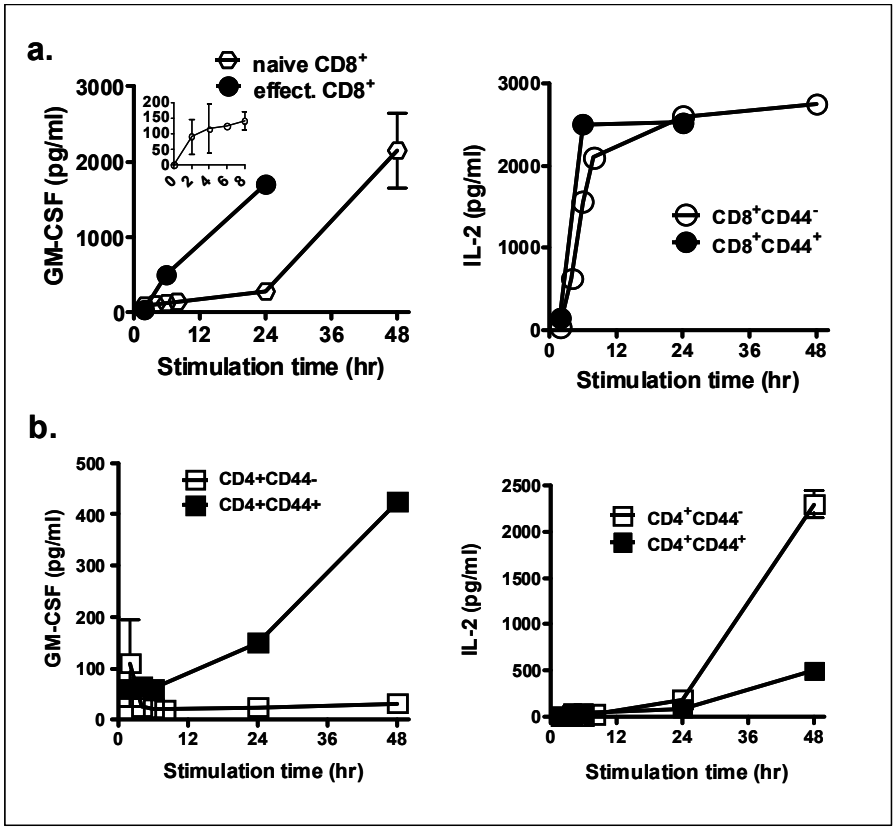

Figure 30: Secretion profile of GM-CSF (left) and IL-2 (right) by both naïve (white dot) and effector (black dot) T cells in a time series. Both $CD8^+$ and $CD4^+$ T cells were isolated from spleens and lymph nodes and then sorted into both effector ($CD44^+$) and naïve ($CD44^-$) subsets. The cells were stimulated by CD3/CD28 crosslinking. Supernatants were then collected after 2 h, 4 h, 6 h, 8 h, 24 h, and 48 h to monitor the GM-CSF secretion in the time series. IL-2 was also monitored to ensure the activation of T cells. This represents two sets of independent experiments.

The secretion profile was summarized in **Fig. 30**. The upper panel shows the $CD8^+$ T cells results (**Fig. 30, a**), while the lower panel is the $CD4^+$ T cell results (**Fig. 30, b**). Consistent with **Fig. 27**, naïve $CD4^+$ T cells did not secret GM-CSF,

whereas the effector $CD4^+$ T cells were potent GM-CSF producers upon stimulation with α-CD3/CD28. For $CD8^+$ T cells, the upper left corner of GM-CSF secretion profile shows the details of the early secretion (before 8 h stimulation). From this figure, we can see that the $CD8^+$ T cells were activated very efficiently upon CD3/CD28 crosslinking, reflected by the fast secretion plateau of IL-2. After 4 h of T cell activation, the secretion of GM-CSF from naïve $CD8^+$ T cells already reached 100 pg/ml, while the one from the effector cells reached 400 pg/ml. From the titration experiment of GM-CSF in the *in vitro* DC maturation assay, this concentration was already enough to stimulate the DC maturation (**Fig. 31**). Above all, we may conclude that the GM-CSF secreted by the activated $CD8^+$ T cells plays a key role in the early phase activation of DCs during infection. Thus the GM-CSF can be defined as the licensing factor.

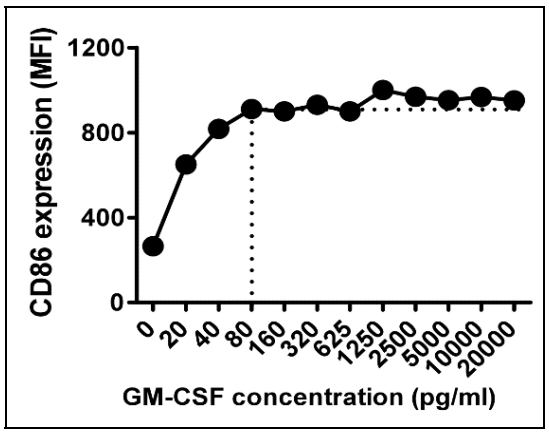

Figure 31: Stimulatory effects of recombinant GM-CSF on FLT3L DCs with a dilution series in DC activation assay. The dilution series of 20 ng/ml to 20 pg/ml recombinant GM-CSF were tested on FLT3L-DCs. After 24 h, the CD86 expression was analyzed by flow cytometry. This was repeated twice with same results.

Furthermore, after 48 h stimulation, the GM-CSF secretion from naïve $CD8^+$ T cells shoot up to a very high level. This might indicate that, during an inflammatory

response, the $CD8^+$ T cell-secreted GM-CSF also functions at the later phase of DC maturation to maintain their activated status or work as a paracrine to stimulate the neighbouring DCs, for the re-enforcement of the immune defense.

We assessed in details the capacity of different subsets of T cells to produce GM-CSF upon α-CD3/CD28 stimulations (**Fig. 32**). We compared the secretion profile of both 'classical' T cells, such as $CD8^+$ T cell subsets and $CD4^+$ T cell subsets, and specialized T cells like $NK1.1^+$ T (NKT) cells, γ/δ T cells, dendritic epidermal T cells (DETC), and regulatory T cells (T_{Reg}).

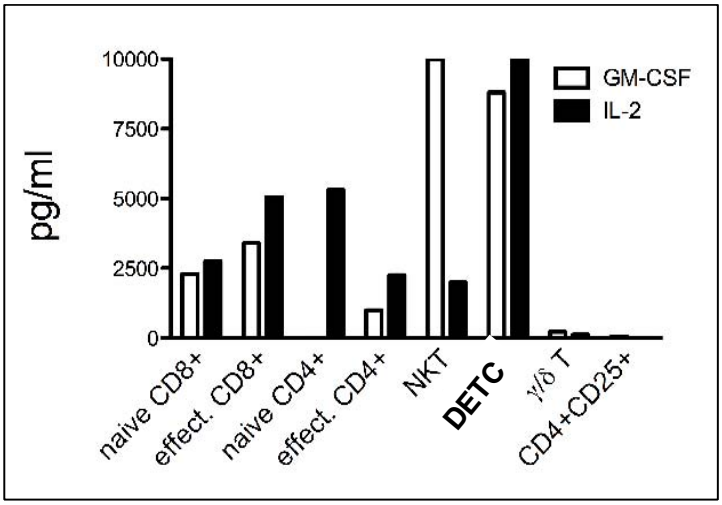

Figure 32: The GM-CSF secretion profile of different T cell subsets. GM-CSF secretion from different specialized T cell subsets after CD3/CD28 crosslinking were measured by ELISA, while IL-2 levels were meantime measured as a positive indicator of T cell activation. This represents two sets of data.

In **Fig. 32**, NKT and DETC cells were efficient to secrete extremely high levels GM-CSF secretion upon activation, indicating the importance of this GM-CSF-mediated DC maturation in their respective microenvironment. On the other hand, γ/δ T cells and T_{Reg}s produced hardly detectable amount of GM-CSF.

We next compared GM-CSF and a panel of classical DC activates in their ability to induce maturation of different DC subpopulations, including *in vitro*-derived FLT3L DCs ($CD11c^+CD11b^+$) and *ex vivo*-isolated spleen DCs (both $CD11c^+CD8^+$ and $CD11c^+CD8^-$). Interestingly, GM-CSF was one of the strongest inducers among TLR-dependent [LPS, CpG, Poly(I:C) and Zymosan] and independent (α-CD40) stimuli when tested on all DC subpopulations (**Fig. 33**). Only plasmocytoid $CD11c^+B220^+$ DCs were unresponsive towards GM-CSF due to the lack of GM-CSF receptor expression (data not shown). GM-CSF mediated upregulation was not limited to CD86 but could also be observed in CD80, CD40, as well as MHC class II expression (data not shown).

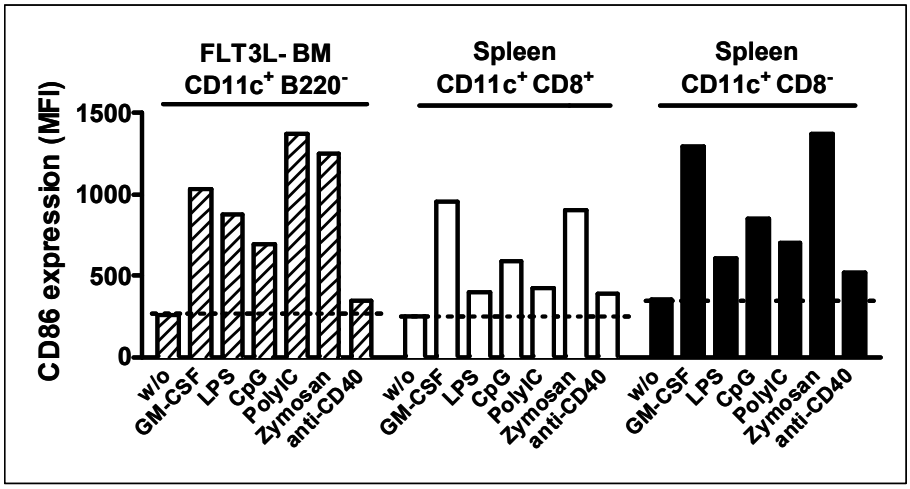

Figure 33: GM-CSF is as potent as other conventional DC stimulators. FLT3L-generated $CD11c^+CD11b^+$ DCs, spleen $CD11c^+CD8^+$ DCs, and spleen $CD11c^+CD8^-$ DCs were incubated for 48 h with 10 ng/ml GM-CSF, 1 μg/ml LPS, 2.5 μM CpG, 50 μg/ml poly(I:C), or 5 μg/ml α-CD40 antibody. CD86 surface expressions on DCs were then analyzed by flow cytometer and showed by mean fluorescence intensity (MFI). This was repeated twice.

Upregulation of costimulatory molecules on GM-CSF licensed DCs correlated with an augmented ability to support T cell proliferation. In fact, both conventional

spleen DC subsets ($CD11c^+CD8^-$ and $CD11c^+CD8^+$) induced more efficiently T cell proliferation upon 14 h stimulation with GM-CSF (**Fig. 34, a**). When GM-CSF priming activity was compared to that of potent TLR agonists, such as CpG, similar enhanced T cell stimulation could be observed (**Fig. 34, b**).

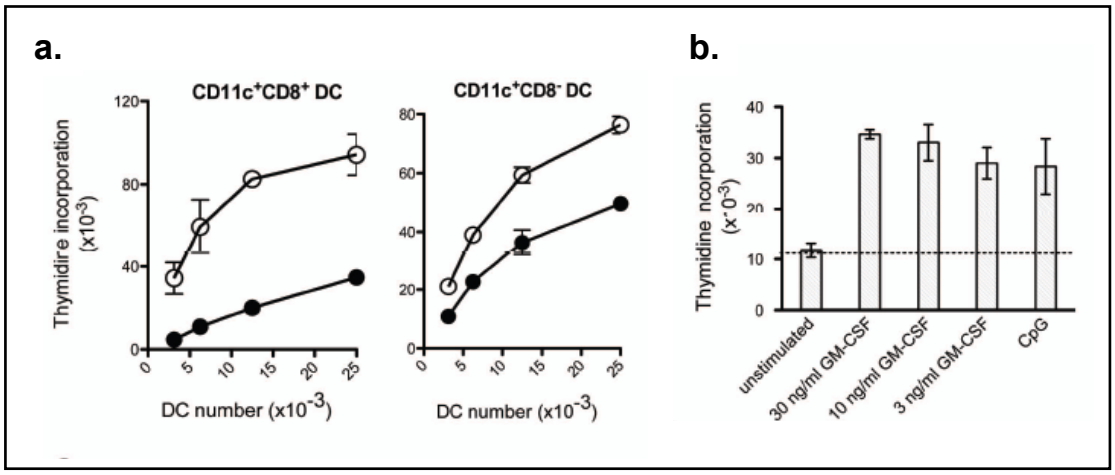

Figure 34: GM-CSF stimulated DCs showed more potent stimulatory roles in T cell proliferation. a) Spleen DCs, including both $CD11c^+CD8^+$ (left panel) and $CD11c^+CD8^-$ (right panel) groups were cultured in the presence (open cycles) and absence (filled cycles) of 10 ng/ml GM-CSF for 24 h. The DCs were then pulsed with OVA peptide and put into culture with OVA-specific $CD4^+$ T cells. 72 h later, T cell proliferation was visualized by thymidine incorporation in a 16 h pulse. b) FLT3L generate $CD11c^+CD11b^+$ DCs were stimulated for 24 h with different concentrations of GM-CSF (30, 10, 3 ng/ml) or with 2.5 µM CpG. After washing away the stimuli, cell were pulsed with OVA and co-cultured with OVA-specific T cells. 72 h later, T cell proliferation was visualized by thymidine incorporation in a 16 h pulse. This is the representitive of two sets of data.

In summary, the GM-CSF is a potent DC stimulator released by activated $CD8^+$ T cells. GM-CSF stimulated DCs support an increased T cell proliferation. The secretion of proinflammatory cytokines and the further induced T_H cell polarization was then within our interest. Data from the lab showed that GM-CSF alone was not able to stimulate proinflammatory cytokine secretion from DCs, while GM-CSF support an increased cytokine release together with other DC stimulators (data not

shown) (158). The synergistic interactions between GM-CSF and other DC stimulators stimulating different PRRs were then the topic of the next study.

5 GM-CSF stimulation alone does not induce the release of proinflammatory cytokines from DCs

The ability of mature DCs to stimulate naïve T cells is mainly determined by the expression levels of MHC and costimulatory molecules. Production of proinflammatory cytokines can influence however the outcome of T_H polarization (e.g., IL-12p70 for T_H1 priming). We measured the effects of GM-CSF on the production of several proinflammatory cytokines such as IL-12p70, IL-6, TNF-α and other DC related cytokines such as IL-10 and IL-2. However, we could not observe any modulation of the secretion of these specific cytokines when GM-CSF was the only stimulus (**Fig. 35**). The only cytokine clearly induced via GM-CSF triggering was MCP-1 (CCL2), a small cytokine belonging to the CC chemokine family involved in the recruitment of T cells as well as other cells including DCs and monocytes. Therefore, although GM-CSF strongly enhances DC maturation that ultimately leads to increased T cell activation, it alone does not trigger the secretion of proinflammatory cytokines, such as IL-12, a strong stimulator of T_H1 and CTL responses (88, 159).

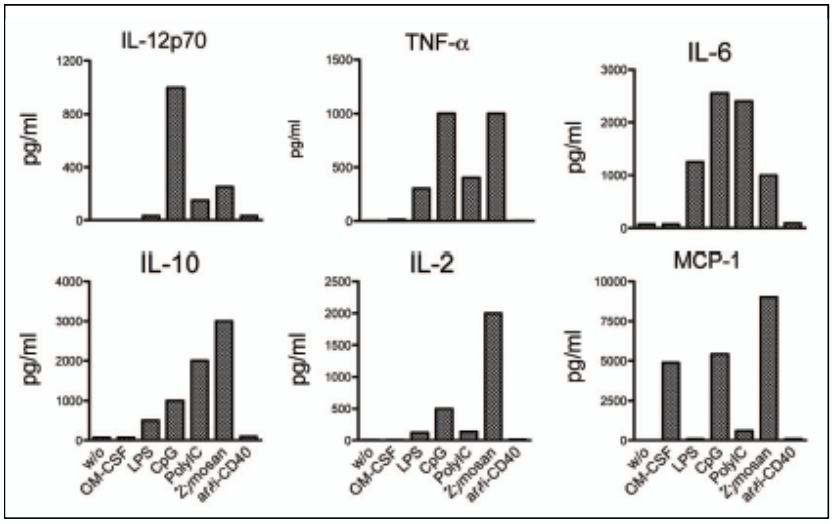

Figure 35: The release of proinflammatory cytokines upon stimulation with GM-CSF or other TLR. The FLT3L-derived BMDCs were stimulated by GM-CSF (10 ng/ml), α-CD40 (10 µg/ml), or several TLR agonists [1 µg/ml LPS, 2.5 µM CpG, 50 µg/ml poly(I:C), or 50 µg/ml zymosan]. After 24 h incubation, the supernatant was screened by ELISA. This was repeated twice to have the same data.

6 GM-CSF as a strong amplifier of β-glucan signaling

It has been described that stimulation of DCs via the CD40 requires microbial priming to induce an optional inflammatory response (160). Furthermore, direct recognition of microbial components by DC is essential for priming of an appropriate T helper cell differentiation (161). Therefore, we tested whether GM-CSF was synergizing with TLR-dependent microbial stimuli in terms of upregulation of proinflammatory cytokines. Interestingly, GM-CSF seems to have a strong facilitating effect for microbial stimuli induced cytokine release. In fact, combinations of GM-CSF with different TLR agonists, including LPS, CpG, Poly(I:C), leaded clearly to augmented IL-12p70 secretion. However, the most dramatic synergism was observed between GM-CSR and curdlan that culminated to more than 10-fold increase in IL-12p70 and 7-fold enhanced TNF-α production.

Enhanced cytokine secretion strictly correlated with a dramatic upregulation of costimulatory molecules on DCs, as shown here for CD86 (**Fig. 36**). Similar synergism could be observed in IL-6 as well as IL-2 secretion (paper submitted). These results show that GM-CSF intensifies and sustains the curdlan-mediated DC activation and that the integration of both signals allows a more effective response to potential invading pathogens than each ligand alone.

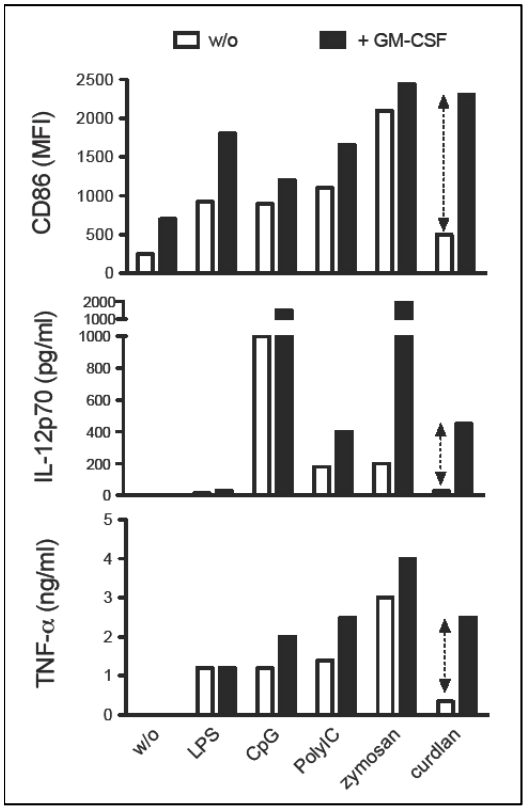

Figure 36: GM-CSF promotes the increased effects of both DC maturation and secretion of proinflammatory cytokines stimulated by other DC stimulators. The different PRR agonists, including LPS (1 μg/ml), CpG (2.5 μM), poly(I:C) (50 μg/ml), zymosan (50 μg/ml), and curdlan (100 μg/ml) were used to stimulate FLT3L-BMDCs, in the presence or absence of 10 ng/ml GM-CSF. After 24 h, CD86 expression was monitored by flow cytometer (upper panel), while IL-12p70 and TNF-α secretion was measured by ELISA (middle and lower panel). This was repeated three times with the same data.

We further analyzed the effects of curdlan/GM-CSF stimulation on IL-1β secretion. IL-1β is a highly potent proinflammatory cytokine, and its secretion depends on a multi-subunit complex called inflammasome. The NF-κB-dependent synthesis of pro-IL-1β is followed by a required danger signal, like ATP, which mediates the activation of caspase-1 and subsequently the pro-form cleavage and cytokine release.

To clarify the role of GM-CSF in IL-1β synthesis, DCs were stimulated for 16 h with curdlan in the absence or in the presence of GM-CSF and pro-IL-1β was monitored at intracellular protein level. Western blot analysis showed 5 times higher amounts of the pro-IL-1β in cells stimulated with the combination of curdlan and GM-CSF compared to cells treated with curdlan alone (**Fig. 37**).

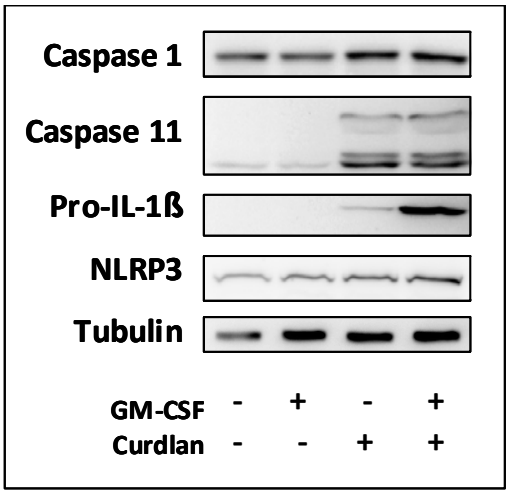

Figure 37: GM-CSF promotes increased synthesis of pro-IL-1β, but not inflammasome components. The FLT3L-derived BMDCs were cultured without or with 10 ng/ml GM-CSF and 100 μg/ml curdlan separately or in combination. After 24 h stimulation, the cells were lysed using lysis buffer and the proteins were loaded for Western analysis to target the expressions of pro-IL-1β and the inflammasome components, including pro-caspase-1, caspase-11, and NLRP3. Tubulin was used as the protein loading control. This is the representitive of two sets of experiments.

Together with pro-IL-1β we measured the components of inflammasome complex, including NLRP3, caspase-1 and caspase-11 in unstimulated and curdlan and/or GM-CSF stimulated cells. We observed that caspase-1 protein levels were similar in all tested conditions, whereas NLRP3 and caspase-11 levels were increased upon stimulation, but without any obvious differences between curdlan and curdlan/GM-CSF treatments (**Fig. 37**).

To test the effect of GM-CSF on the IL-1β production in a 'danger situation', we stimulated FLT3L-derived DCs in the presence of ATP with curdlan alone or in combination with GM-CSF. Single stimuli (GM-CSF or curdlan) did not induce any significant cytokine release, but their combination dramatically enhanced in a dose-dependent manner the secretion of IL-1β (**Fig. 38**). We ruled out the role of GM-CSF as a danger signal itself since it always needs to partner with ATP to boosts the IL-1β release (data not shown). Taken together, these results indicate that DCs require GM-CSF for increased pro-IL-1β synthesis in response to curdlan.

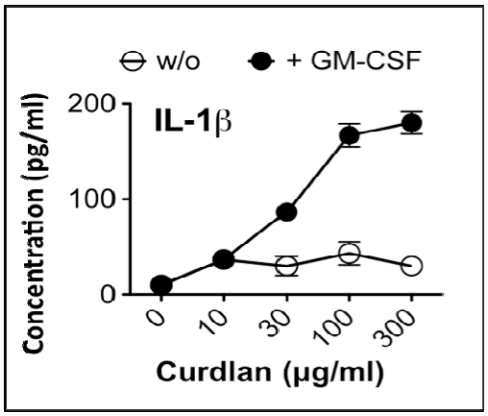

Figure 38: The secretion of IL-1β upon curdlan stimulation was synergistically increased with the addition of GM-CSF. FLT3L-derived BMDCs were stimulated by curdlan with dilution series from 300 to 10 μg/ml in the absence (white dot) or presence (black dot) of 10 ng/ml GM-CSF. After 24 h incubation, 5 mM ATP was added for 2 h. The IL-1β was detected by ELISA.

7 The synergy between GM-CSF and curdlan at NF-κB level

It is commonly accepted that the NF-κB signaling mediates the release of many proinflammatory cytokines. NF-κB activation is a complex event that does not simply lead to protein synthesis, but includes a series of phoshporylation and degradation steps which eventually lead to the nuclear translocation of NF-κB subunits, functioning as transcription factors in the nuclei for regulation of gene expressions. Hence, we focused more in detail on the NF-κB signaling pathways.

We analyzed the effect of our different stimuli on the phosphorylation and degradation of IκBα by stimulating FLT3L-derived $CD11b^+$ BMDCs for 2 h with curdlan and GM-CSF alone or in combination. As shown in **Fig. 39**, co-stimulation with both stimuli resulted in an enhanced IκBα phosphorylation and also degradation when compared to cells stimulated with curdlan or GM-CSF alone.

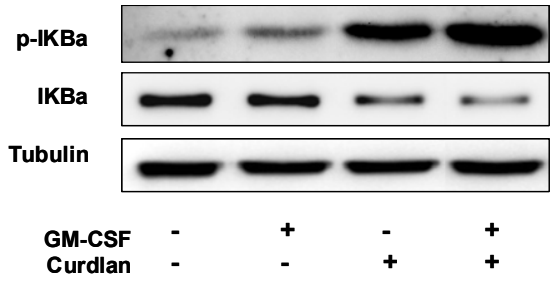

Figure 39: GM-CSF provided the stimulatory signals for IκBα phosphorylation and degradation. The FLT3L-derived BMDCs were put into stimulation without or with 10 ng/ml GM-CSF and 100 μg/ml curdlan separately or the combination for 2 h. Samples were then collected via cell lysis and applied into acrylamide gel for Western blotting. α-phospho-IκBα antibody was used as the primary antibody to detect its activation status. α-IκBα antibody was used to detect the total IκBα protein levels. Tubulin was used as the protein loading control.

Furthermore, we observed that co-stimulation of DCs supported augmented nuclear translocation of different NF-κB subunits. Nuclear fractions of differently stimulated FLT3L-derived $CD11b^+$ BMDCs were prepared with 16 h stimulation. The NF-κB subunit c-Rel was detected by Western blot, while other subunits were measured by NF-κB ELISA. In fact, p65, p50, RelB, p52 as well as c-Rel were clearly detectable in nuclear extracts of DCs co-treated with curdlan and GM-CSF (**Fig. 40**), results that are consistent with the observed increased proinflammatory cytokine and chemokine responses.

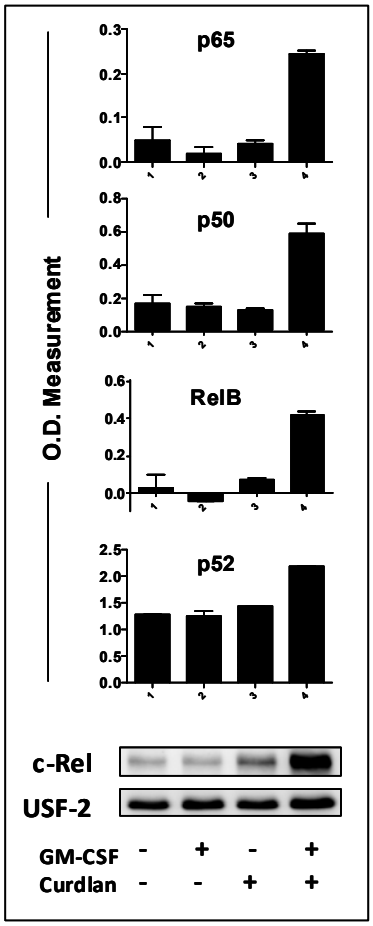

Figure 40: GM-CSF strongly promoted the increased nuclear translocation of all NF-κB subunits. The FLT3L-derived BMDCs were stimulated with either 10 ng/ml GM-CSF or 100 μg/ml curdlan, or in combination of both for 20 h. The nuclear fractions were then

extracted using home-made buffers, followed by Western analysis to target c-Rel. DNA-binding protein USF-2 was used as the loading control. The same nuclear samples as used in c-Rel Western were applied in the NF-κB ELISA to test the other subunits, including p65, p50, RelB and p52. Stimulation conditions were shown below. This is the representitive of two sets of data.

8 Deciphering the signaling integration points

Based on the so far elaborated data, the signaling integration sites for both GM-CSF and curdlan-induced pathways, which boosted the synergistic effects on cytokine release, were especially within the interests to be deciphered. We thus targeted the downstream molecules for both GM-CSF and curdlan signaling pathways.

8.1 Tracking the signaling adaptors of both GM-CSF and curdlan pathways

First we analyzed the signaling pathway induced by engagement of the GM-CSF receptor. An equal phosphorylation pattern of JAK2 and STAT5 could be visualized only in the DCs with GM-CSF stimulation, alone or in combination with curdlan (**Fig. 41**), whereas the unstimulated cells as well as curdlan alone-stimulated cells showed negative results.

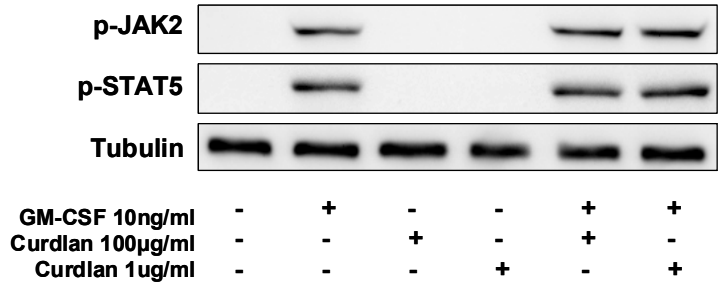

Figure 41: Curdlan does not integrate into the GM-CSF mediated JAK2-STAT5 activation for synergistic effects. The FLT3L-derived BMDCs were stimulated by GM-CSF or curdlan or in combination of both for 5 min. Cells were lysed by lysis buffer and loaded into an acrylamide gel for Western blotting, which analyzed the activation status of JAK2 an STAT5 by using α-phospho-JAK2 and α-phospho-STAT5 antibodies as the primary antobodies, respectively. The GM-CSF concentration here used was 10 ng/ml, while the curdlan concentration was either 100 μg/ml or 1 μg/ml. This was repeated twice.

We next focused on the Dectin-1 mediated NF-κB canonical pathway comprising the kinase Syk as the first upstream molecule. The intracellular staining of phopho-Syk was employed to detect its activation status. From **Fig. 42**, both curdlan and curdlan/GM-CSF induced rapid and equal Syk phosphorylation in DCs, whereas control and GM-CSF stimulation did not, which excluded Syk as an integration point of both signals (curdlan and GM-CSF).

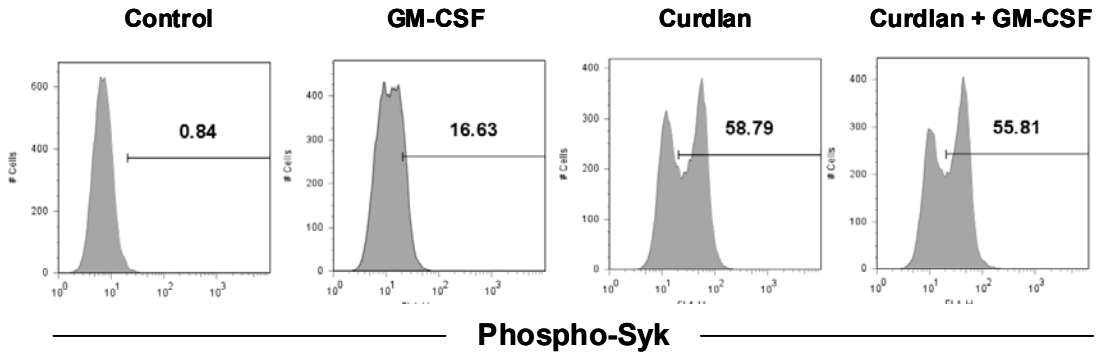

Figure 42: GM-CSF did not further increase the curdlan-induced Syk phosphorylation. FLT3L-derived BMDCs were stimulated by 10 ng/ml GM-CSF or 100 μg/ml curdlan or the combination of both. After 5 min, the cells were fixed with 2% paraformaldehyde in PBS, and permeabilized by 0.1% saponin for α-phospho-Syk antibody intracellular staining. α-Syk antibody was also used in this intracellular staining to capture the levels of total Syk proteins in different samples, which were all at the same level (data not shown), as the standard.

The non-canonicl adaptor Raf-1, downstream of Dectin-1, was also screened via intracellular staining. However, the staining of phospho-Raf-1 was always too weak

to demonstrate the potential differences upon stimulations (data not shown), which might be due to the low targeting resolution of the primary antibody used in the experiment.

The Syk-induced downstream adaptor PLCγ2, which was reported in many other literatures as key player for Syk signaling (80, 162), was also included in our study. The results of its Western blot are given in **Fig. 43**.

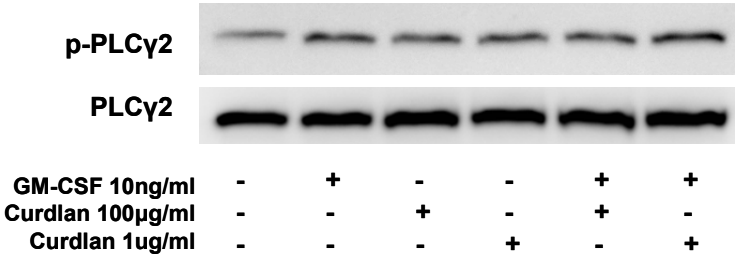

Figure 43: PLCγ2 activation status did not change upon GM-CSF and/or curdlan stimulations. The FLT3L-derived BMDCs were stimulated by GM-CSF or curdlan or the combination of both for 5 min. Cells were lysed by lysis buffer and loaded onto an acrylamide gel for Western blotting, which analyzed the activation status of PLCγ2 by using α-phospho-PLCγ2 as the primary antobody. The GM-CSF concentration used here was 10 ng/ml, while the curdlan concentration was either 100 μg/ml or 1 μg/ml.

Additionally, the intracellular staining of phospho-PLCγ2 was performed and the results are shown in **Fig. 44**.

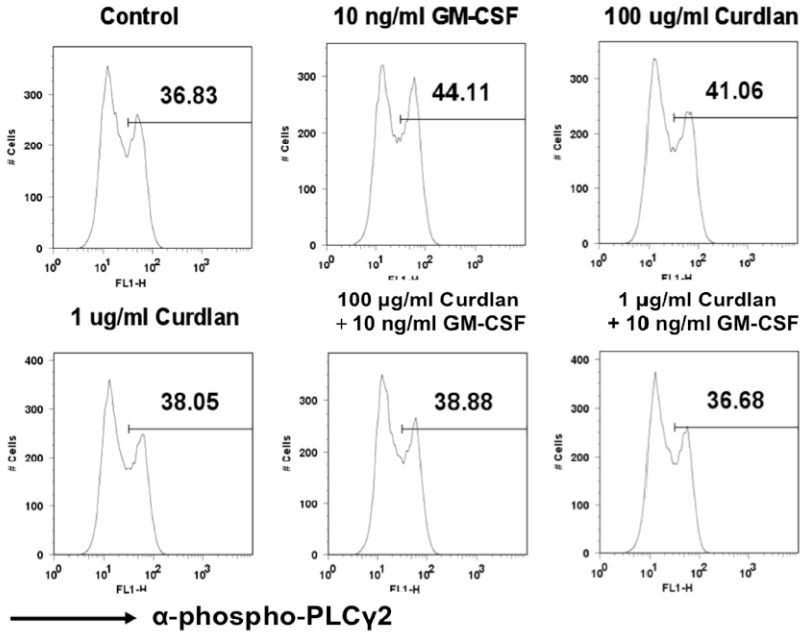

Figure 44: Intracellular staining of phospho-PLCγ2. FLT3L-derived BMDCs were stimulated by 10 ng/ml GM-CSF, 100 μg/ml or 1 μg/ml curdlan or the combination of both. After 5 min stimulation, the cells were fixed with 2% paraformaldehyde in PBS, and permeabilized by 0.1% saponin for phospho-PLCγ2 staining.

From both **Fig. 43** and **Fig. 44**, even after stimulation, the activation of PLCγ2 did not show any significant differences compared with the one from the unstimulated cells. From the published data, FLT3L signaling might trigger PLCγ2 activation, thus the possible explanation of the even activation among untreated and differentially treated DCs could be the pre-activation of PLCγ2 in the FLT3L culture.

In order to remove the stimulatory effects from FLT3L during FLT3L-derived BMDCs' development, the 7-day BMDCs were washed and resuspended into SF-IMDM with 2% FCS without addition of FLT3L for starvation of the cells. After incubation for different time periods, the cells were prepared as usual for Western analysis to visualize PLCγ2. The results were summarized in **Fig. 45**.

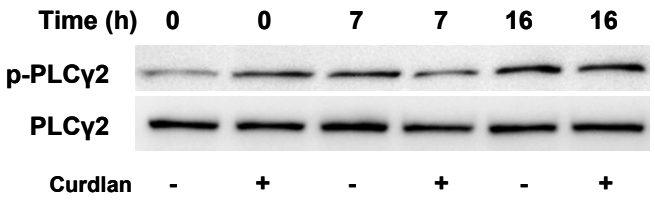

Figure 45: Visulization of PLCγ2 activation status in starvation experiment. The BMDCs from FLT3L culture were washed and incubated in normal medium (SF-IMDM with 2% FCS) for starvation. After different time, 0 h, 7 h and 16 h, the cells were stimulated for 5 min in the presence or absence of curdlan (100 µg/ml) and prepared for Western blotting. α-phospho-PLCγ2 was used to detect the protein activation while α-PLCγ2 was used to detect the total protein levels in the cells.

From the data, starvation via removing FLT3L from the BMDCs did not erase the pre-stimulated PLCγ2 activities. Even after starvation, the cells were showing basal levels of PLCγ2 phosphorylation, which could not be further increased by curdlan stimulation. Therefore, the studies of PLCγ2 did not contribute much to explain the signaling stories in the GM-CSF and curdlan synergy. The same happened to our Syk and Raf-1 studies. In this case, some other adaptor molecules, potentially involved in the signaling transduction, might be targeted to elucidate the signaling integration between these two stimuli.

8.2 The phospho-proteomic approach via ERLIC coupled LC/MS

Aiming to screen for new targets for our signaling studies to figure out the signaling interactions between GM-CSF and curdlan, we thus employed a proteomics approach with the help from Mass Spectrometry. According to Gan, et. al., ERLIC coupled LC/MS could efficiently enrich the phospho-peptides and eventually identify the signaling proteins (163).

However, this large-scale proteomics screening required a much higher abundance of protein samples for a better resolution. In this case, we employed the HOX-B4 transduced BM cells to prepare the FLT3L-derived DCs. The HOX-B4 line allowed a higher proliferation and longer lifespan of the BM cells in culture, as described by Ruedl et. al. (164). With these cells as the source for DC preparation, we could easily increase the amount of cells prepared for proteomics studies. In order to confirm the reliability of using these cells for our studies, functions of HOX-B4 BMDCs were screened using our routine DC maturation assay and the data is given in **Fig. 46**. To summarize, the HOX-B4 BMDCs responded similarly as the normal BMDCs upon stimulations and made a reliable resource for the ERLIC coupled LC/MS studies.

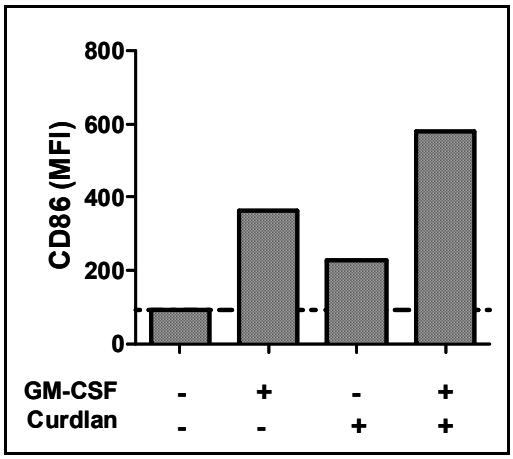

Figure 46: The FLT3L-derived HOX-B4 BMDCs showed similar activation patterns as normally as primary BMDCs in the DC maturation assay. The HOX-B4 transduced BM cells were cultured using FLT3L for 7 days. Cells were screened in the DC maturation assay for their responses upon GM-CSF (10 ng/ml) and curdlan (100 µg/ml) stimulations. CD86 mean fluorescence intensity was used to visualize DC maturation in flow cytometer analysis.

Two samples were successfully prepared and sent for proteomics identification. Sample 1 was the HOX-B4 BM-DCs stimulated with curdlan (100 µg/ml) and

sample 2 was the one stimulated with curdlan (100 μg/ml) combined with GM-CSF (10 ng/ml). Due to the limited resources, we did not include the unstimulated cells or the cells treated with GM-CSF alone.

Table 6 shows a summary of the potential interesting candidates which were differentially phosphorylated upon stimulation with curdlan alone or in combination with GM-CSF. The scores in their respective columns correlated with the levels of phosphorylation. The targeted candidates showed enhanced phosphorylation when applying GM-CSF together with curdlan compared to curdlan alone.

Gene	Curdlan	Curdlan +GM-CSF	Functions
Niban	187	353	Regulation of a.a. phosphorylation
Pak1	87	184	ATP binding, dendrite development, a.a. phosphorylation
Cdc2l1	77	110	ATP binding, a.a. phosphorylation, serine/threonine kinase
Arhgap25	74	196	GTPase activity, intracellular signaling transduction
Arhgap27	67	156	Rac GTPase, Cdc42 GTPase, clathrin-mediated endocytosis
CCr7	65	100	C-C chemokine receptor, G-protein coupled signaling, immune
Prkar2a	50	70	cAMP-dependent protein kinase, a.a. phosphorylation
Prkcd	*-1*	*236*	ATP binding, Ig, IL-10, IL12, Intracellular signling
Naca	*-1*	*178*	Coactivator of JUN, binding to DNA and stabilizing interaction of JUN heterodimer with the target gene promoters
Ptpra	*-1*	*85*	Receptor-type protein tyrosine phosphatase, dephosphorylate and activate Src
Cds2	*-1*	*70*	Second messenger downstream of G-PC receptors and Tyr kinases
Pak2	*-1*	*69*	ATP binding, Ser/Thr, Target of small GTP BP (CDC42, RAC1)
Pi4k2a	*-1*	*68*	1-phosphatidylinsositol 4-kinase activity, ATP binding
Slk	*-1*	*57*	ATP binding, DNA binding, Ser/Thr kinase
Gpn1	*-1*	*53*	ATP binding, nucleoside-triphosphatase
Ptplad1	*-1*	*52*	IkBkinase/NFkB, JNK, Rho protein signaling
CCr2	*-1*	*50*	C-C chemokine receptor, G-PC receptor, humoral immu response
Asap1	*-1*	*49*	ARF GTPse activator, zinx ion binding
Ric8a	*-1*	*47*	Guanyl-nucleotide exchange factor, enhancing G-C R medi-. ERK
Akap8	*-1*	*45*	DNA binding, binds to PKA R11 subunit
CD44	*-1*	*38*	Hyaluronic acid receptor, lymphocyte acti-, recircu- & homing

Table 6: List of candidates for potential signaling studies summarized from ERLIC-coupled LC/MS screening. The samples were prepared from FLT3L-derived HOX-B4 BMDCs. After $CD11b^+$ purification, the cells were stimulated by curdlan (100 µg/ml) (Sample 1) or curdlan in combination with GM-CSF (10 ng/ml) (Sample 2) for 20 min. The cells were then lyzed and standardized for MS sample preparation by in-gel digestion. The digested samples were sent for ERLIC-coupled LC/MS and protein identification. The MS results were studied with referring to literatures and NCBI protein database and potentially targeted candidates for signaling studies were summarized in this table.

From **Table 6**, the enhanced phosphorylation of three molecules, PAK1, Cdc2l1, and PAK2, was especially interesting because Cdc2l1 is the upstream molecule for both PAK1 and PAK2, which transduce the signaling to activate MAPKs, possibly including ERK, p38 and JNK. Therefore, we next focused on the PAK1 analysis. Direct detection of PAK1 phosphorylation from the cell lysate failed because of its low abundance (data not shown). To enrich the protein, immunoprecipitation using α-PAK1 was performed followed by Western blotting to detect both α-p PAK1 and α-PAK1. From **Fig. 47**, the enrichment did not improve much the p-PAK1 detection, whereas the total PAK1 was detected, indicating the success of the immunoprecipitation process. One possible reason for the difficulty to detect PAK-1 is still its low abundance.

Figure 47: Immunoprecipitation followed by Western blotting to detect PAK1. The BMDCs were stimulated in the absence or presence of GM-CSF (10 ng/ml) and curdlan (100 μg/ml). Samples were then subjected to immunoprecipitation using α-PAK1, followed by Western blotting to detect both p-PAK1 and total PAK1.

Besides PAK-1, the functions of the other candidates shown in **Table 6** are not studied yet and need to be investigated further.

8.3 The involvement of MAPKs in the signaling integration

Although PAK1 detection was not successful possibly due to its low abundance, we could still target its downstream molecules, which are MAPKs according to literature (165). Therefore, all of the three well-established MAPK members, including ERK, JNK, and p38, were screened using Western blot to detect their phosphorylation upon stimulation. From **Fig. 48**, the three MAPK molecules showed different activation profiles upon stimulation with GM-CSF or/and curdlan.

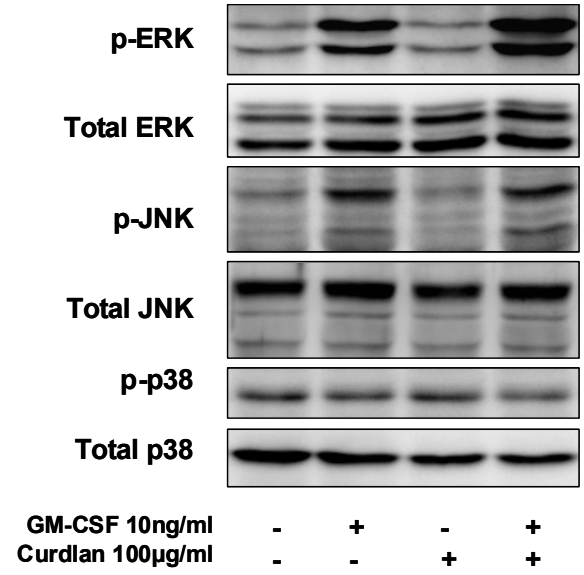

Figure 48: MAPK molecule ERK showed signaling integration for both GM-CSFR and dectin-1 pathways. The FLT3L-derived BMDCs were stimulated by 10 ng/ml GM-CSF or 100 μg/ml curdlan or in combination of both for 20 min. The cells were then lysed and loaded onto an acrylamide gel for Western blotting to detect the phospho-MAPKs, including p-ERK, p-JNK and p-38, while the total protein levels of these molecules were visualized by their respective antibodies as loading standards. This represents two sets of data.

In fact, stimulation of $CD11b^{+}$ FLT3L-derived DCs with GM-CSF induced phosphorylation of two MAPKs, JNK and ERK, whereas no increase above the basal level of phosphorylation was observed in curdlan treated DCs. In the case of

JNK the phosphorylation pattern could not be further augmented by co-treatment with curdlan/GM-CSF, whereas interestingly this was further increased in the case of ERK (**Fig. 48**). Caculation using Fujifilm software demonstrated this increase was 1.5 fold compared with curdlan stimulation along. No apparent differences in the phosphorylation of p38 were observed between the differently stimulated groups, as shown in the lowest panel of **Fig. 48**.

Taken together, we show a higher ERK pathway activity when FLT3L-derived BMDCs were co-stimulated with the combination of curdlan and GM-CSF, which could explain the increased capability of secreting proinflammatory cytokines and chemokines upon this stimulation.

DISCUSSIONS

1 GM-CSF as a major T cell-released DC maturation factor

As introduced, $CD8^+$ T cells mediated the T_H-independent DC maturation to prime the potent CTL responses (96). Using blocking α-GM-CSF antibody or GM-$CSFR^{-/-}$ DCs in our routine DC maturation assay and $CD8^+$ T cells vs DCs co-culture, I proved that the soluble factor involved in this interaction was GM-CSF (158).

GM-CSF was initially described as being able to generate both granulocyte and macrophage colonies from the precursor cells as a result of proliferation and differentiation (166, 167). The studies of GM-CSF were then focused on its roles to mediate multiple inflammatory diseases and autoimmunity, as being a potent proinflammatory cytokine (167, 168), since the proinflammatory functions are associated with the local production of GM-CSF at the site of inflammation. Hence, GM-CSF is described not only as a major regulator to control granulocyte and macrophage lineage populations at all stages of maturation, but also as an effective proinflammatory cytokine (167).

In our lab, the studies of GM-CSF were focused on its DC maturating ability during local infection. With both *in vitro* and *in vivo* approaches, GM-CSF was revealed to be the 'licensing' factor which promotes DC maturation reflected by both upregulated surface markers, including CD80, CD86, and CD40, and increased priming ability for $CD4^+$ T cell clonal expansion. However, GM-CSF signals alone do not prime the production of proinflammatory cytokine from DCs, since additional signals from PAMPs were required. The PAMPs used in our studies include LPS, CpG, poly(I:C), zymosan, and the β-glucan curdlan. In particular, when GM-CSF

was co-applied with curdlan, the most significant increase in cytokine production could be observed.

The DC maturation is a complex process integrating multiple activation stimuli. The nature, intensity and duration of these stimuli tailor the specific DC maturation which can prime a specific T cell response (38). Studies using multiple DC stimuli, including both PAMPs and proinflammatory cytokines, demonstrated that the direct recognition of microbial stimuli by DCs is the prerequisite for efficient DC maturation for the induction of T_H differentiation (161). Recently, a coordinated interaction between NK cells (IFN-γ producer), pathogen associated molecular patterns and $CD4^+$ T cells (CD40L) has been suggested as a combinatorial code for an effective IL-12p70 secretion (38). Herein, in the context of $CD8^+$ T cell/DC crosstalk, we suggest GM-CSF as a major factor in DC activation during T helper independent anti-viral responses. This process can be further regulated by viral PAMPs (as well as by other microbial PAMPs) signaling which efficiently enhances proinflammatory cytokine release by activated DCs. Combination of T cell released GM-CSF and microbial patterns then fully license DCs to prime strong CTLs. Supporting our observations, it was previously shown that GM-CSF is capable to enhance cytokine production in response to LPS and TNF (169) as well as to polarize efficiently T_H1 and T_H2 cells in combination with the yeast cell wall mixture zymosan .

Besides being secreted by $CD8^+$ T cells, GM-CSF can also be secreted $CD4^+$ T cell. However, the later do not secrete GM-CSF in their initial phase of activation, as clearly shown from our data. The GM-CSF secreting T_H effector cells include T_H1, T_H2, and newly defined T_H17. Recent studies revealed that the functions of the proinflammatory cytokine GM-CSF in the development of an autoimmune disease

called experimental autoimmune encephalomyelitis (EAE) which is associated with T_H17 cell responses (170, 171). The proinflammatory GM-CSF involved in this disease development is secreted by T_H17 cells upon stimulation from IL-23. The secreted GM-CSF feedbacks to DCs to induce more IL-23 production and supports further T_H17 activation. In addition, GM-CSF is also involved in the T_H1-mediated initiation of EAE, but the detailed mechanism for disease development is still unknown (172). This finding suggests GM-CSF as a possible target for the treatment of autoimmune diseases.

To summarize the licensing model describing $CD8^+$ T cells mediated DC maturation upon secretion of GM-CSF, the data is schematically demonstrated in **Fig. 49**, in comparison to the originally proposed licensing model.

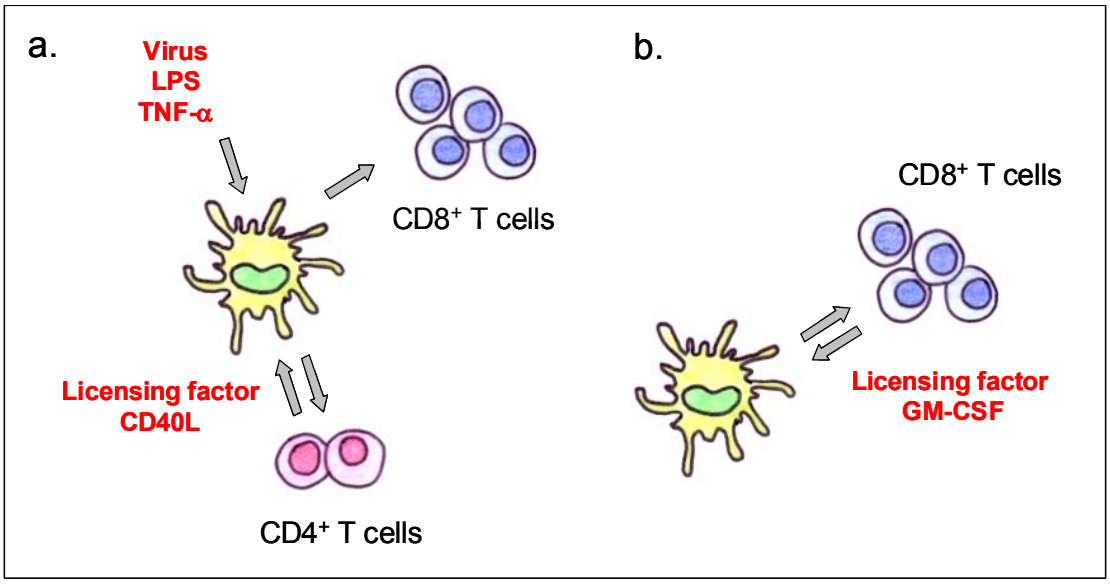

Figure 49: DC needs a license to help T-killer cells. a. In the old 'licensing' model, the licensing signals were provided by either $CD4^+$ T_H cells via CD40-CD40L ligation, or by other stimuli, e.g., virus, LPS, or TNF-α. b. In our T_H-independent 'licensing' model, DC maturation is mediated by GM-CSF, which is secreted by $CD8^+$ T cells. GM-CSF activates DCs to be the potent 'effector' cells which eventually induce T cell clonal expansion.

In the originally proposed 'licensing' model, the licensing signals were provided by either $CD4^+$ T_H cells via CD40-CD40L ligation, or by other stimuli, e.g., virus, LPS, or TNF-α (**Fig. 49, a**) (90-92). In our T_H-independent 'licensing' model, DC maturation is mediated by GM-CSF, which is secreted by $CD8^+$ T cells. GM-CSF activates DCs to be the potent 'effector' cells which eventually induce T cell clonal expansion (**Fig. 49, b**) (96, 158).

2 The T cell-derived licensing factor GM-CSF synergizes with curdlan for antifungal defense

Fungal infections have recently become a major health threat due to a rapidly increased population carrying inmunodeficient conditions, e.g., HIV, organ transplantation, cancer, etc, in which the hosts are extremely susceptible to fungal infections, as well as the emergence of fungi that are resistant to antimycotic drugs (173, 174). Antifungal adaptive immunity needs both T_H1 and T_H17 immune responses (51). IL-17 in T_H17 responses is essential for neutrophil mobilization for antifungal responses, while IFN-γ in T_H1 responses is required to activate neutrophil and the subsequent phogocytosis of fungi.

Dectin-1 is a characteristic CLR which was commonly recognized to be essential for fungal recognition and host responses (151). It recognizes a broad range of fungal species, including *Candida albicans, Aspergillus fumigatus and Pneumocystis carinni*. upon fungal recognition, Dectin-1 participates in the host defense by directly inducing intracellular signals for inflammatory responses,

resulting in pathogen clearance and persistent protection from fungal re-infection, thus linking the adaptive recognitions to adaptive immunity (175).

As an agonist for Dectin-1, the β-glucan curdlan can trigger the production of both proinflammatory and anti-inflammatory cytokines, including IL-2, IL-10 and TNF-α, marking the characteristic activation of Dectin-1 signaling (51, 54). The synergy between GM-CSF and curdlan boosts the secretion of all these cytokines, as well as some other proinflammatory cytokines, including IL-1β, IL-6 and IL-12p70 (paper submitted), while IL-12p70 was not obviously induced by curdlan stimulation alone (54).

IL-12 is a potent proinflammatory cytokine that drives T_H1 development for host defense against invading pathogens. With curdlan alone for stimulation, the IL-12 secretion was merely detected, while in combination with GM-CSF, the secretion was significantly boosted, rendering the elevated T_H1 polarization. The low levels of IL-12 secretion by curdlan might be explained by the fact that most fungi are commensal organisms, which do not induce host clearance (173). However, in the presence of an inflammatory mediator GM-CSF, whose secretion normally resulted from pathogen infection, the IL-12 secretion was efficiently elevated, with the consequence of the enhanced antifungal defense. Different from the report that declared the curdlan-induced antifungal defense biased to T_H17 direction (51), our data demonstrated the strong development of both T_H1 and T_H17 responses, both of which has been previously shown to be efficient antifungal directions.

In the inflammatory responses, the secretion of anti-inflammatory cytokine IL-10 appears to be contradictory. Indeed, the IL-10 secretion was recognized to be beneficial for the host to develop the regulatory T cell responses, for the controlled inflammatory responses and persistence of antifungal immunity for protection from

re-infection (173, 176). Similarly, the synergistically secreted IL-2 might be involved in T_{Reg} development (177).

Pathogen recognition receptors recognize highly conserved microbial and fungal patterns (40, 44, 175). Their engagement results in activation of antigen presenting cells, such as DCs, which efficiently initiate both innate and adaptive immune responses against the pathogen. It became evident during the last years that a simultaneous triggering of different PRRs is required to shape an effective pathogen specific T helper polarizing program in DCs. Synergy between distinct TRIF-coupled TLRs (TLR3 and TLR4) and endosomal TLRs (TRL7 and TLR9) (178) or between TLRs (e.g. TLR2 and TLR4) and non-TLRs (e.g. Dectin-1) (141, 142, 179) tailors a pathogen-specific immune response which is ultimately required for the final clearance of the invading microbes or fungi.

In particular, in antifungal immune responses, a synergy between Dectin-1 and two TLRs, TLR-2 and TLR-4, was extensively described. All three receptors are major recognition sites for fungal species like *Candida albicans* and their simultaneous engagement results in strong cytokine secretion and as a consequence strong antifungal innate and adaptive immunity (54, 141). Studies revealed that the secretion of IL-12 and IL-2 is TLR2 dependent and on the other hand IL-10 production is largely dependent on the major adaptor of Dectin-1, Syk (54).

In this study, we explored the capacity of GM-CSF to synergize with the β-glucan curdlan, a well-known and specific Dectin-1 agonist with immunomodulatory properties. We showed that both stimuli, when applied together, provide a strong inflammatory signature to DCs leading to the formation of potent 'effector' DCs with augmented capacity in priming efficiently T_H1, T_H17 and IL-22 secreting $CD4^+$ T helper cells and in shaping a highly specialized antifungal immune

response (data not shown). These results are in accordance with a previous work of Rosas et al, which demonstrated the crucial effect of GM-CSF in a cellular programming of a proinflammatory Dectin-1 mediated response in macrophage. Using both curdlan and glucan microparticles the authors showed that macrophages do not mount a significant proinflammatory cytokine response upon Dectin-1 engagement, which can be dramatically boosted via GM-CSF co-stimulation (180). They speculated about a GM-CSF mediated alteration of the downstream signaling components of the Syk/CARD9 and NF-κB pathways, but the exact mechanism of action was not clarified.

3 The signaling integration site in the effects of the synergy between GM-CSF and curdlan

In order to elucidate the molecular mechanism underlying this observed synergistic effect between the two different stimuli, we focused on the analysis of known signaling pathways initiated upon curdaln-specific receptor, Dectin-1, as well as GM-CSF receptor engagement. No crosstalk between these two different receptors has been described so far. It is well documented that GM-CSF activates the JAK2/STAT5, Ras/Raf/MAPK as well as PI3K/Akt pathways through its heterodimeric receptor (134). On the other hand, curdlan initiates via Dectin-1 binding a NF-κB canonical pathway comprising the kinase Syk and the adaptor proteins CARD9, BCL10 and MALT1 (52) as well as a NF-κB non-canonical pathway involving the kinase Raf-1 (143).

Dectin-1 mediated fungicidal effector mechanisms include the phagocytosis (142) and production of reactive oxygen species (149), and the later was marked by the involvement of Syk. Syk was initially reported as the key adaptor to mediate Dectin-1 signaling and to elicit a novel pattern recognition pathway, for the translation of the innate PRR recognition patterns into adaptive immune responses (54). Different approaches revealed the Syk-dependent activation of multiple signaling mechanisms, including NF-κB pathway (52, 54), MAPK pathway (181), NFAT pathway (150), and NALP3 inflammasome complex (182). Besides, a Syk-independent pathway induced by Raf-1 was recently reported to mediate the non-canonical NF-κB activation. This non-canonical signaling integrated to the Syk-mediated canonical NF-κB pathway at the Rel protein levels to regulate immune responses (143).

The possible synergistic interactions between GM-CSF and curdlan signaling are illustrated in **Fig. 50**. In summary, Dectin-1 engagement activates both the Syk-dependent canonical NF-κB pathway and the Raf-1-dependent non-canonical NF-κB pathway. GM-CSF signaling synergizes with curdlan signaling for enhanced activation of both canonical and non-canonical NF-κB subunits. Besides, Dectin-1 engagement induces the Syk-dependent NFAT activation and release of reactive oxygen species, and the later promotes NLRP3 inflammasome activation for the release of IL-1β. GM-CSF signaling might contribute to these events by direct activation of NFAT and increased expression of pro-IL-1 β through elevated NF-κB signals. The GM-CSF induced JAK2-STAT5 pathway is not involved in the synergistic interplay between GM-CSF and curdlan signaling, whereas ERK1/2 is activated by both GM-CSF and curdlan signaling. In addition, Dectin-1 signaling

may activate ERK via both Syk- and Raf-1dependent pathways. ERK is a significant integration point for both GM-CSF and curdlan signaling.

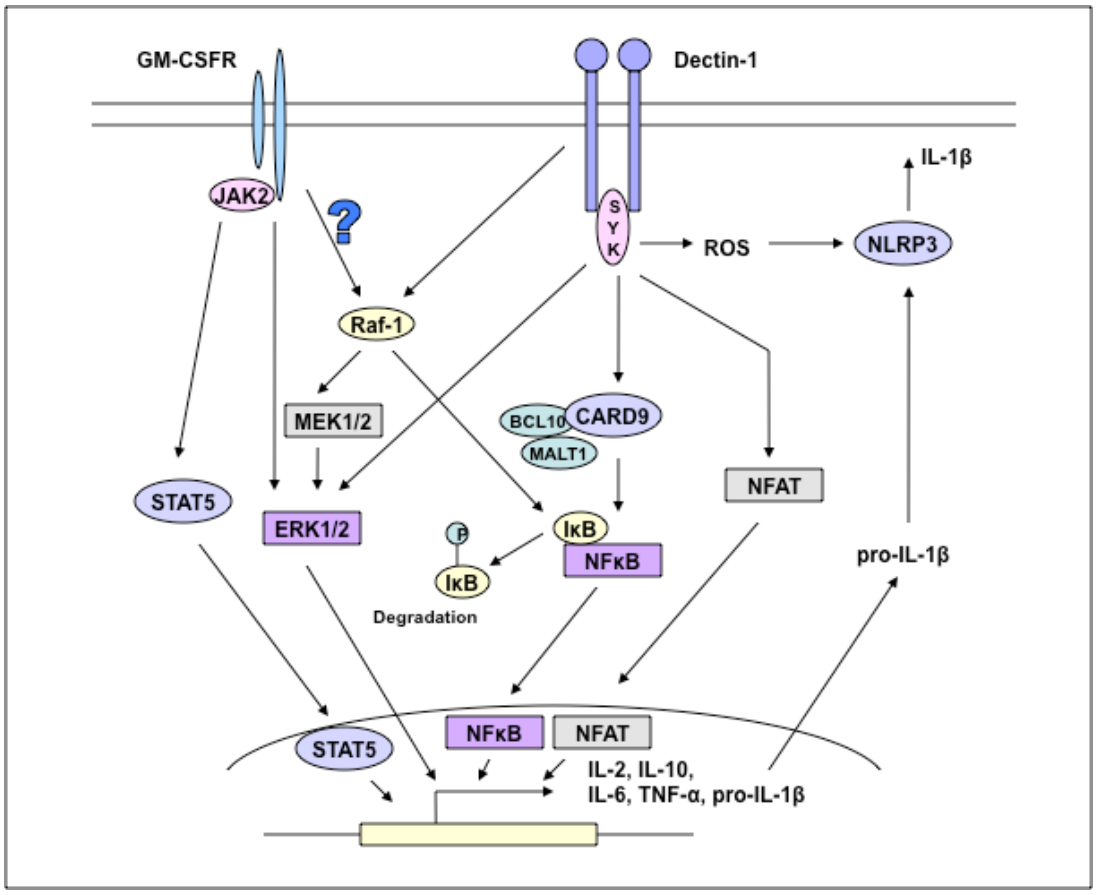

Figure 50: The signaling pathways involved in the synergistic effects between GM-CSF and curdlan. The signaling pathways induced by curdlan and GM-CSF engagement integrate at both NF-κB and MAPK ERK pathways. Other signaling pathways potentially involved in their interactions are NFAT pathway and NLRP3 inflammasome.

3.1 NFAT and inflammasome activation

The observed synergistic release of IL-2 upon combined GM-CSF and curdlan stimulation might reflect the activation of NFAT pathways, which might meanwhile trigger the Syk-dependent release of IL-10 (150). The NFAT activation coupled IL-2 and IL-10 secretion makes Dectin-1 distinct from TLRs, which do not bear this

property. The NFAT activation was proved to be the important antifungal mechanism, confirming the strong association of Dectin-1 with antifungal host defense (183).

The calcineurin-dependent dephosphorylation of NFAT and its nuclear translocation indicate its activation, and this process is normally PLCγ-dependent. As PLCγ2, rather than PLCγ1, is the major player in Dectin-1 induced Syk-dependent signaling (162), we focused on the former in our studies. However, due to the high activation status of this signaling molecule even in the absence of stimuli in our *in vitro* culture, we could not dissect the signaling integration furthermore. Additionally, the nuclear extracts from activated BMDCs were studied by Western blotting to visualize the NFAT subunit (data not shown). However, the blot showed multiple bands at the position matching the size of NFAT subunits. Thus the active form of NFAT protein cannot be clearly visualized. Therefore, we do not have enough supporting data to describe the activation status of NFAT. Further improvements on the experiments might be done aiming to explain the regulation of the NFAT activations.

IL-1β acts in cooperation with IL-23 for the T_H17 differentiation (184, 185), while its release is controlled by the key signaling complex named inflammasome (46). Syk-mediated signaling upon *C. albicans* stimulation was shown to activate the inflammasome in the absence of danger signals. The activated inflammasome function is also coupled with production of antifungal ROS (182). Consistent with this finding, our Western data showed that the curdlan stimulation elevated the expression of both pro-caspase-1 and caspase 11, while the later was more sensitive to curdlan signals. However, we did not monitor the bio-active p10 (caspase-1) release. From literature, Syk-mediated inflammasome activation is controlled by

CARD9 and induces also the pro-IL-1β expression, which is determined by the NF-κB subunit c-Rel (**Fig. 32**). The detailed regulation of pro-IL-1β expression will be discussed later.

3.2 Significance of synergistic NF-κB activation

Syk-mediated NF-κB activation was among the earliest Dectin-1-induced downstream signaling pathways discovered (52, 54). In the canonical pathway, CARD9 plays a key role in signaling transduction to activate p65 nuclear translocation (52). This function is supported by BCL10 and MALT1, which form a scaffold complex with CARD9 to relay the signals to downstream effectors. More evidences confirmed the CARD9-induced canonical NF-κB pathway, with nuclear translocation of two canonical NF-κB subunits, p65 and c-Rel (143). In addition, Syk also induces the non-canonical pathway to activate RelB molecule, which is a non-canonical NF-κB subunit. This signaling is dependent on NIK adaptor (143). Besides Syk, the non-canonical pathway Dectin-1 activation can also be induced by adaptor Raf-1, which was commonly recognized as a key player in the MAPK cascade Raf-1-MEK1/2-ERK1/2 (109). With Raf-1 activation, the non-canonical NF-κB subunit RelB is inactivated while translocated into the nucleus (143).

Although the Raf-1-dependent pathway is Syk-independent, it eventually integrates to the Syk-signaling at the NF-κB levels, to increase the Syk-induced p65 transactivation and to repress the Syk-induced RelB activation (143). This integration is established by the phosphorylation of p65 at Ser276, which results in both RelB inactivation and p65 acetylation. RelB inactivation is determined by the

formation of inactive p65-RelB dimers. And this inactivation efficiently releases the expression of IL-12p40 and IL-1β from RelB repression. In addition, the acetylation of p65 results in elevated expression of IL-10, IL-6, and IL-12p35, while IL-12p40 is upregulated in a RelB-independent manner. However, IL-23p19 expression is regulated by a different pathway and is c-Rel-dependent. Threfore, the p65 transactivation may inhibit its expression, resulting in decreased formation of IL-23, which is a major player for T_H17 development. Raf-1-induced non-canonical NF-κB activation plays the key roles in the tailoring of the cytokine secretion and subsequent T_H effector differentiation, adjusting the T_H lineages to T_H1 with the increased secretion of IL-12. Besides T_H1, the T_H17 differentiation is also regulated.

From our data, the combined effects from GM-CSF significantly elevated the curdlan-induced NF-κB subunits. This applied to all five NF-κB subunits, including p65, p50, RelB, p52, and c-Rel. With curdlan stimulation alone, their activation levels varied, but were generally comparable to control, which is the steady state level. Compared with the data from Gringhuis, et. al., the p65 activation from our data was too low, whereas c-Rel and RelB activation was more significant. The difference in p65 signals might be explained by the FLT3L DCs we used compared with the commonly used GM-CSF DCs. When co-stimulated with GM-CSF, we observed the synergistically elevated activation of all NF-κB subunits, including both canonical and non-canonical ones. Previous studies have demonstrated that Dectin-1 induces all NF-κB subunits activation. This activation depends on the adaptors CARD9 and BCL10, while MALT1 controls only c-Rel activation (174). Based on this information, GM-CSF might potentially target CARD9 or BCL10, for the enhanced curdlan-induced NF-κB signaling, which could be analyzed later.

The elevated RelB and c-Rel translocation might indicate regulatory role of the Raf-1 induced non-canonical NF-κB pathway. The regulated gene might be IL-35. Meanwhile, the augmented activation of the canonical subunits, c-Rel and p65, induces upregulation of IL-1β and IL-6, supporting the T_H17 lineage differentiation, while the IL-12 production drives the T_H1 lineage differentiation (77). The synergistic secretion of IL-10 could also be explained by the canonical NF-κB activation and it is essential for the regulatory T cell functions as mentioned.

3.3 Signaling integration at ERK

The signaling from GM-CSF and curdlan integrate at ERK, which is the typical MAPK molecule regulating cell growth and proliferation (109). The elevated ERK activation was reflected by its amplified phosphorylation upon curdlan/GM-CSF co-stimulation compared with their respective stimulation alone. However, different from previous evidences showing the Syk-induced ERK activation (51, 181), curdlan stimulation from our hands did not augment ERK phosphorylation from its basal levels. This might be again explained by the FLT3L-derived BMDCs we used in the experiments. In contrast, GM-CSF-derived BMDCs were applied in the published studies (51, 181).

ERK activation by GM-CSF signaling has been well documented by many studies for the inhibition of apoptosis and promotion of inflammatory responses (134, 186). In contrast, the zymosan-induced Syk-dependent ERK activation was newly defined (181). Similar to zymosan, curdlan may also elicit ERK activation, although it was not obviously visible from our results. Syk-induced ERK activation transduces the signals for IL-2 and IL-10 expression. This expression is TLR-

independent. With the joint activation signaling from both pathways, the ERK activation was significantly elevated (1.5 fold increase), while the synergistic release of IL-2 and IL-10 might be its consequence.

In contrast to ERK, the JNK and p38 were not detected to play any roles in the synergistic effects between GM-CSF and curdlan. Different from p38, which did not respond to any stimuli, the JNK was activated by GM-CSF signaling, already shown by other studies. However, addition of curdlan did not further elevate its activation.

3.4 The cooperation between different signaling pathways

Upon stimulation of GM/CSF and curdlan, the synergistically activated intracellular signaling pathways include the NF-κB pathway and the ERK pathway, while the activation of the inflammasome and the NFAT pathway is not clearly identified from our data. It was clear that the observed synergistic phenotype resulted from the combined effects of all these pathways, but how they regulate each other to induce the synergistic phenotype is still unclear.

We postulate that the GM-CSF activated ERK signaling may recruit Raf-1 as upstream adaptor. An activated Raf-1 also participates in the non-canonical pathway from curdlan stimulation, to further strengthen this pathway for the augmented release of IL-10 and IL-6. The regulatory role of Raf-1 on NF-κB functions has been described in the synergistic interactions between DC-SIGN and TLRs (140). Consistent with this study, GM-CSF induced Raf-1 plays the same regulatory role for the curdlan-induced NF-κB activations. More evidences comes from the demonstrated regulatory role of MEKK1 on IκBα for its activation (187), while same as Raf-1, MEKK1 belongs to the MAPK kinase kinse family.

The NF-κB signaling might reciprocally regulate the MAPK pathways. A signaling adaptor for NF-κB signaling transduction, Tpl2, was shown to activate ERK signals (188, 189). Whether Tpl2 is employed by Syk-induced NF-κB pathway is still unknown and has to be elucidated.

Last but not least, the signaling scaffold complex, CARD9-BCL2-MALT1, was shown to play an important role in canonical NF-κB signaling transduction and controls the activation of all NF-κB subunits (52, 174), which made this complex an interesting target for the further explanations of the synergistic effects upon combined GM-CSF and curdlan stimulations.

4 Postulation of a new antifungal adjuvant combining GM-CSF and curdlan and its potential delivery approaches

In summary, the synergistic effects between GM-CSF and curdlan activate multiple signaling pathways, including the NF-κB pathway, the MAPK pathway and the NFAT pathway. Here we show that, in the presence of curdlan, GM-CSF can provide a potent inflammatory signal to DCs to ensure a robust production of cytokines and chemokines, and to induce subseμquently T_H cell polarization. Our results strongly suggest that the fungal invasion-induced inflammatory signals are needed to prime and induce effective innate and adaptive immunity for anti-fungal defense. Furthermore, IL-10 and IL-2 produced during fungal infection might be involved in the regulatory functions for the host to control the fungal clearance.

Our findings might be relevant for the design of novel adjuvant formulations which are more effective in priming strong antifungal inflammatory responses. GM-

CSF has been extensively studied for its applications as an adjuvant in cancer treatment, on the other hand, neutralization of GM-CSF was shown to relieve inflammatory and autoimmune diseases (168). Curdlan was recently proposed as a microparticle for vaccine delivery (190, 191). Based on our results, we suggest potentiating its effects via co-administration with GM-CSF.

In conclusion, with the combination of GM-CSF, curdlan might play better roles *in vivo* for DC activation and subsequent derivation into a potent 'natural adjuvant' bearing antifungal functions.

REFERENCES

1. Steinman, R.M., and Z.A. Cohn. 1973. Identification of a novel cell type in peripheral lymphoid organs of mice. I. Morphology, quantitation, tissue distribution. *Journal of Experimental Medicine* 137:1142-1162.
2. Reis E Sousa, C. 2004. Activation of dendritic cells: Translating innate into adaptive immunity. *Current Opinion in Immunology* 16:21-25.
3. Steinman, R.M., D. Hawiger, and M.C. Nussenzweig. 2003. Tolerogenic dendritic cells. Annual Review of Immunology 21:685-711.
4. Steinman, R.M. 2003. The control of immunity and tolerance by dendritic cells. *Pathologie Biologie* 51:59-60.
5. Heath, W.R., and F.R. Carbone. 2009. Dendritic cell subsets in primary and secondary T cell responses at body surfaces. *Nature Immunology* 10:1237-1244.
6. Wilson, N.S., and J.A. Villadangos. 2004. Lymphoid organ dendritic cells: Beyond the Langerhans cells paradigm. *Immunology and Cell Biology* 82:91-98.
7. Shortman, K., and Y.J. Liu. 2002. Mouse and human dendritic cell subtypes. *Nature Reviews Immunology* 2:151-161.
8. Morelli, A.E., and A.W. Thomson. 2007. Tolerogenic dendritic cells and the quest for transplant tolerance. *Nature Reviews Immunology* 7:610-621.
9. Palm, N.W., and R. Medzhitov. 2009. Pattern recognition receptors and control of adaptive immunity. *Immunological Reviews* 227:221-233.
10. Naik, S.H. 2008. Demystifying the development of dendritic cell subtypes, a little. *Immunology and Cell Biology* 86:439-452.
11. Serbina, N.V., and E.G. Pamer. 2006. Monocyte emigration from bone marrow during bacterial infection requires signals mediated by chemokine receptor CCR2. *Nature Immunology* 7:311-317.
12. Yrlid, U., C.D. Jenkins, and G.G. MacPherson. 2006. Relationships between distinct blood monocyte subsets and migrating intestinal lymph dendritic cells in vivo under steady-state conditions. *Journal of Immunology* 176:4155-4162.
13. Gordon, S., and P.R. Taylor. 2005. Monocyte and macrophage heterogeneity. *Nature Reviews Immunology* 5:953-964.
14. Inaba, K., M. Inaba, N. Romani, H. Aya, M. Deguchi, S. Ikehara, S. Muramatsu, and R.M. Steinman. 1992. Generation of large numbers of dendritic cells from mouse bone marrow cultures supplemented with granulocyte/macrophage colony-stimulating factor. *Journal of Experimental Medicine* 176:1693-1702.
15. Inaba, K., R.M. Steinman, M.W. Pack, H. Aya, M. Inaba, T. Sudo, S. Wolpe, and G. Schuler. 1992. Identification of proliferating dendritic cell precursors in mouse blood. *Journal of Experimental Medicine* 175:1157-1167.
16. Sallusto, F., and A. Lanzavecchia. 1994. Efficient presentation of soluble antigen by cultured human dendritic cells is maintained by granulocyte/macrophage colony-stimulating factor plus interleukin 4 and downregulated by tumor necrosis factor α. *Journal of Experimental Medicine* 179:1109-1118.

17. Zhou, L.J., and T.F. Tedder. 1996. CD14+ blood monocytes can differentiate into functionally mature CD83+ dendritic cells. *Proceedings of the National Academy of Sciences of the United States of America* 93:2588-2592.
18. O'Keeffe, M., H. Hochrein, D. Vremec, I. Caminschi, J.L. Miller, E.M. Anders, L. Wu, M.H. Lahoud, S. Henri, B. Scott, P. Hertzog, L. Tatarczuch, and K. Shortman. 2002. Mouse plasmacytoid cells: Long-lived cells, heterogeneous in surface phenotype and function, that differentiate into CD8- dendritic cells only after microbial stimulus. *Journal of Experimental Medicine* 196:1307-1319.
19. Nakano, H., M. Yanagita, and M.D. Gunn. 2001. CD11c+B220+Gr-1+ cells in mouse lymph nodes and spleen display characteristics of plasmacytoid dendritic cells. *Journal of Experimental Medicine* 194:1171-1178.
20. Gilliet, M., W. Cao, and Y.J. Liu. 2008. Plasmacytoid dendritic cells: Sensing nucleic acids in viral infection and autoimmune diseases. *Nature Reviews Immunology* 8:594-606.
21. Di Pucchio, T., B. Chatterjee, A. Smed-Sörensen, S. Clayton, A. Palazzo, M. Montes, Y. Xue, I. Mellman, J. Banchereau, and J.E. Connolly. 2008. Direct proteasome-independent cross-presentation of viral antigen by plasmacytoid dendritic cells on major histocompatibility complex class I. *Nature Immunology* 9:551-557.
22. Yoneyama, H., K. Matsuno, E. Toda, T. Nishiwaki, N. Matsuo, A. Nakano, S. Narumi, B. Lu, C. Gerard, S. Ishikawa, and K. Matsushima. 2005. Plasmacytoid DCs help lymph node DCs to induce anti-HSV CTLs. *Journal of Experimental Medicine* 202:425-435.
23. Curtsinger, J.M., J.O. Valenzuela, P. Agarwal, D. Lins, and M.F. Mescher. 2005. Cutting edge: Type I IFNs provide a third signal to CD8 T cells to stimulate clonal expansion and differentiation. *Journal of Immunology* 174:4465-4469.
24. Vremec, D., J. Pooley, H. Hochrein, L. Wu, and K. Shortman. 2000. CD4 and CD8 expression by dendritic cell subtypes in mouse thymus and spleen. *Journal of Immunology* 164:2978-2986.
25. Villadangos, J.A., and P. Schnorrer. 2007. Intrinsic and cooperative antigen-presenting functions of dendritic-cell subsets in vivo. *Nature Reviews Immunology* 7:543-555.
26. Naik, S.H., D. Metcalf, A. van Nieuwenhuijze, I. Wicks, L. Wu, M. O'Keeffe, and K. Shortman. 2006. Intrasplenic steady-state dendritic cell precursors that are distinct from monocytes. *Nature Immunology* 7:663-671.
27. Shortman, K., and S.H. Naik. 2007. Steady-state and inflammatory dendritic-cell development. *Nature Reviews Immunology* 7:19-30.
28. Liu, K., C. Waskow, X. Liu, K. Yao, J. Hoh, and M. Nussenzweig. 2007. Origin of dendritic cells in peripheral lymphoid organs of mice. *Nature Immunology* 8:578-583.
29. Wilson, N.S., D. El-Sukkari, G.T. Belz, C.M. Smith, R.J. Steptoe, W.R. Heath, K. Shortman, and J.A. Villadangos. 2003. Most lymphoid organ dendritic cell types are phenotypically and functionally immature. *Blood* 102:2187-2194.
30. De Smedt, T., B. Pajak, E. Muraille, L. Lespagnard, E. Heinen, P. De Baetselier, J. Urbain, O. Leo, and M. Moser. 1996. Regulation of dendritic

cell numbers and maturation by lipopolysaccharide in vivo. *Journal of Experimental Medicine* 184:1413-1424.
31. Sung, S.S.J., S.M. Fu, C. Edward Rose Jr, F. Gaskin, S.T. Ju, and S.R. Beaty. 2006. A major lung CD103 (αE)-β7 integrin-positive epithelial dendritic cell population expressing langerin and tight junction proteins. *Journal of Immunology* 176:2161-2172.
32. Bursch, L.S., L. Wang, B. Igyarto, A. Kissenpfennig, B. Malissen, D.H. Kaplan, and K.A. Hogquist. 2007. Identification of a novel population of Langerin+ dendritic cells. *Journal of Experimental Medicine* 204:3147-3156.
33. Poulin, L.F., S. Henri, B. De Bovis, E. Devilard, A. Kissenpfennig, and B. Malissen. 2007. The dermis contains langerin+ dendritic cells that develop and function independently of epidermal Langerhans cells. *Journal of Experimental Medicine* 204:3119-3131.
34. Ginhoux, F., M.P. Collin, M. Bogunovic, M. Abel, M. Leboeuf, J. Helft, J. Ochando, A. Kissenpfennig, B. Malissen, M. Grisotto, H. Snoeck, G. Randolph, and M. Merad. 2007. Blood-derived dermal langerin+ dendritic cells survey the skin in the steady state. *Journal of Experimental Medicine* 204:3133-3146.
35. Reis E Sousa, C. 2006. Dendritic cells in a mature age. *Nature Reviews Immunology* 6:476-483.
36. Sousa, C.R., P.D. Stahl, and J.M. Austyn. 1993. Phagocytosis of antigens by Langerhans cells in vitro. *Journal of Experimental Medicine* 178:509-519.
37. Villadangos, J.A., and W.R. Heath. 2005. Life cycle, migration and antigen presenting functions of spleen and lymph node dendritic cells: Limitations of the Langerhans cells paradigm. *Seminars in Immunology* 17:262-272.
38. Macagno, A., G. Napolitani, A. Lanzavecchia, and F. Sallusto. 2007. Duration, combination and timing: the signal integration model of dendritic cell activation. *Trends in Immunology* 28:227-233.
39. Janeway Jr, C.A. 1989. Approaching the asymptote? Evolution and revolution in immunology. *Cold Spring Harbor Symposia on Quantitative Biology* 54:1-13.
40. Akira, S., S. Uematsu, and O. Takeuchi. 2006. Pathogen recognition and innate immunity. *Cell* 124:783-801.
41. Kawai, T., and S. Akira. 2011. Toll-like Receptors and Their Crosstalk with Other Innate Receptors in Infection and Immunity. *Immunity* 34:637-650.
42. Trinchieri, G., and A. Sher. 2007. Cooperation of Toll-like receptor signals in innate immune defence. *Nature Reviews Immunology* 7:179-190.
43. Iwasaki, A., and R. Medzhitov. 2004. Toll-like receptor control of the adaptive immune responses. *Nature Immunology* 5:987-995.
44. Kawai, T., and S. Akira. 2010. The role of pattern-recognition receptors in innate immunity: Update on toll-like receptors. *Nature Immunology* 11:373-384.
45. Akira, S., and K. Takeda. 2004. Toll-like receptor signalling. *Nature Reviews Immunology* 4:499-511.
46. Schroder, K., and J. Tschopp. The Inflammasomes. *Cell* 140:821-832.
47. Magalhaes, J.G., M.T. Sorbara, S.E. Girardin, and D.J. Philpott. 2011. What is new with Nods? *Current Opinion in Immunology* 23:29-34.
48. Fritz, J.H., L. Le Bourhis, G. Sellge, J.G. Magalhaes, H. Fsihi, T.A. Kufer, C. Collins, J. Viala, R.L. Ferrero, S.E. Girardin, and D.J. Philpott. 2007.

Nod1-Mediated Innate Immune Recognition of Peptidoglycan Contributes to the Onset of Adaptive Immunity. *Immunity* 26:445-459.

49. Creagh, E.M., and L.A.J. O'Neill. 2006. TLRs, NLRs and RLRs: a trinity of pathogen sensors that co-operate in innate immunity. *Trends in Immunology* 27:352-357.
50. Koyama, S., K.J. Ishii, H. Kumar, T. Tanimoto, C. Coban, S. Uematsu, T. Kawai, and S. Akira. 2007. Differential role of TLR- and RLR-signaling in the immune responses to influenza A virus infection and vaccination. *Journal of Immunology* 179:4711-4720.
51. LeibundGut-Landmann, S., O. Groß, M.J. Robinson, F. Osorio, E.C. Slack, S.V. Tsoni, E. Schweighoffer, V. Tybulewicz, G.D. Brown, J. Ruland, and C. Reis e Sousa. 2007. Syk- and CARD9-dependent coupling of innate immunity to the induction of T helper cells that produce interleukin 17. *Nature Immunology* 8:630-638.
52. Gross, O., A. Gewies, K. Finger, M. Schäfer, T. Sparwasser, C. Peschel, I. Förster, and J. Ruland. 2006. Card9 controls a non-TLR signalling pathway for innate anti-fungal immunity. *Nature* 442:651-656.
53. Taylor, P.R., S.V. Tsoni, J.A. Willment, K.M. Dennehy, M. Rosas, H. Findon, K. Haynes, C. Steele, M. Botto, S. Gordon, and G.D. Brown. 2007. Dectin-1 is required for β-glucan recognition and control of fungal infection. *Nature Immunology* 8:31-38.
54. Rogers, N.C., E.C. Slack, A.D. Edwards, M.A. Nolte, O. Schulz, E. Schweighoffer, D.L. Williams, S. Gordon, V.L. Tybulewicz, G.D. Brown, and C. Reis E Sousa. 2005. Syk-dependent cytokine induction by dectin-1 reveals a novel pattern recognition pathway for C type lectins. *Immunity* 22:507-517.
55. Matzinger, P. 1994. Tolerance, danger, and the extended family. *Annual Review of Immunology* 12:991-1045.
56. Beg, A.A. 2002. Endogenous ligands of Toll-like receptors: Implications for regulating inflammatory and immune responses. *Trends in Immunology* 23:509-512.
57. Schnurr, M., F. Then, P. Galambos, C. Scholz, B. Siegmund, S. Endres, and A. Eigler. 2000. Extracellular ATP and TNF-α synergize in the activation and maturation of human dendritic cells. *Journal of Immunology* 165:4704-4709.
58. Wu, L., A. D'Amico, H. Hochrein, M. O'Keeffe, K. Shortman, and K. Lucas. 2001. Development of thymic and splenic dendritic cell populations from different hemopoietic precursors. *Blood* 98:3376-3382.
59. Manz, M.G., D. Traver, T. Miyamoto, I.L. Weissman, and K. Akashi. 2001. Dendritic cell potentials of early lymphoid and myeloid progenitors. *Blood* 97:3333-3341.
60. D'Amico, A., and L. Wu. 2003. The early progenitors of mouse dendritic cells and plasmacytoid predendritic cells are within the bone marrow hemopoietic precursors expressing Flt3. *Journal of Experimental Medicine* 198:293-303.
61. Karsunky, H., M. Merad, A. Cozzio, I.L. Weissman, and M.G. Manz. 2003. Flt3 ligand regulates dendritic cell development from Flt3+ lymphoid and myeloid-committed progenitors to Flt3+ dendritic cells in vivo. *Journal of Experimental Medicine* 198:305-313.

62. Fogg, D.K., C. Sibon, C. Miled, S. Jung, P. Aucouturier, D.R. Littman, A. Cumano, and F. Geissmann. 2006. A clonogenic bone harrow progenitor specific for macrophages and dendritic cells. *Science* 311:83-87.
63. Liu, K., G.D. Victora, T.A. Schwickert, P. Guermonprez, M.M. Meredith, K. Yao, F.F. Chu, G.J. Randolph, A.Y. Rudensky, and M. Nussenzweig. 2009. In vivo analysis of dendritic cell development and homeostasis. *Science* 324:392-397.
64. Randolph, G.J., S. Beaulieu, S. Lebecque, R.M. Steinman, and W.A. Muller. 1998. Differentiation of monocytes into dendritic cells in a model of transendothelial trafficking. *Science* 282:480-483.
65. Randolph, G.J., G. Sanchez-Schmitz, R.M. Liebman, and K. Schäkel. 2002. The CD16+ (FcγRIII+) subset of human monocytes preferentially becomes migratory dendritic cells in a model tissue setting. *Journal of Experimental Medicine* 196:517-527.
66. Barak, V., F. Levi-Schaffer, B. Nisman, and A. Nagler. 1995. Cytokine dysregulation in chronic graft versus host disease. *Leukemia and Lymphoma* 17:169-173.
67. Cebon, J., J.E. Layton, D. Maher, and G. Morstyn. 1994. Endogenous haemopoietic growth factors in neutropenia and infection. *British Journal of Haematology* 86:265-274.
68. Zwierzina, H., S. Schollenberger, M. Herold, F. Schmalzl, and J. Besemer. 1992. Endogenous serum levels and surface receptor expression of GM-CSF and IL-3 in patients with myelodysplastic syndromes. *Leukemia Research* 16:1181-1186.
69. Hikino, H., T. Miyagi, Y. Hua, S. Hirohisa, D.P. Gold, X.K. Li, M. Fujino, T. Tetsuya, H. Amemiya, S. Suzuki, L. Robb, M. Miyata, and H. Kimura. 2000. GM-CSF-independent development of dendritic cells from bone marrow cells in the GM-CSF-receptor-deficient mouse. *Transplantation Proceedings* 32:2458-2459.
70. Vremec, D., G.J. Lieschke, A.R. Dunn, L. Robb, D. Metcalf, and K. Shortman. 1997. The influence of granulocyte/macrophage colony-stimulating factor on dendritic cell levels in mouse lymphoid organs. *European Journal of Immunology* 27:40-44.
71. McKenna, H.J., K.L. Stocking, R.E. Miller, K. Brasel, T. De Smedt, E. Maraskovsky, C.R. Maliszewski, D.H. Lynch, J. Smith, B. Pulendran, E.R. Roux, M. Teepe, S.D. Lyman, and J.J. Peschon. 2000. Mice lacking flt3 ligand have deficient hematopoiesis affecting hematopoietic progenitor cells, dendritic cells, and natural killer cells. *Blood* 95:3489-3497.
72. Xu, Y., Y. Zhan, A.M. Lew, S.H. Naik, and M.H. Kershaw. 2007. Differential development of murine dendritic cells by GM-CSF versus Flt3 ligand has implications for inflammation and trafficking. *Journal of Immunology* 179:7577-7584.
73. Medzhitov, R., and Janeway C, Jr. 2000. Advances in immunology: Innate immunity. *New England Journal of Medicine* 343:338-344.
74. Powell, T.J., C.D. Jenkins, R. Hattori, and G.G. Macpherson. 2003. Rat bone marrow-derived dendritic cells, but not ex vivo dendritic cells, secrete nitric oxide and can inhibit T-cell proliferation. *Immunology* 109:197-208.
75. Steinman, R.M., and M.C. Nussenzweig. 2002. Avoiding horror autotoxicus: The importance of dendritic cells in peripheral T cell tolerance. *Proceedings*

of the National Academy of Sciences of the United States of America 99:351-358.
76. Piccirillo, C.A., and E.M. Shevach. 2004. Naturally-occurring CD4+CD25+ immunoregulatory T cells: Central players in the arena of peripheral tolerance. *Seminars in Immunology* 16:81-88.
77. Zhou, L., M.M.W. Chong, and D.R. Littman. 2009. Plasticity of CD4+ T Cell Lineage Differentiation. *Immunity* 30:646-655.
78. Weaver, C.T., L.E. Harrington, P.R. Mangan, M. Gavrieli, and K.M. Murphy. 2006. Th17: An Effector CD4 T Cell Lineage with Regulatory T Cell Ties. *Immunity* 24:677-688.
79. Boyton, R.J., and D.M. Altmann. 2002. Is selection for TCR affinity a factor in cytokine polarization? *Trends in Immunology* 23:526-529.
80. Geijtenbeek, T.B.H., and S.I. Gringhuis. 2009. Signalling through C-type lectin receptors: Shaping immune responses. *Nature Reviews Immunology* 9:465-479.
81. Ivanov, I.I., B.S. McKenzie, L. Zhou, C.E. Tadokoro, A. Lepelley, J.J. Lafaille, D.J. Cua, and D.R. Littman. 2006. The Orphan Nuclear Receptor RORγt Directs the Differentiation Program of Proinflammatory IL-17+ T Helper Cells. *Cell* 126:1121-1133.
82. Vinuesa, C.G., S.G. Tangye, B. Moser, and C.R. Mackay. 2005. Follicular B helper T cells in antibody responses and autoimmunity. *Nature Reviews Immunology* 5:853-865.
83. Sakaguchi, S., and F. Powrie. 2007. Emerging challenges in regulatory T cell function and biology. *Science* 317:627-629.
84. Zheng, Y., and A.Y. Rudensky. 2007. Foxp3 in control of the regulatory T cell lineage. *Nature Immunology* 8:457-462.
85. Bluestone, J.A., C.R. MacKay, J.J. O'Shea, and B. Stockinger. 2009. The functional plasticity of T cell subsets. *Nature Reviews Immunology* 9:811-816.
86. Yang, X.O., R. Nurieva, G.J. Martinez, H.S. Kang, Y. Chung, B.P. Pappu, B. Shah, S.H. Chang, K.S. Schluns, S.S. Watowich, X.H. Feng, A.M. Jetten, and C. Dong. 2008. Molecular Antagonism and Plasticity of Regulatory and Inflammatory T Cell Programs. *Immunity* 29:44-56.
87. Osorio, F., S. LeibundGut-Landmann, M. Lochner, K. Lahl, T. Sparwaser, G. Eberl, and C. Reis e Sousa. 2008. DC activated via dectin-1 convert Treg into IL-17 producers. *European Journal of Immunology* 38:3274-3281.
88. Lee, Y.K., H. Turner, C.L. Maynard, J.R. Oliver, D. Chen, C.O. Elson, and C.T. Weaver. 2009. Late Developmental Plasticity in the T Helper 17 Lineage. *Immunity* 30:92-107.
89. Lanzavecchla, A. 1998. Licence to kill. *Nature* 393:413-414.
90. Schoenberger, S.P., R.E.M. Toes, E.I.H. Van Dervoort, R. Offringa, and C.J.M. Melief. 1998. T-cell help for cytotoxic T lymphocytes is mediated by CD40-CD4OL interactions. *Nature* 393:480-483.
91. Bennett, S.R.M., F.R. Carbone, F. Karamalis, R.A. Flavell, J.F.A.P. Miller, and W.R. Heath. 1998. Help for cytotoxic-T-cell responses is mediated by CD4O signalling. *Nature* 393:478-480.
92. Ridge, J.P., F. Di Rosa, and P. Matzinger. 1998. A conditioned dendritic cell can be a temporal bridge between a CD4 + T-helper and a T-killer cell. *Nature* 393:474-478.

93. Bennett, S.R.M., F.R. Carbone, F. Karamalis, J.F.A.P. Miller, and W.R. Heath. 1997. Induction of a CD8+ cytotoxic T lymphocyte response by cross-priming requires cognate CD4+ T cell help. *Journal of Experimental Medicine* 186:65-70.
94. Fujii, S.I., K. Liu, C. Smith, A.J. Bonito, and R.M. Steinman. 2004. The linkage of innate to adaptive immunity via maturing dendritic cells in vivo requires CD40 ligation in addition to antigen presentation and CD80/86 costimulation. *Journal of Experimental Medicine* 199:1607-1618.
95. Bachmann, M.F., R.M. Zinkernagel, and A. Oxenius. 1998. Cutting edge commentary: Immune responses in the absence of costimulation: Viruses know the trick. *Journal of Immunology* 161:5791-5794.
96. Ruedl, C., M. Kopf, and M.F. Bachmann. 1999. CD8+ T cells mediate CD40-independent maturation of dendritic cells in vivo. *Journal of Experimental Medicine* 189:1875-1883.
97. Banchereau, J., and R.M. Steinman. 1998. Dendritic cells and the control of immunity. *Nature* 392:245-252.
98. Osorio, F., and C. Reis e Sousa. 2011. Myeloid C-type Lectin Receptors in Pathogen Recognition and Host Defense. *Immunity* 34:651-664.
99. Pasparakis, M. 2009. Regulation of tissue homeostasis by NF-B signalling: Implications for inflammatory diseases. *Nature Reviews Immunology* 9:778-788.
100. Ghosh, S., and M.S. Hayden. 2008. New regulators of NF-κB in inflammation. *Nature Reviews Immunology* 8:837-848.
101. Ghosh, S., and M. Karin. 2002. Missing pieces in the NF-κB puzzle. *Cell* 109:S81-S96.
102. Perkins, N.D. 2007. Integrating cell-signalling pathways with NF-κB and IKK function. *Nature Reviews Molecular Cell Biology* 8:49-62.
103. Bonizzi, G., and M. Karin. 2004. The two NF-κB activation pathways and their role in innate and adaptive immunity. *Trends in Immunology* 25:280-288.
104. Hayden, M.S., and S. Ghosh. 2004. Signaling to NF-κB. *Genes and Development* 18:2195-2224.
105. Debra, S., Z. Weih, B. Yilmaz, and F. Weih. 2001. Essential role of RelB in germinal center and marginal zone formation and proper expression of homing chemokines. *Journal of Immunology* 167:1909-1919.
106. Garrington, T.P., and G.L. Johnson. 1999. Organization and regulation of mitogen-activated protein kinase signaling pathways. *Current Opinion in Cell Biology* 11:211-218.
107. Chang, L., and M. Karin. 2001. Mammalian MAP kinase signalling cascades. *Nature* 410:37-40.
108. Treisman, R. 1996. Regulation of transcription by MAP kinase cascades. *Current Opinion in Cell Biology* 8:205-215.
109. Krishna, M., and H. Narang. 2008. The complexity of mitogen-activated protein kinases (MAPKs) made simple. *Cellular and Molecular Life Sciences* 65:3525-3544.
110. Leppä, S., R. Saffrich, W. Ansorge, and D. Bohmann. 1998. Differential regulation of c-Jun by ERK and JNK during PC12 cell differentiation. *EMBO Journal* 17:4404-4413.

111. Liu, R., T. Itoh, K.I. Arai, and S. Watanabe. 1997. Activation of c-Jun N-terminal kinase by human granulocyte macrophage-colony stimulating factor in BA/F3 cells. *Biochemical and Biophysical Research Communications* 234:611-615.
112. Robinson, M.J., and M.H. Cobb. 1997. Mitogen-activated protein kinase pathways. *Current Opinion in Cell Biology* 9:180-186.
113. Shen, Y.H., J. Godlewski, J. Zhu, P. Sathyanarayana, V. Leaner, M.J. Birrer, A. Rana, and G. Tzivion. 2003. Cross-talk between JNK/SAPK and ERK/MAPK pathways: Sustained activation of JNK blocks ERK activation by mitogenic factors. *Journal of Biological Chemistry* 278:26715-26721.
114. Bagrodia, S., B. Derijard, R.J. Davis, and R.A. Cerione. 1995. Cdc42 and PAK-mediated signaling leads to Jun kinase and p38 mitogen- activated protein kinase activation. *Journal of Biological Chemistry* 270:27995-27998.
115. Shaw, J.P., P.J. Utz, D.B. Durand, J.J. Toole, E.A. Emmel, and G.R. Crabtree. 1988. Indentification of a putative regulator of early T cell activation genes. *Science* 241:202-205.
116. Müller, M.R., and A. Rao. NFAT, immunity and cancer: A transcription factor comes of age. *Nature Reviews Immunology* 10:645-656.
117. Macian, F. 2005. NFAT proteins: Key regulators of T-cell development and function. *Nature Reviews Immunology* 5:472-484.
118. Mancini, M., and A. Toker. 2009. NFAT proteins: Emerging roles in cancer progression. *Nature Reviews Cancer* 9:810-820.
119. Jain, J., P.G. McCaffrey, V.E. Valge-Archer, and A. Rao. 1992. Nuclear factor of activated T cells contains Fos and Jun. *Nature* 356:801-804.
120. Strober, W., P.J. Murray, A. Kitani, and T. Watanabe. 2006. Signalling pathways and molecular interactions of NOD1 and NOD2. *Nature Reviews Immunology* 6:9-20.
121. Mariathasan, S., and D.M. Monack. 2007. Inflammasome adaptors and sensors: Intracellular regulators of infection and inflammation. *Nature Reviews Immunology* 7:31-40.
122. Broz, P., K. Newton, M. Lamkanfi, S. Mariathasan, V.M. Dixit, and D.M. Monack. Redundant roles for inflammasome receptors NLRP3 and NLRC4 in host defense against Salmonella. *Journal of Experimental Medicine* 207:1745-1755.
123. Kanneganti, T.D., N. Ozören, M. Body-Malapel, A. Amer, J.H. Park, L. Franchi, J. Whitfield, W. Barchet, M. Colonna, P. Vandenabeele, J. Bertin, A. Coyle, E.P. Grant, S. Akira, and G. Núňez. 2006. Bacterial RNA and small antiviral compounds activate caspase-1 through cryopyrin/Nalp3. *Nature* 440:233-236.
124. Hornung, V., F. Bauernfeind, A. Halle, E.O. Samstad, H. Kono, K.L. Rock, K.A. Fitzgerald, and E. Latz. 2008. Silica crystals and aluminum salts activate the NALP3 inflammasome through phagosomal destabilization. *Nature Immunology* 9:847-856.
125. Kanneganti, T.D., M. Lamkanfi, Y.G. Kim, G. Chen, J.H. Park, L. Franchi, P. Vandenabeele, and G. Núňez. 2007. Pannexin-1-Mediated Recognition of Bacterial Molecules Activates the Cryopyrin Inflammasome Independent of Toll-like Receptor Signaling. *Immunity* 26:433-443.

126. Arai, K., F. Lee, A. Miyajima, S. Miyatake, N. Arai, and T. Yokota. 1990. Cytokines: Coordinators of immune and inflammatory responses. *Annual Review of Biochemistry* 59:783-836.
127. Riopel, J., M. Tam, K. Mohan, M.W. Marino, and M.M. Stevenson. 2001. Granulocyte-macrophage colony-stimulating factor-deficient mice have impaired resistance to blood-stage malaria. *Infection and Immunity* 69:129-136.
128. Miyajima, A., A.L.F. Mui, T. Ogorochi, and K. Sakamaki. 1993. Receptors for granulocyte-macrophage colony-stimulating factor, interleukin-3, and interleukin-5. *Blood* 82:1960-1974.
129. Sato, N., K. Sakamaki, N. Terada, K.I. Arai, and A. Miyajima. 1993. Signal transduction by the high-affinity GM-CSF receptor: Two distinct cytoplasmic regions of the common β subunit responsible for different signaling. *EMBO Journal* 12:4181-4189.
130. Schlessinger, J. 2000. Cell signaling by receptor tyrosine kinases. *Cell* 103:211-225.
131. Hansen, G., T.R. Hercus, B.J. McClure, F.C. Stomski, M. Dottore, J. Powell, H. Ramshaw, J.M. Woodcock, Y. Xu, M. Guthridge, W.J. McKinstry, A.F. Lopez, and M.W. Parker. 2008. The Structure of the GM-CSF Receptor Complex Reveals a Distinct Mode of Cytokine Receptor Activation. *Cell* 134:496-507.
132. Armitage, J.O. 1998. Emerging applications of recombinant human granulocyte-macrophage colony-stimulating factor. *Blood* 92:4491-4508.
133. Matsuguchi, T., Y. Zhao, M.B. Lilly, and A.S. Kraft. 1997. The cytoplasmic domain of granulocyte-macrophage colony-stimulating factor (GM-CSF) receptor α subunit is essential for both GM-CSF-mediated growth and differentiation. *Journal of Biological Chemistry* 272:17450-17459.
134. Klein, J.B., M.J. Rane, J.A. Scherzer, P.Y. Coxon, R. Kettritz, J.M. Mathiesen, A. Buridi, and K.R. McLeish. 2000. Granulocyte-macrophage colony-stimulating factor delays neutrophil constitutive apoptosis through phosphoinositide 3-kinase and extracellular signal-regulated kinase pathways. *Journal of Immunology* 164:4286-4291.
135. Bozinovski, S., J.E. Jones, R. Vlahos, J.A. Hamilton, and G.P. Anderson. 2002. Granulocyte/macrophage-colony-stimulating factor (GM-CSF) regulates lung innate immunity to lipopolysaccharide through Akt/Erk activation of NFκB and AP-1 in vivo. *Journal of Biological Chemistry* 277:42808-42814.
136. Liontos, L.M., D. Dissanayake, P.S. Ohashi, A. Weiss, L.L. Dragone, and C.J. McGlade. 2011. The Src-like adaptor protein regulates GM-CSFR signaling and monocytic dendritic cell maturation. *Journal of Immunology* 186:1923-1933.
137. Zelensky, A.N., and J.E. Gready. 2005. The C-type lectin-like domain superfamily. *FEBS Journal* 272:6179-6217.
138. Geijtenbeek, T.B.H., S.J. Van Vliet, A. Engering, B.A. T Hart, and Y. Van Kooyk. 2004. Self- and nonself-recognition by C-type lectins on dendritic cells. In Annual Review of Immunology. 33-54.
139. Kerrigan, A.M., and G.D. Brown. Syk-coupled C-type lectin receptors that mediate cellular activation via single tyrosine based activation motifs. *Immunological Reviews* 234:335-352.

140. Gringhuis, S.I., J. den Dunnen, M. Litjens, B. van het Hof, Y. van Kooyk, and T.H. Geijtenbeek. 2007. C-Type Lectin DC-SIGN Modulates Toll-like Receptor Signaling via Raf-1 Kinase-Dependent Acetylation of Transcription Factor NF-κB. *Immunity* 26:605-616.
141. Dennehy, K.M., G. Ferwerda, I. Faro-Trindade, E. Pyz, J.A. Willment, P.R. Taylor, A. Kerrigan, S.V. Tsoni, S. Gordon, F. Meyer-Wentrup, G.J. Adema, B.J. Kullberg, E. Schweighoffer, V. Tybulewicz, H.M. Mora-Montes, N.A.R. Gow, D.L. Williams, M.G. Netea, and G.D. Brown. 2008. Syk kinase is required for collaborative cytokine production induced through Dectin-1 and Toll-like receptors. *European Journal of Immunology* 38:500-506.
142. Gantner, B.N., R.M. Simmons, S.J. Canavera, S. Akira, and D.M. Underhill. 2003. Collaborative induction of inflammatory responses by dectin-1 and toll-like receptor 2. *Journal of Experimental Medicine* 197:1107-1117.
143. Gringhuis, S.I., J. den Dunnen, M. Litjens, M. van der Vlist, B. Wevers, S.C.M. Bruijns, and T.B.H. Geijtenbeek. 2009. Dectin-1 directs T helper cell differentiation by controlling noncanonical NF-κB activation through Raf-1 and Syk. *Nature Immunology* 10:203-213.
144. Robinson, M.J., D. Sancho, E.C. Slack, S. LeibundGut-Landmann, and C.R. Sousa. 2006. Myeloid C-type lectins in innate immunity. *Nature Immunology* 7:1258-1265.
145. Lanier, L.L. 2005. NK cell recognition. In Annual Review of Immunology. 225-274.
146. Di Carlo, F.J., and J.V. Fiore. 1958. On the composition of zymosan. *Science* 127:756-757.
147. Underhill, D.M., A. Ozinsky, A.M. Hajjar, A. Stevens, C.B. Wilson, M. Bassetti, and A. Aderem. 1999. The Toll-like receptor 2 is recruited to macrophage phagosomes and discriminates between pathogens. *Nature* 401:811-815.
148. Kataoka, K., T. Muta, S. Yamazaki, and K. Takeshige. 2002. Activation of macrophages by linear (1→3)-β-D-glucans. Implications for the recognition of fungi by innate immunity. *Journal of Biological Chemistry* 277:36825-36831.
149. Underhill, D.M., E. Rossnagle, C.A. Lowell, and R.M. Simmons. 2005. Dectin-1 activates Syk tyrosine kinase in a dynamic subset of macrophages for reactive oxygen production. *Blood* 106:2543-2550.
150. Goodridge, H.S., R.M. Simmons, and D.M. Underhill. 2007. Dectin-1 stimulation by Candida albicans yeast or zymosan triggers NFAT activation in macrophages and dendritic cells. *Journal of Immunology* 178:3107-3115.
151. Brown, G.D. 2006. Dectin-1 : A signalling non-TLR pattern-recognition receptor. *Nature Reviews Immunology* 6:33-43.
152. Kim, T.D., R. Hyun Jeong, C. Hyun Il, C.H. Yang, and J. Kim. 2000. Thermal behavior of proteins: Heat-resistant proteins and their heat-induced secondary structural changes. *Biochemistry* 39:14839-14846.
153. Shu, L., W. Yin, H. Zhuang, and Z. Hua. 2006. Comparison of gene expression profiles in mouse primary T cells under normal and prolonged activation. *Blood Cells, Molecules, and Diseases* 37:64-75.
154. Wang, M., D. Windgassen, and E.T. Papoutsakis. 2008. Comparative analysis of transcriptional profiling of CD3+, CD4+ and CD8+ T cells

identifies novel immune response players in T-Cell activation. *BMC Genomics* 9:
155. Stentz, F.B., and A.E. Kitabchi. 2004. Transcriptome and proteome expression in activated human CD4 and CD8 T-lymphocytes. *Biochemical and Biophysical Research Communications* 324:692-696.
156. Kotenko, S.V., L.S. Izotova, O.V. Mirochnitchenko, E. Esterova, H. Dickensheets, R.P. Donnelly, and S. Pestka. 2001. Identification of the functional interleukin-22 (IL-22) receptor complex. The IL-10R2 chain (IL-10Rβ) is a common chain of both the IL-10 and IL-22 (IL-10-related T cell-derived inducible factor, IL-TIF) receptor complexes. *Journal of Biological Chemistry* 276:2725-2732.
157. Min, L., S.A.B.M. Isa, W. Shuai, C.B. Piang, F.W. Nih, M. Kotaka, and C. Ruedl. 2010. Cutting edge: Granulocyte-macrophage colony-stimulating factor is the major CD8+ T cell-derived licensing factor for dendritic cell activation. *Journal of Immunology* 184:4625-4629.
158. Min, L., S.A.B.M. Isa, W. Shuai, C.B. Piang, F.W. Nih, M. Kotaka, and C. Ruedl. Cutting edge: Granulocyte-macrophage colony-stimulating factor is the major CD8+ T cell-derived licensing factor for dendritic cell activation. *Journal of Immunology* 184:4625-4629.
159. Kapsenberg, M.L. 2003. Dendritic-cell control of pathogen-driven T-cell polarization. *Nature Reviews Immunology* 3:984-993.
160. Schulz, O., A.D. Edwards, M. Schito, J. Aliberti, S. Manickasingham, A. Sher, and C. Reis e Sousa. 2000. CD40 triggering of heterodimeric IL-12 p70 production by dendritic cells in vivo requires a microbial priming signal. *Immunity* 13:453-462.
161. Spörri, R., and C. Reis e Sousa. 2005. Inflammatory mediators are insufficient for full dendritic cell activation and promote expansion of CD4+ T cell populations lacking helper function. *Nature Immunology* 6:163-170.
162. Xu, S., J. Huo, K.G. Lee, T. Kurosaki, and K.P. Lam. 2009. Phospholipase Cγ2 is critical for Dectin-1-mediated Ca2+ flux and cytokine production in dendritic cells. *Journal of Biological Chemistry* 284:7038-7046.
163. Gan, C.S., T. Guo, H. Zhang, S.K. Lim, and S.K. Sze. 2008. A comparative study of electrostatic repulsion-hydrophilic interaction chromatography (ERLIC) versus SCX-IMAC-based methods for phosphopeptide isolation/enrichment. *Journal of Proteome Research* 7:4869-4877.
164. Ruedl, C., H.J. Khameneh, and K. Karjalainen. 2008. Manipulation of immune system via immortal bone marrow stem cells. *International Immunology* 20:1211-1218.
165. Déléris, P., M. Trost, I. Topisirovic, P.L. Tanguay, K.L.B. Borden, P. Thibault, and S. Meloche. 2011. Activation loop phosphorylation of ERK3/ERK4 by group I p21-activated kinases (PAKs) defines a novel PAK-ERK3/4-MAPK-activated protein kinase 5 signaling pathway. *Journal of Biological Chemistry* 286:6470-6478.
166. Burgess, A.W., and D. Metcalf. 1980. The nature and action of granulocyte - macrophage colony stimulating factors. *Blood* 56:947-958.
167. Hamilton, J.A. 2002. GM-CSF in inflammation and autoimmunity. *Trends in Immunology* 23:403-408.
168. Hamilton, J.A. 2008. Colony-stimulating factors in inflammation and autoimmunity. *Nature Reviews Immunology* 8:533-544.

169. Brissette, W.H., D.A. Baker, E.J. Stam, J.P. Umland, and R.J. Griffiths. 1995. GM-CSF rapidly primes mice for enhanced cytokine production in response to LPS and TNF. *Cytokine* 7:291-295.
170. Codarri, L., G. Gyülvészii, V. Tosevski, L. Hesske, A. Fontana, L. Magnenat, T. Suter, and B. Becher. 2011. RORγ3t drives production of the cytokine GM-CSF in helper T cells, which is essential for the effector phase of autoimmune neuroinflammation. *Nature Immunology* 12:560-567.
171. El-Behi, M., B. Ciric, H. Dai, Y. Yan, M. Cullimore, F. Safavi, G.X. Zhang, B.N. Dittel, and A. Rostami. 2011. The encephalitogenicity of TH 17 cells is dependent on IL-1- and IL-23-induced production of the cytokine GM-CSF. *Nature Immunology* 12:568-575.
172. McGeachy, M.J. 2011. GM-CSF: The secret weapon in the TH 17 arsenal. *Nature Immunology* 12:521-522.
173. Romani, L. 2004. Immunity to fungal infections. *Nature Reviews Immunology* 4:11-23.
174. Gringhuis, S.I., B.A. Wevers, T.M. Kaptein, T.M.M. van Capel, B. Theelen, T. Boekhout, E.C. de Jong, and T.B.H. Geijtenbeek. Selective c-Rel activation via Malt1 controls anti-fungal TH-17 immunity by dectin-1 and dectin-2. *PLoS Pathogens* 7:
175. Brown, G.D., J. Herre, D.L. Williams, J.A. Willment, A.S.J. Marshall, and S. Gordon. 2003. Dectin-1 mediates the biological effects of β-glucans. *Journal of Experimental Medicine* 197:1119-1124.
176. Netea, M.G., R. Sutmuller, C. Hermann, C.A.A. Van Der Graaf, J.W.M. Van Der Meer, J.H. Van Krieken, T. Hartung, G. Adema, and B.J. Kullberg. 2004. Toll-Like Receptor 2 Suppresses Immunity against Candida albicans through Induction of IL-10 and Regulatory T Cells. *Journal of Immunology* 172:3712-3718.
177. Malek, T.R., and A.L. Bayer. 2004. Tolerance, not immunity, crucially depends on IL-2. *Nature Reviews Immunology* 4:665-674.
178. Napolitani, G., A. Rinaldi, F. Bertoni, F. Sallusto, and A. Lanzavecchia. 2005. Selected Toll-like receptor agonist combinations synergistically trigger a T helper type 1 -polarizing program in dendritic cells. *Nature Immunology* 6:769-776.
179. Ferwerda, G., F. Meyer-Wentrup, B.J. Kullberg, M.G. Netea, and G.J. Adema. 2008. Dectin-1 synergizes with TLR2 and TLR4 for cytokine production in human primary monocytes and macrophages. *Cellular Microbiology* 10:2058-2066.
180. Rosas, M., K. Liddiard, M. Kimberg, I. Faro-Trindade, J.U. McDonald, D.L. Williams, G.D. Brown, and P.R. Taylor. 2008. The induction of inflammation by dectin-1 in vivo is dependent on myeloid cell programming and the progression of phagocytosis. *Journal of Immunology* 181:3549-3557.
181. Slack, E.C., M.J. Robinson, P. Hernanz-Falcón, G.D. Brown, D.L. Williams, E. Schweighoffer, V.L. Tybulewicz, and C. Reis e Sousa. 2007. Syk-dependent ERK activation regulates IL-2 and IL-10 production by DC stimulated with zymosan. *European Journal of Immunology* 37:1600-1612.
182. Gross, O., H. Poeck, M. Bscheider, C. Dostert, N. Hannesschläger, S. Endres, G. Hartmann, A. Tardivel, E. Schweighoffer, V. Tybulewicz, A. Mocsai, J. Tschopp, and J. Ruland. 2009. Syk kinase signalling couples to the Nlrp3 inflammasome for anti-fungal host defence. *Nature* 459:433-436.

183. Greenblatt, M.B., A. Aliprantis, B. Hu, and L.H. Glimcher. Calcineurin regulates innate antifungal immunity in neutrophils. *Journal of Experimental Medicine* 207:923-931.
184. Gerosa, F., B. Baldani-Guerra, L.A. Lyakh, G. Batoni, S. Esin, R.T. Winkler-Pickett, M.R. Consolaro, M. De Marchi, D. Giachino, A. Robbiano, M. Astegiano, A. Sambataro, R.A. Kastelein, G. Carra, and G. Trinchieri. 2008. Differential regulation of interleukin 12 and interleukin 23 production in human dendritic cells. *Journal of Experimental Medicine* 205:1447-1461.
185. Acosta-Rodriguez, E.V., G. Napolitani, A. Lanzavecchia, and F. Sallusto. 2007. Interleukins 1β and 6 but not transforming growth factor-β are essential for the differentiation of interleukin 17-producing human T helper cells. *Nature Immunology* 8:942-949.
186. Bozinovski, S., J.E. Jones, R. Vlahos, J.A. Hamilton, and G.P. Anderson. 2002. Granulocyte/macrophage-colony-stimulating factor (GM-CSF) regulates lung innate immunity to lipopolysaccharide through Akt/Erk activation of NFκB and AP-1 in vivo. *Journal of Biological Chemistry* 277:42808-42814.
187. Lee, F.S., J. Hagler, Z.J. Chen, and T. Maniatis. 1997. Activation of the IκBα kinase complex by MEKK1, a kinase of the JNK pathway. *Cell* 88:213-222.
188. Banerjee, A., R. Gugasyan, M. McMahon, and S. Gerondakis. 2006. Diverse Toll-like receptors utilize Tpl2 to activate extracellular signal-regulated kinase (ERK) in hemopoietic cells. *Proceedings of the National Academy of Sciences of the United States of America* 103:3274-3279.
189. Dumitru, C.D., J.D. Ceci, C. Tsatsanis, D. Kontoyiannis, K. Stamatakis, J.H. Lin, C. Patriotis, N.A. Jenkins, N.G. Copeland, G. Kollias, and P.N. Tsichlis. 2000. TNF-α induction by LPS is regulated posttranscriptionally via a Tpl2/ERK-dependent pathway. *Cell* 103:1071-1083.
190. Kim, B.S., I.D. Jung, J.S. Kim, J.H. Lee, I.Y. Lee, and K.B. Lee. 2000. Curdlan gels as protein drug delivery vehicles. *Biotechnology Letters* 22:1127-1130.
191. Hunter Jr, K.W., R.A. Gault, and M.D. Berner. 2002. Preparation of microparticulate β-glucan from Saccharomyces cerevisiae for use in immune potentiation. *Letters in Applied Microbiology* 35:267-271.